PROTEOMICS BASED SEARCH FOR NOVEL SIK2 SUBSTRATES INVOLVED IN ENDOPLASMIC RETICULUM HOMEOSTASIS

by

Tuncay Şeker

B.S., Molecular Biology and Genetics, Boğaziçi University, 2007

M.S., Molecular Biology and Genetics, Boğaziçi University, 2009

Submitted to the Institute for Graduate Studies in
Science and Engineering in partial fulfillment of
the requirements for the degree of
Doctor of Philosophy

Graduate Program in Molecular Biology and Genetics

Boğaziçi University

2017

To my beloved family...

ACKNOWLEDGEMENTS

I would like to express my sincere gratitude to my supervisors Assist. Prof. Necla Birgül İyison and Assoc. Prof. Ferruh Özcan for their encouragement and tremendous support throughout my long and challenging PhD years. Your advices and guidance have been priceless.

I would like to express my appreciation to my thesis committee members Assoc. Prof. İbrahim Yaman, Assist. Prof. Umut Şahin, Assoc. Prof. Asuman Demiroğlu-Zergeroğlu and Assist. Prof. Can Murathan Erişti for accepting to be in my jury and spending their valuable time in evaluating and criticizing this work.

I would like to thank all the current and former CSL members İzzet Akiva, Burçin Duan Şahbaz, Tolga Aslan, Aida Shahraki, Gizem Sınmaz, Ayşe Nur Kayabaşı, Ruçhan Karaman, Ali İşbilir, Vahap Kapıkıran and Emine Dindar for their friendship and cooperation. I will always remember all the great memories we shared. I would also like to thank all the trainees worked with me for their small and big contributions to this thesis.

I am also thankful to GTÜ-Obedia-Lab members especially Betsi Köse and Soner Türküner for their help and friendship. Betsi made big contribution to this thesis.

I would like to thank Yaman-Lab members Ayşin Demirkol, Can Gürkaşlar, Beren Aylan and Kübra Zırhlıoğlu for their great help, cooperation and friendship. Discussions with İbrahim Yaman have been insightful and illuminating for me.

I am also appreciative to all the students who have taken Bio241 and Bio409 courses for their brilliant questions and comments, as they contributed to the improvement of my teaching skills.

I would like to offer my special thanks to my friends in the MBG department especially Mahmut Can Hız, Xalid Bayramlı, Ece Terzioğlu Kara and Duygu Dağlıkoca for their help and friendship. I also owe my special gratitude to my close friends Erdinç Çamlıbel, Sabri Kızanlık, Caner Korkmaz, Merve Özen-Kızanlık, Yeliz Yılmaz-Korkmaz and Özge Yılmaz for their support and encouragement.

My deepest gratitude goes to my dear friends and sisters Zeynep Özcan and Gizem Gül. I am indebted to them for their encouragement toward completing this never ending story. Every time I lost my way and hope, their positive energies and comments helped me in this struggle.

I am deeply grateful to all my professors in the department for improving my knowledge and raising me academically throughout my undergraduate and graduate years.

Lastly, I would like to express my appreciation to my family for their support with endless love throughout my life.

This work was supported by the Scientific and Technological Research Council of Turkey (TÜBİTAK) Fund 112T274.

ABSTRACT

PROTEOMICS BASED SEARCH FOR NOVEL SIK2 SUBSTRATES INVOLVED IN ENDOPLASMIC RETICULUM HOMEOSTASIS

As a result of high calorie diet and low physical activity, obesity has become widespread worldwide in the last two decades. Obesity, which is a risk factor for many diseases including diabetes, hypertension, and fatty liver, threatens human health considerably. Molecular studies aiming the treatment of obesity and related metabolic diseases are mostly concerned with the regulation of the feeding behaviours and metabolic pathways. SIK2, having a central role in metabolic pathways, is considered as a pharmacological target in the development of therapeutic drugs against metabolic diseases. Recent studies have shown that Endoplasmic Reticulum (ER) stress is involved in the pathological development of metabolic diseases and SIK2 plays a key role in maintaining protein homeostasis in response to ER stress. However, the molecular details have not yet been fully understood. In this study, to elucidate the role of SIK2 in ER stress response we searched for the novel ER-resident substrates of SIK2 by LC-MS/MS-based proteomic analysis. IRS4 and CHIP, considered as candidate proteins after proteomic analysis, were found to interact with SIK2 by co-immunoprecipitation experiments. In the subsequent co-IP experiments, it was also found that IRS4 interacts with the ER stress sensor protein IRE1. A series of experiments have been carried to further investigate the possible roles of IRS4 on ER-stress response and it has been concluded that IRS4 has a regulatory role on the XBP1-splicing activity of IRE1 and the degradation of the ERAD substrate CD3δ. To sum up, results of this study reveal novel protein interactions which will help better understanding the molecular function of SIK2 in maintaining proteostasis in response to ER stress.

ÖZET

SIK2'NİN ENDOPLASMİK RETİKULUM HOMEOSTAZI İLE İLİŞKİLİ YENİ SUBSTRATLARININ PROTEOMİKS TEMELLİ YAKLAŞIMLA ARAŞTIRILMASI

Yüksek kalorili beslenme ve düşük fiziksel aktivitenin bir sonucu olarak, obezite son yirmi yılda dünya çapında yaygınlaşmıştır. Diyabet, hipertansiyon ve karaciğer yağlanması gibi birçok hastalık için risk faktörü olan obezite, insan sağlığını önemli ölçüde tehdit etmektedir. Obezite ve ilgili metabolik hastalıkların tedavisini amaçlayan moleküler çalışmalar çoğunlukla beslenme davranışlarının ve metabolik sinyal yolaklarının regülasyonu ile ilgilidir. Metabolik yolaklarda merkezi bir rol oynayan SIK2, metabolik hastalıklara karşı teröpatik ilaç geliştirmede bir farmakolojik hedef olarak görülmektedir. Son çalışmalar, Endoplazmik Retikulum (ER) stresinin metabolik hastalıkların patolojik gelişiminde yer aldığını ve SIK2'nin bu strese yanıt olarak protein homeostazını sağlamada kilit bir rol oynadığını göstermiştir. Ancak, moleküler ayrıntılar henüz tam olarak anlaşılamamıştır. Bu çalışmada, ER stresi yanıtında SIK2'nin rolünü aydınlatmak için, LC-MS/MS tabanlı proteomik yaklaşımla SIK2'nin ER-yerleşik yeni substratlarını araştırdık. Analiz sonrası, aday proteinler olarak ele alınan IRS4 ve CHIP proteinlerinin eş immün çöktürme (co-IP) deneyleriyle SIK2 ile etkileşime girdiği saptanmıştır. İnsülin ve leptin sinyalinin adaptör moleküllerinden biri olan IRS4'ün devamında ER stres sensörü olan IRE1 ile de etkileşime girdiği tespit edilmiştir. IRS4'ün ER stresi yanıtı üzerindeki etkisine dair bir takım deneyler yapılmış ve bunun neticesinde XBP1 kırpılmasında ve ERAD substratı olan rekombinant CD3δ'nın yıkımında düzenleyici rolü olabileceği bulunmuştur. Özet olarak bu çalışma, ER stres yanıtında SIK2'nin protein homeostasindeki rolünü anlamaya yardımcı olacak yeni protein etkileşimleri sunmaktadır.

TABLE OF CONTENTS

LIST OF FIGURES

LIST OF TABLES

LIST OF SYMBOLS

A	Adenine
C	Cytosine
°C	Centigrade Degree
G	Guanine
g	Gravity
m	Meter
M	Molar
ml	Mililiter
mM	Milimolar
ng	Nanogram
P	Proline
S	Serine
T	Thymine
V	Volt
w	Weight
Y	Tyrosine
u	Unit
α	Alpha
β	Beta
γ	Gamma
Δ	Delta
δ	Delta
κ	Kappa
μg	Microgram
μl	Microliter
μM	Micromolar

LIST OF ACRONYMS/ABBREVIATIONS

AgRP	Agouti-related protein
AMP	Adenosine monophosphate
AMPK	Adenine monophosphate-activated protein kinase
ATF4	Activating transcription factor 4
ATF6	Activation transcription factor 6
BCA	Bicinchoninic acid
BSA	Bovine serum albumin
Ca	Calcium
cAMP	Cyclic AMP
CHIP	The carboxyl-terminus of Hsc70 interacting protein
CHOP	C/EBP homologus protein
cDNA	Complementary deoxyribonucleic acid
CRTC2	CREB regulated transcription coactivator 2
DMEM	Dulbecco's modified eagle's medium
DNA	Deoxyribonucleic acid
dNTP	Deoxyribonucleotide triphosphate
eIF2α	Eukaryotic translation initiation factor 2
ER	Endoplasmic reticulum
ERAD	Endoplasmic reticulum-associated protein degradation
EtBr	Ethidium bromide
EtOH	Ethanol
FBS	Fetal bovine serum
IP	Immunoprecipitation
IRE1	Inositol-requiring enzyme 1
IRS4	Insulin receptor substrate 4
KI	Kinase inactive
LB	Luria-Bertani
mRNA	Messenger ribonucleic acid

NaCl	Sodium chloride
PAGE	Polyacrylamide gel electrophoresis
PCR	Polymerase chain reaction
PERK	PKR-like ER kinase
POMC	Pro-opiomelanocortin
PPARγ	Peroxisome proliferator-activated receptor gamma
PVDF	Polyvinilidin difluoride
RNA	Ribonucleic acid
rpm	Revolutions per minute
RT-PCR	Reverse transcriptase-polymerase chain reaction
SDS	Sodium dodecyl sulphate
SIK2	Salt-inducible kinase 2
SREBP	SRE-binding protein
TRAF2	TNF receptor-associated factor 2
UPR	Unfolded protein response
UPS	Ubiquitin proteasome system
WAT	White adipose tissue
WT	Wildtype

1. INTRODUCTION

1.1. Obesity and Diabetes

Obesity, which has become an epidemic worldwide, is defined by the World Health Organization (WHO) as a health condition in which the body mass index (BMI) for the adult individuals is greater than 30 kg/m^2[1]. According to WHO estimates, approximately 13% of the world's adult population (over 600 million) is obese. Since obesity is associated with diabetes, cardiovascular diseases, certain types of cancers and hyperlipidemia [2], obese individuals are at a considerable risk.

Diabetes is a metabolic disease in which blood glucose level cannot be maintained in the normal range over a prolonged period. Approximately 500 million adults in 2014 had diabetes, and the prevalence of diabetes among adults worldwide has nearly doubled since 1980 [3]. Type-1 diabetes, known as insulin-dependent or juvenile diabetes, results from the failure of insulin secretion from pancreatic β-cells. Type 2 diabetes, which is characterized by insensitivity to the insulin hormone, accounts for 90-95% of all diabetes cases [3]. The prevelance of type-2 diabetes increases worldwide in parallel to obesity, sedentary lifestyle and urbanization. Despite the need for urgent therapeutic interventions, effective therapeutic approaches for ameliorating or preventing type-2-diabetes have limited success [4]. Current studies aiming anti-obesity drug development, mainly focuses on the pharmacological control of the medio-basal hypothalamic neural circuits, which have regulatory roles on the feeding behaviors, and the restoration of impaired metabolic pathways in peripheral tissues and the liver.

1.1.1. Regulation of Food Intake and Energy Expenditure

Adipose tissues and the central nervous system, mainly the hypothalamus, have pivotal roles in food intake regulation (see Figure 1.1) [5]. Within the arcuate nucleus of the hypothalamus, neuronal populations, which are characterized by the expres-

sion of specific neuropeptides, regulate energy balance [6]. These neurons respond to some hormonal stimuli like leptin, insulin and ghrelin by expressing anorexigenic (e.g. POMC) [7] and orexigenic (e.g. NPY) [8] neuropeptides.

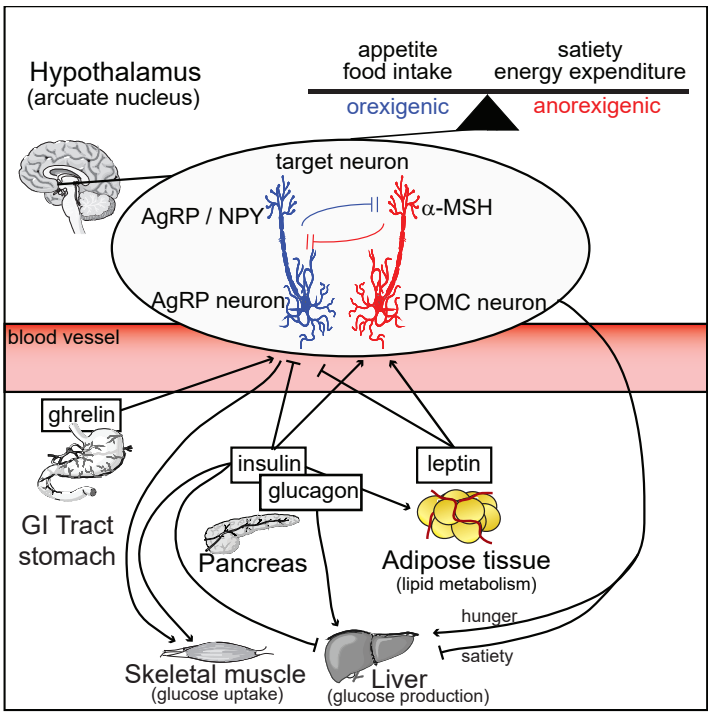

Figure 1.1. Regulation of energy homeostasis.

Leptin, secreted from white adipose tissues, is the key hormone that reduces nutrient uptake and increases energy expenditure through the action on hypothalamic neurons[9]. Leptin stimulates neurons expressing pro-opiomelanocortin (POMC), which is processed into the anorexigenic melanocortin peptides (alpha, beta, and gamma MSH) [10]. After the discovery of this anti-obesity feature, it is thought to be useful as a therapeutic agent in the treatment of obesity. Indeed, recombinant leptin therapy has been particularly successful in leptin-deficient patients [11]. However, circulating blood leptin levels were found to be high in most obese individuals and diet-induced rodent models [12, 13]. This insensitivity to elevated leptin levels has led to the idea that "leptin resistance" and conseqently impairment in leptin sinaling is one of the important factors in the pathological development of obesity and obesity-related diseases.

Insulin, which is secreted by pancreatic β-cells in response to elevated blood glucose level, controls glucose uptake and production in insulin-sensitive tissues such as skeletal muscle, adipose tissue and the liver. It also exerts an anorexigenic action through inhibiting AgRP (agouti-related peptide) [14] and activating POMC [15] neurons. Impaired insulin sensitivity is the hallmark and primary cause of type 2 diabetes.

1.1.2. Molecular Background

Elevated free fatty acid [16, 17], cellular inflammation [18, 19], endoplasmic reticulum (ER) stress [20, 21] and defective autophagy [22, 23, 24] are the main factors in the aetiology and pathogenesis of obesity related metabolic diseases. Insulin resistance following increased adipocity is the common pathological condition in type 2 diabetes.

Adipose tissue has been considered as an active endocrine organ since the discovery of secreting leptin and several cytokines including tumour necrosis factor-α (TNF-α), IL-1β [25], adiponektin [26] and resistin [27]. These cytokines, known as adipokines have been implicated in the development of insulin resistance and type-2-diabetes [28, 29]. It has been shown in various mouse models that inflammatory pathways, such as the nuclear factor κB (NF-κB) pathway, become active within a few days after a high fat diet [17, 30]. Increased expression of proinflammatory cytokines, like TNF-α and interleukin-6 (IL-6), have inhibitory actions on insulin signaling [31]. Inhibitor of kB kinase (IKKb), an upstream kinase of NF-κB, phosphorylates and inhibits IRS1, which is an effector of insulin signaling [32]. Inhibition of inflammation can result in improvements in insulin sensitivity in adipose tissue [31, 33]. Improvements in leptin sensitivity have also been observed in AgRP neurons upon genetic and pharmacological inhibition of the NF-κB pathway [34].

Leptin and insulin regulate food intake through modulating the JAK2/STAT3 and AKT/FOXO pathways, respectively, in leptin/insulin-receptor expressing hypothalamic neurons [35, 36, 37]. STAT3 and FOXO transcription factors have opposing roles on the transcriptional activity of POMC and AgRP genes. During the fasting state,

FOXO transcription factors positiveley and negatively regulate the AgRP and POMC gene expression, respectively. Upon leptin delivery, orexigenic effect of FOXO is reversed by STAT3 occupancy on their promoter regions resulting in increased POMC and decreased AgRP mRNA expression [38]. Studies show that *Foxo1* deletion in AgRP and POMC neurons leads to anorexigenic efffects in mice [39, 40]. SOCS3 and PTP1B, negative regulators of leptin signaling, mRNA levels have been demonstrated to be increased in obese mice [41].

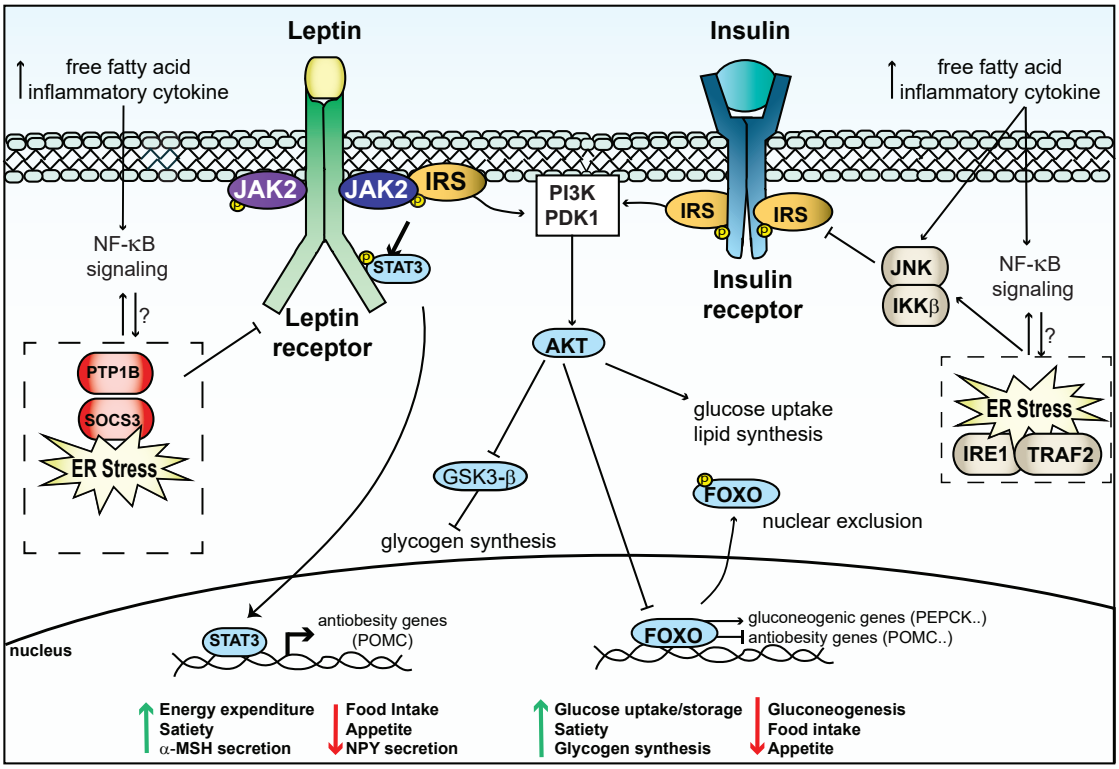

Figure 1.2. Molecular mechanisms of leptin and insulin resistance.

Hyperinsulinemia, which is a characteristic of type-2 diabetes [42] and a response to compensate insufficient insulin action against increased blood glucose level, is thought to be one of the primary contributors to the development of insulin resistance [43]. Increased fat deposits in the body can cause free fatty acids (FFA) to be released from the adipocytes into the plasma. Elevated blood FFA acid level leads to various pathological conditions, such as inflammation and ER stress, in peripheral tissues and the hypothalamus [44, 45, 46]. Free fatty acid is known to inhibit insulin signaling through modulating protein kinases (e.g. JNK and PKC) [47] and lead to development

of insulin resistance [48]. FFA also activates NF-κB pathway by toll-like receptor 4 (TLR4) [49]. The mechanism of FFA-mediated insulin resistance and inflammation remains unclear.

In the last decade, perturbation of biological processes in the endoplasmic reticulum and related response mechanisms have been linked to the development of obesity-induced leptin/insulin resistance and type 2 diabetes [20].

1.2. Endoplasmic Reticulum (ER) Stress

The endoplasmic reticulum (ER) is a subcellular organelle where newly synthesized secretory and transmembrane proteins are folded into their native form with the help of lumenal chaperones and foldases before they are transported to the Golgi apparatus. Under certain conditions, as in the case of an imbalance between the protein folding load and the ER folding capacity, proteins can fail to fold into their correct formation. Disturbances in the ER function leads to accumulation and aggregation of unfolded or misfolded proteins in the ER lumen, a cellular condition termed 'ER stress'.

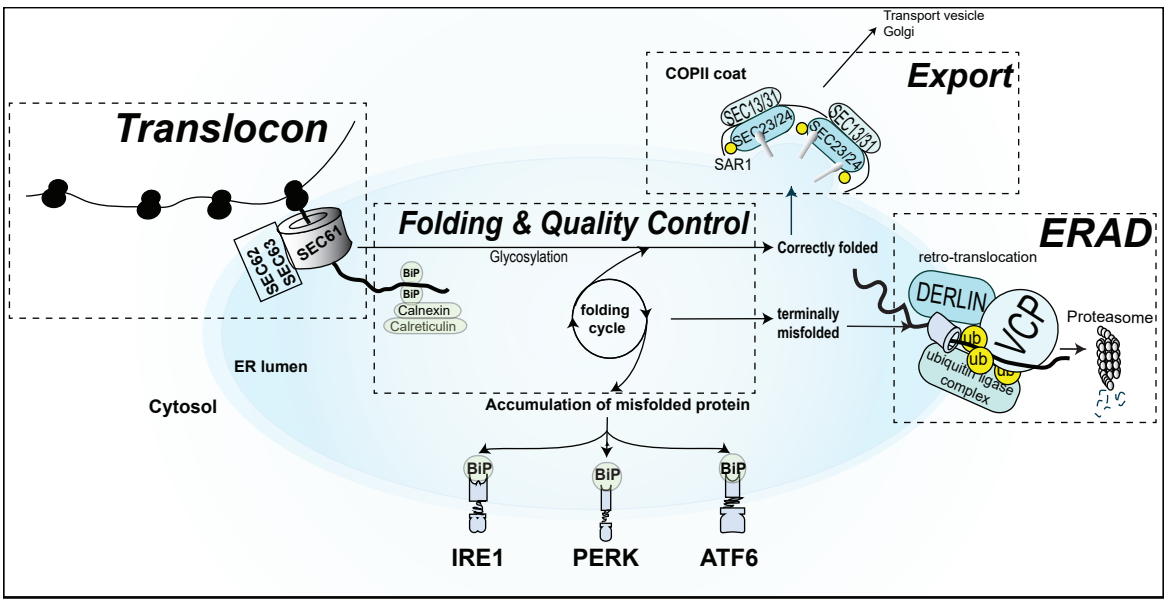

Figure 1.3. Molecular functions of the ER.

1.2.1. Unfolded Protein Response (UPR)

Different physiological perturbations including insufficient folding capacity of ER, alteration in calcium level, diminished protein glycosylation caused by glucose deprivation, impaired redox balance and genetic mutation can cause ER stress. The eukaryotic cells have evolved an adaptive mechanism called 'unfolded protein response(UPR)' [50] to restore ER homeostasis.

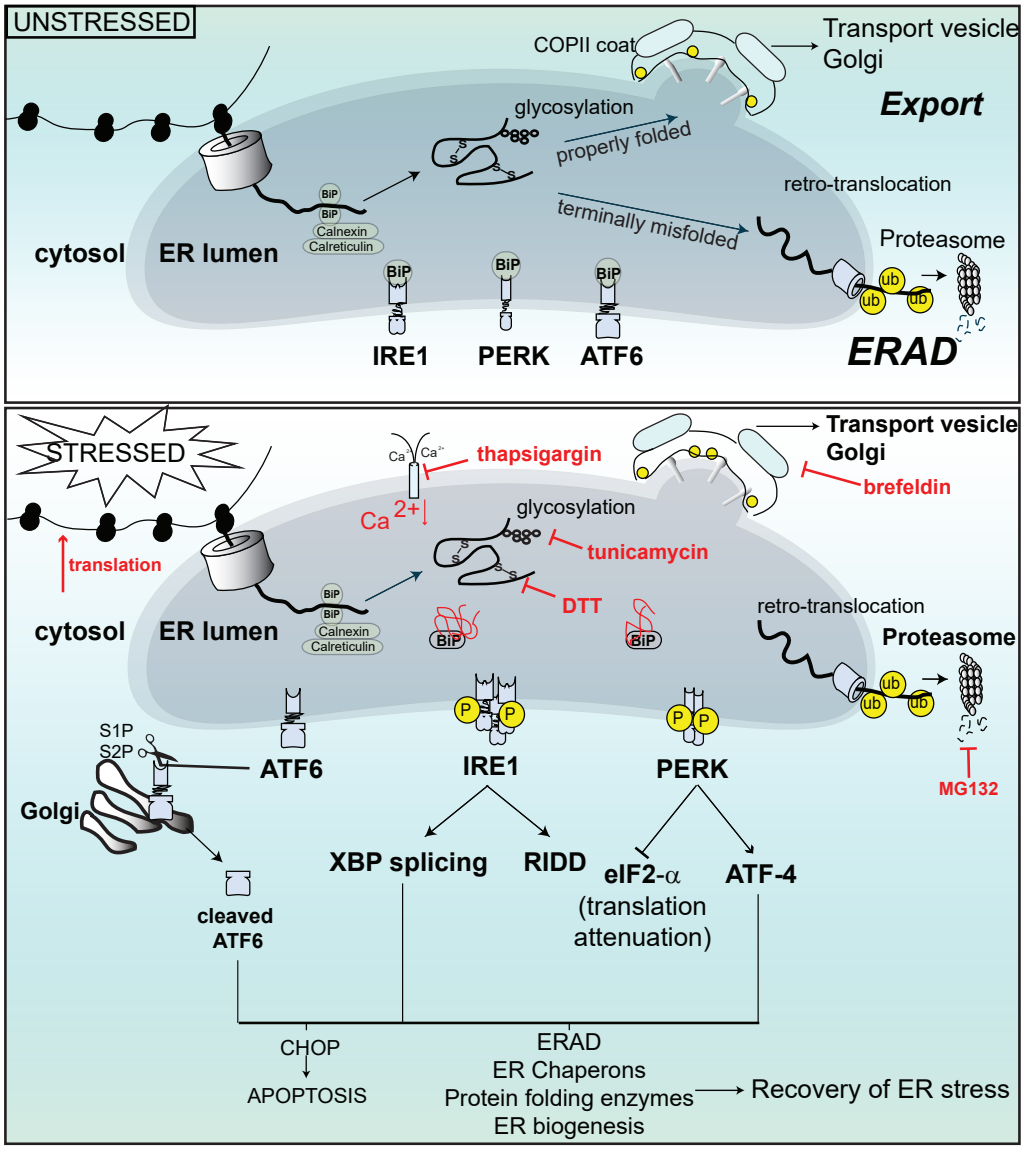

Figure 1.4. UPR sensors and ER stress signaling pathways.

The UPR alleviates the accumulation of misfolded proteins by increasing the ER folding capacity through upregulating the expression of folding-related proteins [51], reducing the ER protein load by attenuation of protein synthesis [52] and promoting the degradation of misfolded proteins through ubiquitin-proteosome system (UPS) [53, 54] and autophagy [55, 56]. If the ER homeostasis is not restored, cells can undergo apoptotic cell death [57, 58] which is also triggered by the UPR system.

UPR system comprises integrated signaling pathways activated by three classes of ER-localized transmembrane sensors including IRE1 (inositol-requiring transmembrane kinase/endonuclease 1), PERK (PKR-like ER kinase), and ATF6 (activating transcription factor 6) (Figure1.4). Under unstressed conditions these transmembrane proteins are in inactive state maintained by the binding of the ER chaperone BiP (immunoglobulin heavy chain binding protein) to their lumenal domains [59]. ER stress causes binding of BiP to unfolded proteins and its dissociation from the sensor proteins. Subsequently this dissociation leads to the activation of IRE1, PERK and ATF6 [59]. Recent studies also suggest that unfolded protein binding to sensor proteins can also activate the UPR [60, 61, 62].

1.2.2. IRE1

IRE1 signaling is the most conserved branch of the UPR among the eukaryotes. IRE1 has a lumenal amino-terminal domain, a transmembrane region, and a cytosolic carboxy-terminal domains having kinase and endoribonuclease activities. Upon ER stress and BiP dissociation, IRE1 dimerizes and trans-autophosphorylates. Trans-autophosphorylation of the kinase domain activates IRE1 endoribonucleolytic activity [63]. The active endoribonuclease domain of IRE1 splices precursor XBP1 (X-box binding protein 1) mRNA by removal of intervening fragment [64, 65]. This unconventional splicing of XBP-1 mRNA generates a spliced form (known as sXBP1) encoding an active transcription factor, which regulates UPR target genes including ER chaperones and components of ERAD machinery [65, 66]. The RNase activity of IRE1 also functions in the degradation of ER localized mRNAs (e.g. insulin, scara3), which is known

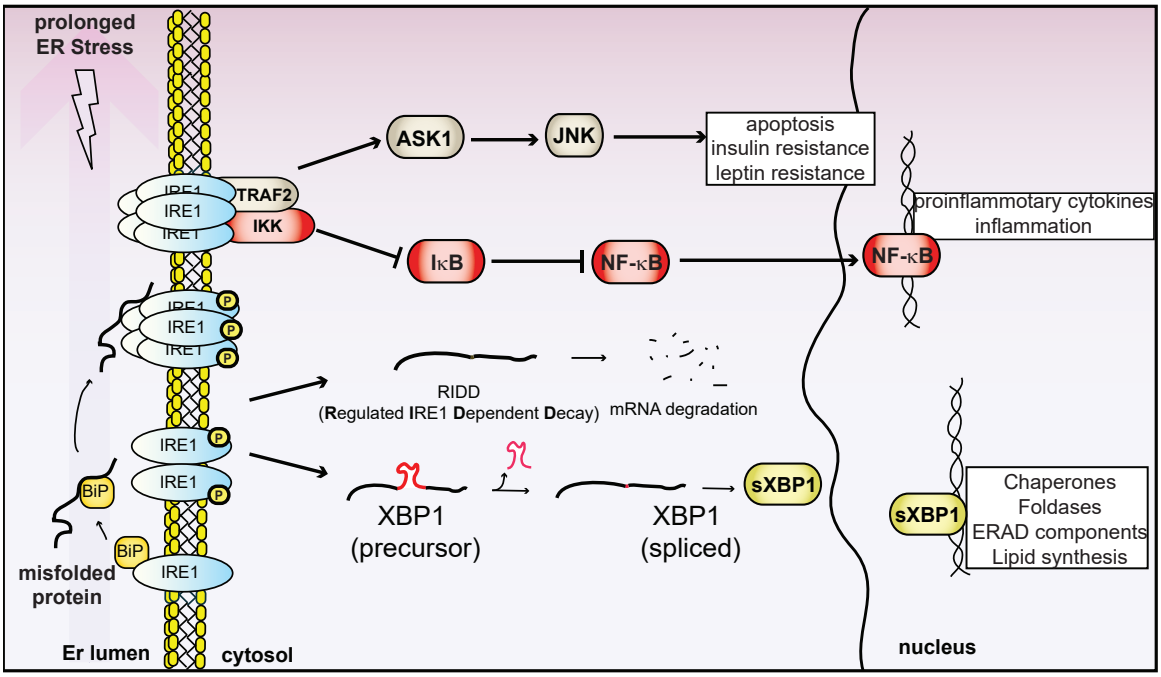

Figure 1.5. IRE1 signaling.

as RIDD (Regulated IRE1-dependent mRNA decay) [67]. In this way, RIDD reduces the ER protein load through decreasing the number of nascent proteins entering the ER.

IRE1 can regulate apoptosis and autophagy through interaction with TRAF2 (TNF-receptor-associated factor 2 factor 2). Recruitment of TRAF2 to IRE1 promotes activation of ASK1 (Apoptosis signal-regulating kinase1) and the JNK pathway [68, 69], which triggers the apoptotic events [70]. IRE1 can regulate the autophagic activity under ER stress [71] through JNK-mediated activation of the autophagy-related gene Beclin1 [72]. Beclin1 mRNA level is also regulated transcriptionally by spliced XBP1 [73].

1.2.3. PERK

Upon ER stress, PERK similar to IRE1 dimerizes and transautophosphorylates. Activated PERK phosphorylates the alpha subunit of eukaryotic initiation factor 2 [52], which causes translational attenuation and reduction in the protein-folding load of the

ER by decreasing the rate of initiation of mRNA translation. Inhibitory effect of PERK on translation machinery seems to be global. However, PERK can selectively increase translation of activating transcription Factor 4 (ATF4), resulting in the upregulation of its target genes [74]. ATF4 translation is repressed under unstressed condition by the presence of two upstream open reading frames (uORFs). Upon ER stress, limited availability of active eIF2α leads to ribosome skipping of inhibitory uORF in the 5'UTR upstream of the ATF4 mRNA[75]. ATF4 induces the expression of the CHOP transcription factor as well as genes involved in ER function. CHOP mediates the apoptotic response to ER stress [76] by down-regulating anti-apoptotic protein BCL2 [77].

1.2.4. ATF6

Following ER stress, ATF6 translocates from the ER to the Golgi apparatus, where it is processed to its active form through sequential cleavage by the serine site 1 (S1P) and site 2 (S2P) proteases [78]. This processed cytosolic 50-kD DNA-binding domain (named as ATF6f) of ATF6 is released to the cytosol and subsequently it penetrates into the nucleus and regulates UPR-related genes such as BiP and CHOP [79].

1.2.5. Endoplasmic Reticulum-Associated Degradation (ERAD) and Cellular Proestasis

Inefficient folding capacity of the ER or conditions disrupting proper folding of ER resident proteins, promote oligomerization and aggregation of misfolded proteins in the ER lumen. In order to prevent the formation of toxic aggregates, terminally misfolded proteins are directed to the ER-associated protein degradation (ERAD) pathway. Terminally misfolded proteins are retro-translocated from the ER lumen to the cytosol where they are degraded by the ubuquitin-proteasome system [54] or autophagy [55, 56]. When the protein degradation pathways fail or are insufficient, misfolded protein aggregates are delivered to the microtubule orginizing center (MTOC) where they

are surrounded by the intermediate filament protein of vimentin [80]. These cage-like structures, named aggresome, alleviate the proteotoxicity of protein aggregates in the cytosol and serve as holding station for the clearance of misfolded proteins [81] (See Figure1.6). ER stress-induced autophagy is thought to be a compensatory response

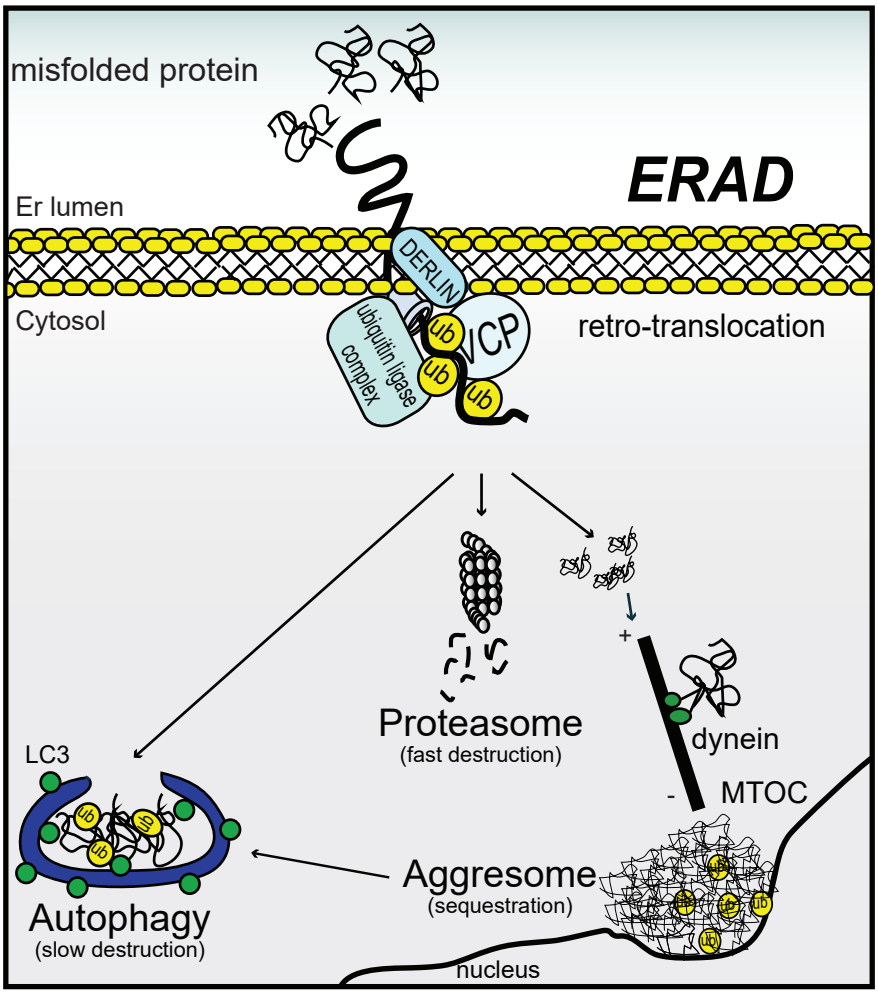

Figure 1.6. The ERAD pathway.

when unfolded proteins can not be eradicated by the UPS. The three UPR branches regulate autophagy during ER stress in different molecular paths on both protein and transcriptional levels. These paths are mainly AKT-MTOR signaling [82], AMPK signaling [83], and transcriptional regulation of autophagy-related genes [84, 85]. Negative regulation of autophagy by the UPR has also been reported in some pathological conditions in neuronal context. Pharmacological induction of ER stress causes inhibition in autophagic activity through the IRE1/TRAF pathway resulting accumulation

of the mutant huntingtin protein [86]. XBP1 interacts with the FOXO1 transcription factor, which regulates the expression of autophagy-related genes, subsequently leads to its proteasomal degradation [87]. In a study investigating the cross-talk between ER stress and autophagy in the context of metabolic diseases, decreased autophagic activity has been observed in obese mice, and the autophagic recovery led to improvements in insulin resistance [22]. Besides, in the same study, suppressed autophagic activity in non-obese mice was shown to induce ER stress and insulin resistance.

1.2.6. ER stress and Metabolic Pathways

Chronic ER stress in obesity is thought to be induced by increased demand for protein synthesis, specifically insulin to decrease blood glucose level, increased lipid synthesis for fat storage and elevated free-fatty acid levels caused by leakage from adipocytes exceeding fat storage capacity.

Involvement of ER stress in metabolic pathways has been shown in various studies. Suppression of ER stress has been reported to improve insulin sensitivity [88, 89, 90]. RNAi-mediated know-down of IRE1 in the liver results in reduced gluconeogenesis and increased glucose tolerance in diabetic mice [91]. Insufficient XBP1 activity also leads to the development of insulin resistance upon high fat feeding in mice [20]. Besides, ectopically over-expression of XBP1 in the liver of diabetic mice restores insulin sensitivity [87]. It has been observed that tunicamycin, a chemical agent that induces ER stress, causes hepatic lipid accumulation [92]. Furthermore, administration of chemical chaperones reducing ER stress restores glucose homeostasis and insulin sensitivity in type-2-diabetic (ob/ob) mice [93] and partially in humans [94].

Impaired ER function inhibits leptin signaling and contributes to development of leptin resistance in the hypothalamus [95]. Pharmacologically-induced ER stress causes leptin resistance and increased food intake in mice [96]. 4-phenyl butyric acid (4-PBA) and tauroursodeoxycholic acid (TUDCA), well-known chemical chaperones,

can reduce ER stress and alleviate leptin resistance [95]. ER stress also induces insulin resistance in the brain along with leptin resistance [97].

1.2.7. ER Stress and Inflammation

IRE1-TRAF2 complex can initiate an inflammatory response through the activation of the IKK-NF-κB [98] and JNK/AP-1 [99] pathways, which up-regulate the expression of pro-inflammatory cytokines (e.g. IL1β, TNF-α) [68, 100, 101]. Supressing inflammation gives some beneficial metabolic effects in diet-induced obese mice [102, 103]. The NF-κB pathway can also be activated through PERK and ATF-6 branches [104, 105]. It has also been reported in several studies that inflammation triggers ER stress by inflammatory cytokines such as TNF-α [106].

1.3. Salt-Inducible Kinase Family

Salt-inducible kinases (SIKs), are serine/threonine kinases belonging to the AMP-activated protein kinase family. SIKs have important cellular functions in energy homeostasis, including the regulation of glucose and fat metabolism in the liver [107] and adipose tissue[108, 109, 110]. SIK family is composed of three identified members (SIK1-3). SIK1 was firstly identified in myocardial cells of the developing mouse heart (named as *msk*, myocardial SNF1-like kinase) [111] and then cloned from the adrenocortical tissues of high-salt diet–fed rats (renamed as SIK, Salt-inducible kinase) [112]. Based on the cDNA sequence of *Sik*, two isoforms (SIK2 and SIK3, previous isoform renamed as SIK1) were identified from human and mouse genome database search [113].

1.3.1. SIK2

SIK2, firstly identified in mouse adipose tissue, was found to be induced during the preadipocyte-adipocyte differentiation in 3T3-L1 cells and white adipose tissue (WAT) of *db/db* diabetic mice [114]. In the same study, SIK2 phosphorylates insulin

receptor substrate-1 (IRS1), an important regulator of insulin signaling, at the Ser-789 residue which has an inhibitory effect on insulin pathway and been elevated in insulin-resistant animals [115]. This finding proposed that SIK2 might have a role in the development of insulin resistance and type 2 diabetes.

In response to stress and hormonal stimuli, SIK2 suppresses lipid and glucose synthesis in adipocytes and hepatocytes [116, 110]. SIK2 has been found to inhibit CRTC2 (TORC2) activity, which is a regulator of gluconeogenesis, through its phosphorylation and nuclear exlusion in HEK-293T cells [117]. Later, it has been demonstrated that insulin decreases gluconeogenic gene expression during re-feeding through SIK2-mediated CRTC2 phospho-inhibition in mouse liver and primary hepatocytes [118]. In the same study, RNA-mediated knock-down of SIK2 induces CRTC2 activity and gluconeogenic gene expression (e.g. *Pepck* and *G6Pase*). It has been shown that SIK2 decreases hepatic lipogenesis through inhibitory phosphorylation on p300 [116]. p300, an acetyl transferase, can activate carbohydrate-responsive element-binding protein (ChREBP) which is a master regulator of fatty acid synthesis and lipogenic genes (e.g. *Fasn* and *Acc*) [116]. In the same study, decreased SIK2 activity has also been observed in livers of *ob/ob* and high-fat diet-fed mice. SIK2 is tought to be required for glucose uptake in rodent adipocytes through the regulation of GLUT4 expression by the phosphorylation of histone deacetylase 4 (HDAC4) [109, 110]. Recently, it has been shown that SIK2 regulates insulin secretion in the MIN6 pancreatic β-cells through phosphorylation of CDK5R1/p35 [119].

1.3.2. SIK2 and Protein Degradation Pathway

Previously, in our lab by using GPS2.1 program [120] ERAD components were scanned for SIK2 phosphorylation motif and p97/VCP (p97/Valosin-containing Protein), which is an ATPase playing a key role in ERAD pathway by extracting misfolded proteins from the ER lumen for the proteoasomal degradation [121], was found to be a putative phosphorylation target for SIK2 [122]. This phosphorylation site has been later reported to be important for the VCP ATPase activity and degradation of ERAD

substrates [123]. In a recent study, SIK2 has also been found to participate in the autophagic process [124].

1.4. Insulin Receptor Substrates(IRS) and IRS4

The Insulin receptor substrates (IRSs) play key roles in both insulin and leptin signaling. Insulin binding to the insulin receptor (IR), causes the recruitment and phosphorylation of IRS proteins on their tyrosine residues [125]. Apart from insulin, leptin and some other cytokines, like interleukins, can cause IRS phosphorylation [126, 127]. Each IRS proteins possesses an NH2-terminal pleckstrin homology (PH) domain, a phosphotyrosine binding domain (PTB) domain, and a carboxy-terminal region. The carboxy-terminal region contains potential tyrosine phosphorylation sites acting in transducing insulin action through binding to the src Homology 2 (SH2)-containing downstream effector proteins including phosphatidylinositol 3-kinase (PI3K) [128]. This interaction leads to activation of the protein kinase B (Akt) molecule [128], which is required for the stimulation of the cellular effects of insulin [129]. There are four known members of the IRS family (1 to 4). Several studies have previously shown the importance of the IRS proteins in the development of insulin resistance [32, 130]. A double-knockout experiment indicates that activation of the Foxo1 transcription factor has been observed in the liver of mice lacking both IRS1 and IRS2 resulting the development of hyperinsulinemia and insulin resistance [131]. IRS2 deletion in the hypothalamus of mice leads to hyperglycemia and obesity [132]. However, deletion of IRS3 or IRS4 has not caused any detectable phenotypic defect [133, 134]. On the other hand, IRS4 along with IRS3 have been suggested to act as a negative regulators in IGF signaling through supressing the IRS1 and IRS2 function in embryonic fibroblast cells [135]. It has been shown that IRS4 is not required for adipocyte differentiation but have a compensatory role in impaired differentiation process in IRS1-KO cells [136]. IRS1 and IRS2 are ubiqitously expressed throughout the rat forebrain, whereas IRS4 is restricted to the hypothalamus, specifically the ventral hypothalamus and arcuate nucleus [137]. The negative regulatory proteins in leptin signaling cytokine signal repressors (SOCS) SOCS2, SOCS6, and SOCS7 proteins, and the leptin receptor have

been identified as IRS4 interaction partners in N38 hypothalamic cells [138].

1.5. CHIP E3 ligase

The carboxyl-terminus of Hsc70 interacting protein (CHIP), which is a chaperone associated E3 ligase, has been identified in an interaction screen as a Hsc/p70 interacting protein [139]. CHIP mediates ubiqutination and degradation of mis/unfolded proteins along with the Hsc70/Hsp40 chaperone system [140, 141, 142]. CHIP participates in the ER quality control by functioning in the degradation of various ERAD substrates including the cystic-fibrosis transmembrane-conductance regulator (CFTR) [143]. Apart from its role in proteasomal degradation, recently it has been shown that CHIP regulates the IRE1/TRAF2/JNK pathway under ER stress through ubiquitination of IRE1 [144].

CHIP has been recently revealed to suppress adipocyte differentiation through proteasomal degdatation of PPARγ, which is a master regulator of adipogenesis [145]. Overexpression of CHIP in MCF7 and MCF10A cells results in AKT-mediated inhibition of the Forkhead box O (FoxO) transcription factors FoxO1, FoxO3, and FoxO4, which transcriptonally regulates apoptotic proteins and metabolic enzymes [146].

CHIP negatively regulates NF-KB signaling in MCF7 and HCT-116 cells through degradation of TRAF2 [147] and p65 [148], respectively. CHIP also together with Hsp70 inhibits TNF-alpha induced apoptosis in HeLa cells by promoting proteasomal degradation of ASK1 (apoptosis signal-regulating kinase 1) [149].

CHIP plays roles in the regulation of autophagic flux and aggresome formation. Knockdown of CHIP induces autophagosome formation through the AKT/mTOR pathway [150]. CHIP mediates the ubiquitination and the binding of the misfolded proteins to histone deacetylase 6 (HDAC6), which subsequently promotes dynein-dependent sequestration of misfolded proteins to the MTOC [151].

2. PURPOSE

In eukaryotic cells, secretory and transmembrane proteins are processed by folding machinery in the ER lumen for their correct conformation. Accumulation of unfolded/misfolded proteins in the ER lumen causes ER stress, which activates cellular responses to restore the protein homeostasis. Prolonged ER stress may turn physiological responses into pathological outcomes such as fat accumulation, insulin resistance and apoptotic cell death. Chronic ER stress, dysregulation of insulin/leptin signaling are common metabolic outcomes observed in obesity and type 2 diabetes. However, the role of ER stress and its regulators in the pathogenesis of metabolic diseases are not fully understood. SIK2 is a key regulatory kinase having roles in metabolic pathways, autophagy and the ERAD pathway. The involvement of SIK2 in these biological processes led us strongly to investigate its possible roles in the unfolded protein response.

In this study, the first goal was to identify potential ER-localized SIK2 substrates by isolating ER fraction of 293T cells expressing the wildtype and kinase inactive forms of SIK2 under ER stress condition, followed by analysis of phospho-proteome profile. As a continuation of the study, next objective was to perform functional assays examining effects of the candidate proteins, obtained from phospho-proteomic analysis, on the UPR.

Overall, throughout the work, it was aimed to elducidate the possible roles of SIK2 in the ER stress response by identifying its potential ER-resident substrates and examining the effects of these candidate proteins on the UPR, mainly IRE1/XBP1 signaling and the ERAD pathway.

3. MATERIALS

3.1. General Kits, Enzymes and Reagents

Table 3.1. List of kits, enzymes and reagents.

Name	**Supplier**
BCA Protein Assay Kit	Thermo, USA
Complete EDTA free PI (Protease Inhibitor) cocktail	Roche, Switzerland
Dulbecco's Modified Eagle Medium (DMEM)	Gibco, USA
DNA Molecular Weight Marker GeneRuler 1 kb DNA Ladder	Thermo, USA
Fetal Bovine Serum (FBS)	Gibco, USA
Genopure Plasmid Midi Kit	Roche, Switzerland
High Pure Plasmid Isolation Kit	Roche, Switzerland
ImProm-II Reverse Transcription System	Promega, USA
MinElute Gel Extraction Kit	Qiagen, Germany
Penicillin/Streptomycin (10X)	Hyclone, USA
Phusion High-Fidelity DNA Polymerase	NEB, USA
Protein Molecular Weight Marker	Thermo, USA
Restriction Endonucleases	Thermo, USA
T4 DNA Ligase	NEB, USA
Taq DNA polymerase	Thermo, USA
Trypsin-EDTA (0.5 mM EDTA,0.025% Trypsin)	Hyclone, USA
Turbofect Transfection Reagent	Thermo, USA
Western Blotting Luminol Reagent Super Signal West Femto Maximum Sensitivity Kit	Thermo, USA

3.2. Chemicals

Table 3.2. Chemicals used in this study.

Name	**Supplier**
Acetic Acid	Merck, USA
Acrylamide	AppliChem, Germany
Agar	Conda, Spain
Agarose E	Conda, Spain
Ammonium Persulfate (APS)	Sigma-Aldrich, USA
Ampicillin	Roche, Switzerland
B-Mercaptoethanol	Merck, USA
Boric Acid	Sigma-Aldrich, USA
Bovine Serum Albumin (BSA)	AppliChem, Germany
Bromophenol Blue	Fluka, USA
Calcium chloride dehydrate	AppliChem, Germany
D-Glucose	Sigma-Aldrich, USA
DMSO	Sigma-Aldrich, USA
EDTA	AppliChem, Germany
Epoxomicin	ApexBio, Taiwan
Ethanol	Emsure, Germany
Ethidium Bromide	Sigma-Aldrich, USA
Glycerol	Sigma-Aldrich, USA
Glycine	Applichem, Germany
HEPES	Sigma-Aldrich, USA
Isopropanol	Emsure, Germany
Kanamycin	Fluka, USA
Magnesium Chloride	Sigma-Aldrich, USA
Methanol	Emsure, Germany
N, N, N', N'-tetramethylethylenediamine (TEMED)	AppliChem, Germany
N,N'-Methylenebisacrylamide	Sigma-Aldrich, USA

Table 3.2. Chemicals used in this study (cont.).

Name	**Supplier**
NP-40	AppliChem, Germany
Paraformaldehyde	Sigma-Aldrich, USA
Phosphate Saline Buffer (PBS)	Gibco, UK
Sodium Chloride (NaCl)	Fisher Scientific, USA
Sodium Deoxycholate	Sigma-Aldrich, USA
Sodium Dodecyl Sulfate (SDS)	AppliChem, Germany
Sodium Fluoride	Merck, USA
Sodium Hydroxide	Sigma-Aldrich, USA
Tris-Base	AppliChem, Germany
Tris-Cl	AppliChem, Germany
Triton X-100	AppliChem, Germany
Tryptone	Sigma-Aldrich, USA
Tween 20	Sigma-Aldrich, USA
Yeast Extract	Conda, Spain
EZMix Tryptone	Sigma-Aldrich, USA
Thapsigargin	Santa-Cruz, USA
VR23	Selleckchem, USA

3.3. Biological Materials

3.3.1. Bacterial Strains

E. coli TOP10 bacterial strain (genotype: F- mcrA Δ(mrr-hsdRMS-mcrBC) φ80lacZΔM15 ΔlacX74 recA1 araD139 Δ(araleu) 7697 galU galK rpsL (StrR) endA1 nupG) was used for cloning and plasmid isolation purposes.

3.3.2. Mammalian Cell Lines

Human embryonic kidney cell line HEK293T was purchased from ABMGood (British Columbia, Canada).

3.4. Buffers and Solutions

3.4.1. Bacterial Culture Solutions and Antibiotics

Table 3.3. Solutions and antibiotics used in bacterial cultures.

Solution/Buffer	**Content**
Luria-Bertani medium (LB)	10 g Tryptophan 5g Yeast Extract 10g NaCl Distilled water up to 1 L, autoclaved
LB Agar	10g Tryptophan 5g Yeast Extract 10g NaCl 15g Agar Distilled water up to 1 L, autoclaved
Ampicillin stock	100 mg/ml in 70% Ethanol Sterilized by filtration and stored at -20°C 100 μg/ml (working concentration)
Kanamycin stock	50mg/ml in distilled water Sterilized by filtration and stored at -20°C 50μg/ml (working concentration)

3.4.2. DNA Gel Electrophoresis

Table 3.4. DNA Gel Electrophoresis buffers and solutions.

Solution/Buffer	**Content**
50X Tris-Acetic acid EDTA (TAE)	242 g Tris base 18.61 g EDTA 57.1 ml Glacial Acetic Acid distilled water upto 1L
TE Buffer	10mM Tris–HCl 1mM EDTA, pH 8.0
Ethidium bromide (EtBr)	10mg/ml (stock solution) 0.5µg/ml (working solution)
6X DNA Gel Loading Buffer	10 mM Tris-HCl (pH 7.6) 0.03% Bromophenol blue 60% Glycerol 60 mM EDTA
10X Orange G DNA Loading Buffer	0.5% Orange G 50% Glycerol

3.4.3. Endoplasmic Reticulum Isolation Solutions

Table 3.5. Buffers and solutions used in ER isolation.

Solution/Buffer	**Content**
ER Isolation Buffer	10 mM HEPES (pH: 7.8) 250 mM sucrose 25 mM KCl 1 mM EGTA 1X Protease Inhibitor Cocktail 1X Phosphatase Inhibitor Cocktail

Table 3.5. Buffers and solutions used in ER isolation (cont.).

Solution/Buffer	**Content**
Protein Extraction Buffer	7 M Urea
	2 M Thiourea
	CHAPS (2%, w/v)
	50 mM DTT
	1X Protease Inhibitor Cocktail
	1X Phosphatase Inhibitor Cocktail

3.4.4. Cell Lysis Buffers

Table 3.6. Buffers used in cell lysis and immunoprecipitation.

Solution/Buffer	**Content**
NP-40 Cell Lysis Buffer	150 mM NaCl
	50 mM Tris-Cl pH 7.4
	2 mM EDTA
	1% NP-40
	0.5% Sodium deoxycholate
	5 mM NaF
	1mM Sodium othovanadate (Na_3VO_4)
	1X Protease Inhibitor Cocktail
IP Lysis Buffer	145 mM NaCl
	20mM Tris-HCl (pH 8.0)
	2mM EDTA
	0.2% NP40
	1X Protease inhibitor cocktail
	1X Phosphatase inhibitor cocktail

3.4.5. Western Blotting Buffer and Solutions

Table 3.7. Buffers and solutions used in PAGE and Western Blotting.

Solution/Buffer	**Content**
10X SDS Running Buffer	30.3 g Tris base 144 g Glycine 10 g SDS distilled water upto 1 L
10X Transfer Buffer	30.3 g Tris base 144 g Glycine distilled water upto 1 L
1X Transfer Buffer	100 ml 10X Transfer Buffer 200 ml Methanol 700 ml distilled water
1X Tris Buffered Saline with Tween-20 (TBS-T)	20 ml Tris.Cl (1M, pH 7.4) 37.5 ml NaCl (4M) 10 ml Tween-20 (10%) distilled water upto 1 L
Western Blot Blocking Solution	5% non-fat milk powder in 1X TBS-T or 3% BSA in 1X TBS-T
5X SDS-PAGE Loading Dye	200 mM Tris-Cl pH 6.8 10% SDS 50% Glycerol 25% β-mercaptoethanol 0.01% Bromophenol Blue
Stripping Solution	6.25 mL Tris-HCl (1M, pH 6.8) 20ml SDS (10%) 0.8 ml β-mercaptoethanol distilled water upto 100 ml

3.5. Nucleic Acids

3.5.1. Plasmids

Table 3.8. Plasmids used in this study.

Construct	**Origin**	**Vector backbone**
Empty pcDNA4-HisC	Invitrogen, USA	
Empty sYFP-N1	This Study	pSYFP-N1
mCherry2-N1	Addgene #54517	
pCMV-3Tag-6	Agilent #240200	
HIS-SIK2-WT	(Kuser, 2011)[152]	pcDNA4-HisC
HIS-SIK2-KI	(Kuser, 2011)[152]	pcDNA4-HisC
FLAG-SIK2-WT	This study	pCMV-3xFLAG-7.1
pcDNA3-IRE1	Addgene #13009	pcDNA3
HIS-IRE1	This study	pcDNA4-HisC
FLAG-IRE1	This study	pCMV-3xFLAG-7.1
FLAG-IRS4	University of Dundee, MRC-PPU Reagents #DU36186	pcDNA5-FRT-TO-FLAG
IRS4-mCherry	This study	mCherry2-N1
IRS4-sYFP	This study	pSYFP-N1
XBP1-eYFP	This study	pEYFP-N2
CD3δ-GFP	This study	pEGFP-N2
FLAG-IRS4-ΔPH	This study	pCMV-3Tag-6
FLAG-IRS4-ΔPH-PTB	This study	pCMV-3Tag-6
FLAG-IRS4-ΔPH-PTB-Gly	This study	pCMV-3Tag-6
FLAG-IRS4-ΔC	This study	pCMV-3Tag-6

Table 3.8. Plasmids used in this study (cont.).

Construct	**Origin**	**Vector backbone**
FLAG-CHIP	This study	pCMV-3xFLAG-7.1
FLAG-CHIP-ΔN	This study	pCMV-3xFLAG-7.1

3.5.2. Oligonucleotides

Primers used in polymerase chain reactions, sequencing and cloning were purchased from Macrogen Inc. (Seoul, South Korea). Primers that were used in this study are tabulated in Table 3.9.

Table 3.9. Primers used in this study.

Primer ID	**Sequence (5'-3')**	**Application**	***RE sites**
CD3d_1F	GCCAAGCTTATGGAACATAGCACGTTTCTCTCTG	cloning	HindIII
CD3d_2R	AGGGCCCCTTGTTCCGAGCCCAGTTTC	cloning	ApaI
IRE1_1F	AAAAGAATTCATGCCGGCCCGGCGGCTGCT	cloning	EcoRI
IRE1_2R	AAACTCGAGGAGGGCGTCTGGAGTCACT	cloning	XhoI
IRE1_3F	AAAAAGCTTATGCCGGCCCGGCGGCTGCT	cloning	HindIII
IRS4_1Fcl	AAAAAGCTTATGGCGAGTTGCTCCTTCAC	cloning	HindIII
IRS4_2Rcl	AGGGCCCCCCGACCTCTTTTGGGAGAGT	cloning	ApaI
IRS4_3F_del_PH	AAAAAGCTTATGCCCTTCTATAAAGATGTGTGG	cloning	HindIII
IRS4_4F_del_PH_PTB	AAAAAGCTTATGTACAGAGCCCGCTGCCGCAGC	cloning	HindIII
IRS4_5F_del_gly	AAAAAGCTTATGGAAGATTCAAGAGGGTACATG	cloning	HindIII
IRS4_6R_delC	AGGGCCCCGTACCCTCTTGAATCTTCA	cloning	ApaI
SIK2_1Fcl	AAAAGATCTGGGCCCAGCATGGTCATGGCGGAT	cloning	BglII-ApaI
SIK2_2Rcl	AAAGTCGACTCGAGCTAATTCACCAGGACATACC	cloning	XhoI-SalI
SIK2_3Fcl	GAATCTGGCTAGAACCAAAG	cloning	
SIK2_3Rcl	AAACTCGAGATTCACCAGGACATACCCGT	cloning	XhoI
SIK2_4Rcl	CTGCACTTTGTTCAACTCTA	cloning	
SIK2_5F	AAAGCGGCCGCGTCATGGCGGATGGCCCGAGGCAC	cloning	NotI
SIK2_6R	AAAGGGCCCCTAATTCACCAGGACATACCCGT	cloning	ApaI
SIK2_7F	AAAAAGCTTGTCATGGCGGATGGCCCGAGGCAC	cloning	HindIII
SIK2_8Rcl	AAAAAGCTTATTCACCAGGACATACCCGTT	cloning	HindIII
STUB1_1F	AAAAAGCTTATGAAGGGCAAGGAGGAGAAG	cloning	HindIII
STUB1_2R	AAAGGATCCGTAGTCCTCCACCCAGCCATT	cloning	BamHI
STUB1_3F_delN	AAAAAGCTTATGCCGAGCGCGCAGGAGCTC	cloning	HindIII
XBP1_1F_cl	AAAAAGCTTGAGCTATGGGCCTTGTAGTTGAGAAC	cloning	HindIII
XBP1_2R_cl	AGGGCCCTTAAATCTGAAGAGTCAATACCGC	cloning	ApaI

Table 3.9. Primers used in this study (cont.).

Primer ID	**Sequence (5'-3')**	**Application**	***RE sites**
XBP1_forw	TGCTGAGTCCGCAGCAGGTG	RT-PCR	
XBP1_rev	GCTGGCAGGCTCTGGGGAAG	RT-PCR	
YFPreverse	AGCGGCCGCTTACTTGTACAGCTCGTCCAT	sequencing	
cherry_rev	TCGCCCTTGCTCACCATGGT	colony PCR	

F and R in primer ID denote forward and reverse primer respectively.

*RE sites: Restriction enzyme cutting site

3.6. Antibodies

3.6.1. Antibodies

Table 3.10. Antibody concentrations and suppliers.

Antibody	**Host/isotype**	**Dilution**	**Supplier(cat.no.)**	**kDA**
SIK2	Rabbit	1:1000	Cell Signal-6919	130
IRE1	Rabbit	1:1000	Cell Signal-3294	130
BiP	Rabbit	1:1000	Cell Signal-3177	78
VCP	Mouse	1:10000	Sigma	97
TRAF2	Rabbit	1:1000	Cell Signal-4724	
CHIP	Rabbit	1:1000	Cell Signal-2080	32
Phospho-SAPK/JNK	Rabbit	1:1000	Cell Signal-4668	46-54
JNK	Rabbit	1:1000	Cell Signal-9258	46-54
IRS4	Rabbit	1:1000	Origene-TA303856	∼160
LC3B	Rabbit	1:1000	Sigma-L7543	16-18
p62/SQSTM1	Rabbit	1:1000	Sigma-p0067	62
Ubiquitin	Mouse	1:2000	Sigma	
β-actin	Mouse	1:2000	Santa-Cruz-sc47778	45
GAPDH	Rabbit	1:1000	Santa-Cruz-sc25778	39
GFP	Rabbit	1:1000	Santa-Cruz	
HIS	Mouse	1:100	Santa-Cruz	
Mouse IgG	HRP	1:5000	Cell Signal-7076	

Table 3.10. Antibody concentrations and suppliers (cont.)

Antibody	**Host/isotype**	**Dilution**	**Supplier(cat.no.)**	**kDA**
Rabbit IgG	HRP	1:5000	Santa-Cruz-sc2004	

3.7. Disposable Labware

3.7.1. Disposable Labware

Table 3.11. List of disposable labware used in this study.

Cell Culture Petri Dishes (145mm, 100 mm, 60 mm)	TPP, Switzerland
Cell Scraper	TPP, Switzerland
Centrifuge Tubes (15 ml, 50 ml)	TPP, Switzerland
Cover Slips	VWR, USA
Cryovial Tubes (2ml)	Greiner Bio One, UK
Microfuge Tubes (0.5ml, 1.5ml, 2ml)	Axygen, USA
Micropipette Tips	Axygen, USA
Multiwell Plates (6-well, 12-well, 24-well, 96-well)	TPP, Switzerland
Pasteur Pipettes	Hartenstein
PCR Tubes (0.2ml)	Axygen, USA
Petri Dishes for bacterial growth	Fırat Plastik, Turkey
Pippette Tips (Bulk)	CAPP, Denmark
Pippette Tips (filtered)	CAPP, Denmark
Serological Pipettes (5ml, 10ml, 25ml)	CAPP, Denmark
Syringe Filter Units (0.22 m, 0.45 m)	EMD Millipore, USA
Syringes (1ml, 5ml, 10ml, 50ml)	Set Medikal, Turkey
Test Tubes (0.2 ml, 0.5 ml, 1.5 ml, 2 ml)	Axygen, USA

3.8. Equipment

Table 3.12. Equipment used in this study.

Agarose Gel Electrophoresis System	Mini-sub Cell GT, BioRad, USA
Autoclave	Midas 55, Prior Clave, UK
Balances	DTBH 210, Sartorius, GERMANY Electronic Balance VA 124, Gec Avery, UK
Carbon dioxide tank	Genc Karbon, TURKEY
Cell culture incubator	Hepa Class 100, Thermo, USA
Centrifuges	Ultracentrifuge J2MC, Beckman Coulter, USA Mini Centrifuge 17307-05, Cole Parmer, USA Centrifuge 5415R, Eppendorf, USA Centrifuge, Allegra X-22, Beckman Coulter, USA
Cold room	Birikim Elektrik Soğutma, TURKEY
Deepfreezers	-20°C, Arçelik, TURKEY -70°C Freezer, Harris, UK -80°C ULT Freezer, Thermo, USA -150°C, MDF-1156, Sanyo,Japan
Documentation System	Gel Doc XR System, Bio-Doc, ITALY Stella, Raytest, Germany G-BOX Chemi XX6, Syngene, UK
Electrophoresis Equipments	Mini-Protean III Cell, Bio-Rad, USA
Freezing Container	Mr.Frosty, Nalgene, Thermo, USA
Heat blocks	DRI-Block DB-2A, Techne, UK

Table 3.12. Equipment used in this study (cont.).

Hemocytometer	Improved Neubauer, Weber Scientific International Ltd, UK
Ice Machine	Scotsman Inc., AF20, ITALY
Laboratory Bottles	Isolab, Germany
Laminal flow cabinet	Labcaire BH18, UK
Luminometer	Fluoroskan Ascent FL, Thermo Electron, USA.
Magnetic Stirrers	M221 Elektro-mag, TURKEY Clifton Hotplate Magnetic Stirrer, HS31, UK
Micropipettes	Finnpipette, Thermo, USA
Microplate Reader	680, Biorad, USA
Microscopes	Inverted Microscope, CKX41, Olympus, JAPAN Fluoroscence Microscope, Observer.Z1, Zeiss, GERMANY
Microwave oven	M1733N, Samsung, MALAYSIA
pH meter	WTW pH330i, GERMANY
Pipettor	Pipetus-akku,Hirscmann Labogerate, GERMANY
Power Supply	Biorad, USA
Refrigerators	2082C, Arçelik, TURKEY 4030T, Arçelik, TURKEY
Shakers	VIB Orbital Shaker, InterMed, DENMARK Lab-Line Universal Oscillating Shaker, USA
Softwares	Quantity One, Bio-Rad, ITALY

Table 3.12. Equipment used in this study (cont.).

	ImageJ, Image Analysis Software, NIH, USA Roche Diagnostics, SWITZERLAND XStella 1.0, Stella, GERMANY
Spectrophotometer	Agilent 8453, USA NanoDrop 1000, USA
Thermocyclers	Gene Amp. PCR System 2700, Applied Biosystems, USA
Vacuum pump	KNF Neuberger, USA
Vortex	Vortexmixer VM20, Chiltern Scientific, UK
Water baths	TE-10A, Techne, UK
Water purification system	UTES, TURKEY

4. METHODS

4.1. Molecular Cloning

4.1.1. Polymerase Chain Reaction (PCR)

Phusion (NEB, USA) and *Taq* polymerases (Thermo, USA) were used for cloning purposes. For the amplification of DNA fragments to be cloned, the Phusion High-Fidelity DNA polymerase was used and the PCR reaction mix was prepared according to Table 4.1. *Taq* DNA polymerase was routinely used in colony PCR reaction for checking cloned constructs. The PCR condition for both DNA polymerases is summarized in Table 4.3.

Table 4.1. PCR reaction mix for Phusion DNA Polymerase.

Component	**volume for 20µl Reaction**	**Final Concentration**
Nuclease-free water	up to 20µl	
5X Phusion HF buffer	4µl	1X
10mM dNTPs	0.4µl	200µM
10µM Forward Primer	1µl	0.5µM
10µM Reverse Primer	1µl	0.5µM
Template DNA	variable	10ng
DMSO	0.6µl	3%
Phusion (2u/µl)	0.2µl	0.4u per 20µl reaction

4.1.2. Restriction Enzyme Digestion of DNA

Restriction enzyme digestion reactions were performed in 20µl reaction volumes with the appropriate reaction buffer and condition according to manufacturer's recommendations. Reaction tubes were incubated at 37°C for 30 minutes or 3-4 hours using FastDigest (Thermo, USA) or conventional restriction enzymes, respectively.

Table 4.2. PCR reaction mix for Taq DNA Polymerase.

Component	**volume for 25µl Reaction**	**Final Concentration**
Nuclease-free water	up to 25µl	
$MgCl_2$ (20mM)	2µl	2mM
10X Taq Buffer	2.5µl	1X
10mM dNTPs	0.3µl	400µM
10 µM Forward Primer	1µl	0.4µM
10 µM Reverse Primer	1µl	0.4µM
Template DNA	variable or picked colony	10ng
DMSO	1.25µ	5%
Taq DNA polymerase (5 u/µl)	0.2µl	1u per 25µl reaction

Table 4.3. Standard PCR protocols for the *Taq* and Phusion DNA Polymerases.

	Taq		**Phusion**		
Step	**Temperature**	**Time**	**Temperature**	**Time**	**Cycle**
Initial denaturation	95°C	3 min	98°C	30 sec	1
Denaturation	95°C	30 sec	98°C	10 sec	28-32
Primer annealing	55°C	30 sec	64-68°C	15 sec	
Elongation	72°C	1 min per 1 kb	72°C	20 sec per 1 kb	
Final elongation	72°C	5 min	72°C	7min	1
Hold	4°C	∞	4°C	∞	

4.1.3. Agarose gel electrophoresis

To prepare 1% Agarose gel, 0.5 g of Agarose was melted in 50 ml 1X TAE buffer by heating using a microwave oven and after cooling the solution to room temperature 5 µl ethidium bromide (final concentration of 0.5 µg/ml) was added to allow UV-light detection of the DNA. Mixture was cast in an agarose tray. After the gel was polymerized, it was placed in an electrophoresis chamber containing 1X TAE buffer. 6X DNA loading dye was mixed with DNA samples to a final concentration of 1X. Samples were loaded in the gel and it was run at 100 Volt constant voltage for 20-30 minutes. Gels were visualized under UV light using the GelDoc image documentation system (BioRad, USA).

4.1.4. Extraction of DNA Samples from Agarose Gel

DNA sample was excised from agarose gel using a razor blade under UV light. The gel was placed into a 1.5ml centrifuge tube and weighted. DNA fragment in the gel was purified with spin columns using the PCR purification kit (Qiagen, USA) according to manufacturer's protocol.

4.1.5. Ligation

Ligation of linearized plasmid DNA and inserts were performed using T4 DNA Ligase (NEB, USA) according to manufacturer's instruction. For each 10µl of reaction volume, 50-100ng digested plasmid and inserts were mixed with 1:1 or 1:3 molar ratio. The reaction was carried out at room temperature for 30 min and inactivated at 65°C for 10 min.

4.1.6. Preparation of Chemically Competent *E.coli* Cells

5ml of LB medium was inoculated with a 100 µl aliquot of the *E. coli* DH5α strain from glycerol stock, and grown at 37°C overnight while shaking at 200 rpm.

Then, 25 ml LB was inoculated with 250 µl of the overnight culture. Cells were grown until optical density at 590 nm reached to 0.4-0.6. Cells were centrifuged at 4000 g for 10 min at 4°C. The pellet was resuspended in 12.5 ml of ice-cold sterile 50mM $CaCl_2$ and incubated on ice for 30 min. Cells were centrifuged again (4000g for 10 min at 4°C) and the pellet was resuspended in 2.5 ml ice-cold sterile 50 mM $CaCl_2$. 50-200 µL of this preparation was used for transformations. For long term storage at -80°C, 100 µl of cell aliqouts including 10% of glycerol were flash-frozen in liquid nitrogen.

4.1.7. Transformation of the Chemically Competent TOP10

A vial of competent cells was thawed on ice for 15 min and 10-50 ng plasmid or ligation mix (15-20%) was added. After incubation on ice for 20-30 min, the vial was placed in 42°C heat-block for 1 min, and then immediately on ice for 2 min. 500 µl LB medium was added onto cells. Cells were incubated for 1 hr at 37°C with vigorous shaking (200rpm). After 1 hour incubation, 100 µl of the cell suspension was spread on appropriate antibiotic-containing LB-agar plates and cells were grown overnight at 37°C, in an inverted position.

4.1.8. Colony PCR

Colony PCR was routinely performed for screening positive clones in agar plates. First, each colony was picked from agar plate with a pipette tip and mixed with 25ul of PCR solution containing Taq polymerase (Thermo, USA) and other additives, which are described in manufacturer's protocol. PCR was performed in a thermal cycler with the conditon given in Table 4.3. PCR products were run in 1% agarose gel.

4.1.9. Plasmid Purification

Plasmid purifications were carried out with Genopure and High Pure Plasmid Isolation Kits (Roche, Germany), for midi/maxi and mini isolation scales respectively, according to the manufacturer's protocols. Plasmids that would be used in transfections

were purified with midi or endotoxin free maxi gravity flow kits to yield transfection grade plasmids. Quality of plasmids was checked by spectrophotometric measurements and agarose gel electrophoresis. $OD_{260/280}$ was between 1.8-2.00.

4.1.10. Semi-Quantitative Reverse Transcriptase Mediated PCR (RT-PCR) and XBP-1 splicing assays

cDNA synthesis was performed with ImPromII Reverse Transcription System Kit (Promega,USA) according to manufacturer's protocol. 1 μg of total RNA was used for each reaction. At the end of the reaction, cDNA is diluted to a final volume of 100 μl. 1-2% of cDNA synthesized from 1 μg total RNA was used as template in PCR reactions. RT-PCR was performed with the help of Taq DNA polymerase, according to the condition in in Table 4.3. For XBP1 splicing assay, 28 cycles for denaturation, annealing and elongation steps were set in PCR protocol.

4.2. Cell Culture Methods

4.2.1. Growth and Maintenance of HEK-293T Cells

HEK-293T cells were routinely grown on 10 cm cell culture dish in DMEM containing 10% FBS, 1% Penicillin/Streptomycin and 4.5 g/l glucose (high-glucose). Cells were cultivated in 5% CO2-supplemented incubator at 37°C. Media were kept at 4°C and warmed to 37°C in a sterile water bath before use.

4.2.2. Passaging

The cells were passaged before reaching 90% confluence. The growth medium was aspirated and the cells were washed once with pre-warmed 1X calcium and phosphate-free PBS. In order to remove the monolayer cells from the surface, trypsin (0.025 per cent, ready to use) was added to the petri dish and cells were incubated at 37°C for 3-5 min. 2-3 volumes of fresh medium was added to inactivate trypsin and the suspension

was pipetted gently to disperse the cells. The cells were transferred to fresh petri dishes in a 1:5 ratio for standard passaging.

4.2.3. Cryopreservation

Cells were harvested by trypsinization and neutralized with 10 volumes of growth medium. The cells were counted in a haemocytometer and precipitated 3 min at 500g. The pellet was suspended in freezing medium (5% DMSO, 10% FBS and 85% DMEM). 1ml of this solution was placed into 2 ml screw capped-cryotubes. The tubes were waited in isopropanol containing freezing-box at -80°C overnight. Following day, main stocks were transferred into the liquid nitrogen storage tank. The number of cells frozen in a single vial was between 1-2 millions.

4.2.4. Thawing

One vial of frozen cell line was taken from the nitrogen tank and thawed immediately in 37°C (at most) water bath. After cells were thawed, they were transferred in a falcon tube and 4ml fresh medium was added. Cells were precipitated for 3 min at 500 g. The pellet was resuspended in an adequate amount of medium and transferred to a fresh petri dish.

4.2.5. Transient Transfection of 293T cells

Transfections were carried out with the the Turbofect (Thermo) *in vitro* transfection reagent. The amount of plasmid and the volume of were determined according to the manufacturer's protocol. Cells were seeded the day before transfection to obtain 70-80% confluency at the day of transfection. 4 hours after transfection, media were replaced with certain amount of fresh growth medium.

4.2.6. RNA Extraction from HEK-293T cells

Total RNA isolation is performed with RNeasy RNA Isolation kit (Qiagen, USA) according to manufacturer's protocol. Total RNA concentration is measured by nanodrop spectrophotometer and DNA contamination is checked by the $OD_{260/280}$ ratio (between 2 and 2.2). Total RNA integrity is checked by loading the samples on 1% agarose gel. Purified RNA samples were stored at -20°C for short term and -80°C for long term storage.

4.2.7. Thapsigargin Treatment

500.000-1.000.000 cells and 2.000.000-3.000.000 cells were seeded into 60 mm or 100 mm cell-culture dishes, respectively. Next day, either thapsigargin (1μM, final concentration) or DMSO as vehicle control were added to the media of the cells. Cells were harvested 6 hours after treatment or at indicated time point for further analysis.

4.3. Endoplasmic Reticulum (Microsome) Isolation

50.000.000-60.000.000 (3x150mm cell culture plates) 293T cells were harvested by trypsinization and rinsed with PBS twice. Cells were centrifuged and resuspended in 3 ml of fresh ER Isolation Buffer containing 10 mM HEPES (pH: 7.8), 250 mM sucrose, 25 mM potassium chloride, 1 mM EGTA and protease/phosphatase inhibitors (Thermo). Samples were incubated for 30 min on ice and homogenized using dounce homogenizer (300 rpm, 20 strokes). In each homogenization step, 1.5 ml of cell suspension volume was used. Homogenates were centrifuged at 1000 g for 10 min at 4°C. Nuclear and cellular pellets were stored at -20°C for further applications. Supernatants were transferred into new Eppendorf tubes and centrifuged at 12.000g for 15 min at 4°C. Mitochondrial pellets were also stored at -20°C. Post-mitochondrial supernatants were transferred into ultracentrifuge tubes and centrifuged at 100.000g for 60 min at 4°C. Then the microsomal pellets were resuspended in protein extraction buffer containing Urea (7 M), Thiourea (2 M), CHAPS (2%, w/v), DTT (50 mM), and

phosphatase/protease inhibitors (Roche). Protein concentration was determined using Pierce 660nm assay (Thermo). Samples were stored at -80°C until further applications.

4.4. Preparation of Protein Sample for LC-MS/MS Analysis

4.4.1. Protein Quantification

For the quantification of protein concentrations, 660 nm assay (Pierce) was used. Protein samples and bovine serum albumin (BSA) dilutions ranging from 0.05 to 2 mg/ml were mixed with 150 µl of 660 nm assay reagent. After 5 minutes incubation at room temperature, absorbances were measured at 660 nm. Unknown sample concentrations were calculated from the standard curve.

4.4.2. Methanol-Chloroform Precipitation

200 µg of ER protein extracts were mixed with 800 µl methanol, 200 µl chloroform and 600 µl water. Samples were vortexed and centrifuged at 10000 g for 1 min. Methanol/water mix on the top of the interface was removed without disturbing the interface. 800 µl methanol was added to wash the samples. Tubes were vortexed vigorously and centrifuged at 14000g for 5 min. After centrifugation, two additional washing steps with cold methanol were performed. After the last centrifugation, supernatants were removed and pellets were air dried for 5 min. Samples were stored at -80°C until shipment.

4.5. Co-Immunoprecipitation (Co-IP)

4.5.1. Preparation of Lysates

48 hours after transfection, cells were treated with 1 µM thapsigargin or DMSO (as vehicle control) for indicated time points. Before cell lysis, the media of treated cells were aspirated and cells were rinsed with 1X PBS. 500 µl of IP-lysis buffer con-

taining 0.2% NP40, 150 mM NaCl, 20 mM Tris-Cl (pH:8.0), 2 mM EDTA and 1X phosphatase/protease inhibitors (Thermo) was added on the cells. Lysates were harvested using a cell scraper and were transferred into a 1.5ml Eppendorf tube. For complete lysis and shearing the DNA, lysates were passed through an insulin-syringes with 21-gauge needle (4-5 times) and incubated on ice for 30 min. After incubation, samples were centrifuged at 14000 g for 15 min at 4°C. 10% of the lysate was taken as input control for western blotting. Before starting immunoprecipitation protocol, 20 µl of protein A/G-agarose (Santa-Cruz) beads was added to the lysates for pre-clearing to decrease non-specific protein-bead interaction. After incubating the lysate-bead mixes for 30 min at 4°C, they were precipitated at 1000g for 1 min at 4°C. Then the supernatant were transferred into new Eppendorf tube to continue with IP protocol.

4.5.2. Immunoprecipitation using the anti-HIS antibody and FLAG-agarose bead

1 µg primary anti-HIS antibody was added to the lysates containing 1 mg total protein. Antibody-lysate mix was incubated for 1 hour at 4°C before adding 20µl of Protein A/G agarose bead (Santa-Cruz). To immunoprecipate the FLAG-tagged recombinant proteins, cell extracts with 1mg total protein were mixed with 40µl of the equilibrated anti-FLAG-M2 agarose beads (Sigma) after. For equilibration, beads were washed three times with IP lysis buffer and centrifuged at 500g for 3 minutes. Then, tubes were incubated overnight in cold room on a rocker. After incubation, antibody-bead-protein complexes were centrifuged at 4°C for 5 min at 1000 g and washed three times with 500 µl of IP-lysis buffer. If FLAG-agarose beads were used, samples were precipitated at 500 g for 3 min. After the last washing step, immunoprecipitates were resuspended in 50 µl of IP-lysis buffer containing 1X SDS-loading dye and heated at 95°C for 5 min. For western blotting, 25µl of sample was used to detect the specific immunoprecipitated protein. 2% of the pre-immunoprecipitation lysates were used as input control.

4.6. SDS-PAGE Gel Electrophoresis and Western Blotting

4.6.1. Cell Lysis and Protein Extraction

Protein lysates from HEK-293T cells were prapared in NP-40 lysis buffer. Cells were washed once with 1X PBS and lysis buffer was directly added onto the cells. Plates were incubated on ice for 15 minutes before scraping cells. Then, cells lysates were collected into 1.5 ml centrifuge tubes and homogenized using syringes. After additional incubation on ice for 30 min, lysates were centrifuged 10 min at 14000g at 4°C. After centrifugation, supernatants were transferred into new eppendorf tubes. Protein lysates were stored at -20°C for short term storage.

4.6.2. Protein Quantificaiton and Bicinchoninic acid (BCA) Assay

For the quantification of protein concentrations, BCA Assay kit (Pierce) was used. Protein samples and bovine serum albumin (BSA) dilutions ranging from 0.125 to 2 mg/ml were mixed with 200 µl of BCA Working Solution. After 30 minutes incubation at 37°C absorbances were measured at 592 nm. Unknown sample concentrations were calculated from the standard curve.

4.6.3. SDS-PAGE and Western Blot

SDS-PAGE gels were casted, run and transferred using Mini-Protean cell and Mini Trans-blot cell (BioRad) systems. Routinely, 10% running gels (with the 29:1 acrylamide:bis-acrylamide ratio) were cast. After polymerization of the separating gel a 5% stacker gel (with the same cross linker ratio) was prepared. Protein samples were prepared in 1X SDS-PAGE dye. 3-4 µl of the pre-stained protein marker (Thermo Scientific Inc.) was used as the molecular weight standard. Samples were heated at 95°C for 10 min, vortexed, and spin, loaded into the wells formed by the combs in the stacker gel. Samples were run at 80-100V until the BPB front entered the running gel and then the voltage was increased up to 120V. Runs were stopped when the BPB

front left the running gel.

Table 4.4. Preparation of SDS-PAGE gels.

	Resolving Gel	**Stacking Gel**
ddH2O	3.65 ml	1.82 ml
1.5 M Tris.Cl (pH 8.8)	2.25 ml	–
1 M Tris.Cl (pH 6.8)	–	313 µl
SDS 20% (w/v)	45 µl	13 µl
Acrylamide Bis-acrylamide (30%-0.8 w/v)	3 ml	335 µl
APS 10% (w/v)	56.5 µl	21 µl
TEMED	13 µl	6 µl

Proteins were transferred onto PVDF membranes (Thermo Scientific Inc.) for 2 hrs at 100V in cold-room. After transfer, blots were blocked in 5% non-fat milk for 1 hr at room temperature with shaking using orbital shaker at around 100 rpm. After washing the membrane in TBST buffer twice, blots were incubated at 4°C overnight in the 5% BSA solution containing specific primary antibody with the appropriate concentrations recommended by the supplier. After primary incubation and washing steps, membrane was incubated in 5% non-fat milk solution containing HRP-conjugated secondary antibody for 1-2 hour(s) at room temperature. Then, membranes were washed 3 times in TBST with 5 min interval. By using western blotting luminol detection kit (Cell Signaling) protein bands were visualized with Stella Imaging Station (Raytest).

4.7. GO-term and Pathway Enrichment Analysis

GO-term and pathway enrichment analyses were performed using the online bioinformatic platform DAVID (release 6.8 [153]). Significant enriched pathways and terms were filtered according to their Benjamini adjusted p-values (<0.1).

5. RESULTS

5.1. Over-expression of SIK2 under thapsigargin treatment and ER isolation

To identify novel ER-resident substrates of SIK2 under ER stress condition, as a first step 293T cells were transiently transfected with the SIK2-WT (wildype) and SIK2-KI (kinase-inactive) constructs. Thapsigargin, a chemical agent causing calcium depletion in the ER by inhibiting Ca^{2+} ATPase (SERCA)[154], is commonly used as an inducer of ER stress. Cells were harvested 6 hours after thapsigargin treatment for ER isolation. SIK2 over-expression and ER-stress induction were checked with Western Blotting (Figure 5.1). BiP, a well-established ER stress marker, protein level change was observed in order to confirm the stimulatory effect of thapsigargin on ER stress.

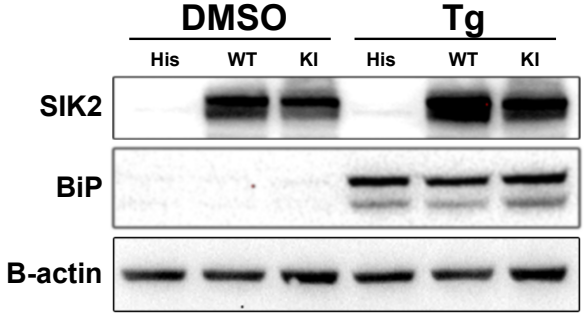

Figure 5.1. SIK2 over-expression in 293T cells under thapsigargin-induced ER stress. (Tg:Thapsigargin(1 μM, 6 hrs), His: empty His construct, WT:SIK2-wildtype, KI:SIK2-kinase inactive)

5.1.1. Preparation of ER fraction for LC-MS/MS analysis

ER fractions (microsomes) of the cells were collected after homogenization and differential centrifugation steps (See Section 4.3). Western Blotting was performed using the anti-Calnexin antibody as ER marker to check ER microsome enrichment (Figure 5.2).

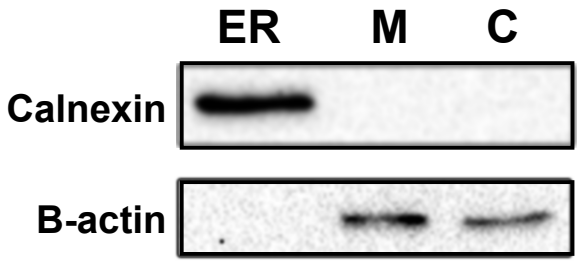

Figure 5.2. Western blotting of sub-cellular fractions. Calnexin was used as ER marker. (M: mitochondrial fraction C: cytosol).

5.2. LC-MS/MS Sub-Proteome Analysis

After observation of SIK2 overexpression, ER-stress induction (Figure 5.1) and the enrichment of the ER microsomes (Figure 5.2) protein samples were precipitated and sent to the Yale Proteomics Center (New Haven, Connecticut, USA) for label-free LC-MS/MS analysis to identify and quantify phospho-peptides/proteins in each sample. LC-MS/MS raw data were processed using the Progenesis QI software by the center. Processed data showing identified proteins and peptide abundance scores were sent to us as separated list for each sample. Analysis was performed with proteins that have at least two unique peptides with scores higher than 95% confidence and at a FDR smaller than 1%. Same confidence and FDR ratio filters were also used for phospho-proteome analysis. The flow diagram summarizing the work from the beginning of sample preparation to the analysis part was illustrated in Figure 5.3.

In the full-proteome (phospho + non-phospho) data, increased BiP (ER stress marker) and SIK2 (over-expressed protein) protein levels were observed as expected (Figure 5.4). Besides, the Ser770 residue of VCP/p97, which is a known SIK2 substrate [123], was found to be phosphorylated in only thapsigargin-treated SIK2-wt-overexpressing cells.

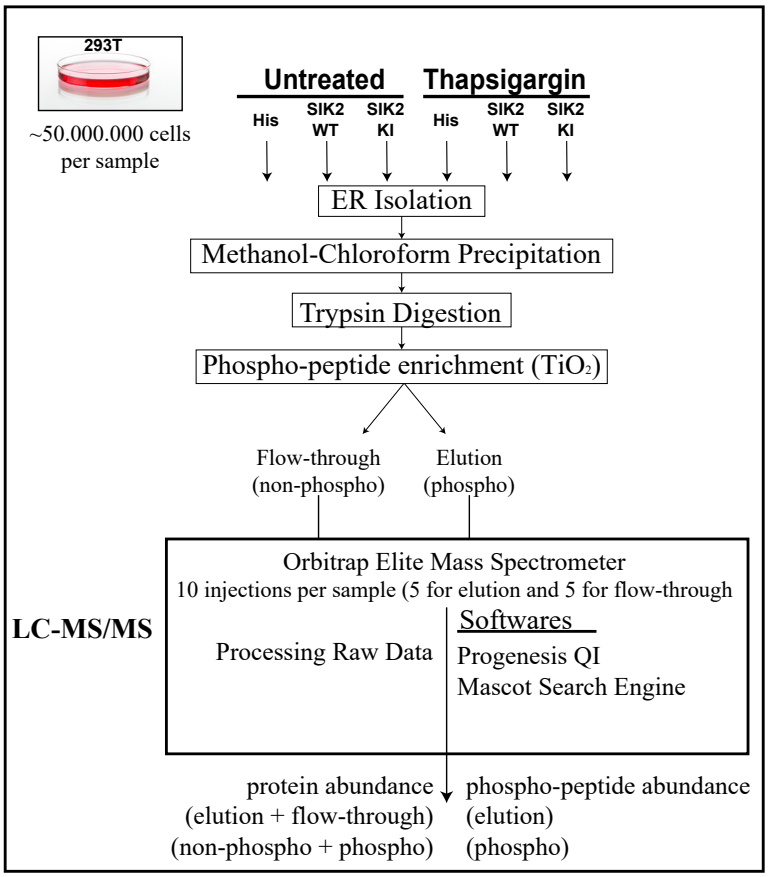

Figure 5.3. Flow-chart of the LC-MS/MS based label-free quantitative proteomic work.

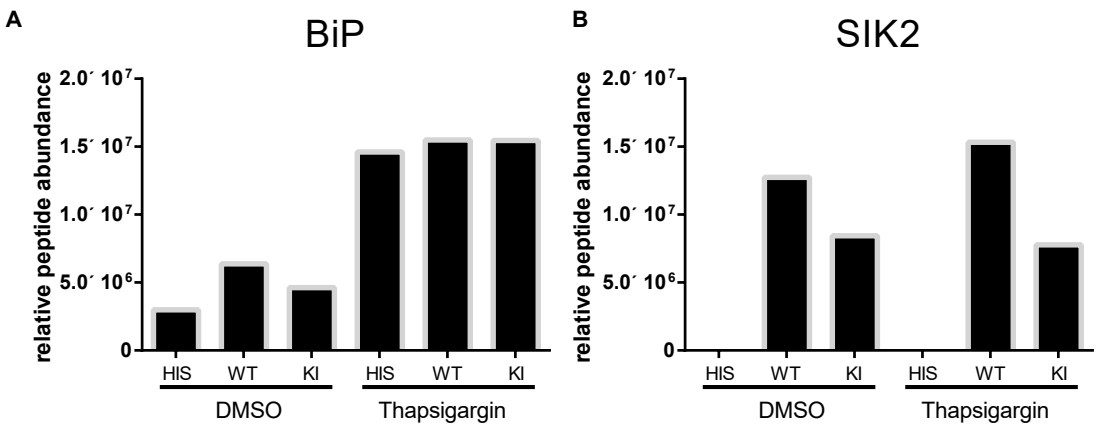

Figure 5.4. Peptide Abundances of BiP and SIK2 in control (HIS) and SIK2-overexpressing (WT and KI) 293T cells either untreated or treated with thapsigargin (1 μM, 6 hrs).

Number of proteins and phospho-peptides identified in LC-MS/MS quantitative proteome analysis for each sample were summarized in Table 5.1 and Table 5.2. 2447 different proteins were identified when proteins in all samples were combined. In GO-term annotation enrichment analysis, ER-related GO-terms (e.g. "endoplasmic reticulum", "endoplasmic reticulum lumen") or molecules having roles in the ER (e.g. "molecular chaperones", "ER to Golgi transport vesicle") were indeed found to be enriched in these identified proteins (Table 5.3). Filters of "minimum 2 fold increase" or "minimum 0.5 fold decrease" were used to prepare UP and DOWN protein lists, respectively, for further gene enrichment analyses.

Table 5.1. Number of proteins identified in proteome (phospho + non-phospho) analysis for each sample (HIS: control sample, WT:SIK wildtype, KI:SIK2 kinase inactive, UP/DOWN: proteins/peptides whose peptide abundances increased/decreased in thapsigargin samples respectively).

	UP	**DOWN**	**TOTAL**
HIS	297	402	**1799**
WT	541	332	**1934**
KI	374	390	**1805**
samples combined			**2447**

Table 5.2. Number of proteins and peptides identified in phospho-proteome analysis (HIS: control, WT:SIK2-wildtype, KI:SIK2-kinase inactive, UP,DOWN: proteins/peptides whose peptide abundances increased/decreased in thapsigargin sample respectively).

	UP		**DOWN**		**TOTAL**	
	peptide	protein	peptide	protein	peptide	protein
HIS	430	274	583	361	2168	876
WT	711	406	412	293	2281	901
KI	357	237	558	337	2026	810
filter: WT-tg / WT: min 2 fold WT_up but KI_not_up					**290**	**201**
samples combined					**3197**	**1080**

Table 5.3. Functional annotation term enrichment analysis for the whole protein set identified in the LC-MS/MS proteome analysis.

Category	Term	#	%	F.E.	p-Value
GOTERM_CC_FAT	signal recognition particle. endoplasmic reticulum targeting	6	0.30	7.1	2.90E-04
GOTERM_CC_FAT	rough endoplasmic reticulum membrane	7	0.30	5.5	4.40E-04
GOTERM_CC_FAT	rough endoplasmic reticulum	12	0.50	4.3	2.00E-05
GOTERM_CC_FAT	endoplasmic reticulum lumen	24	1.00	2.1	4.70E-04
GOTERM_CC_FAT	endoplasmic reticulum part	74	3.10	1.5	2.10E-04
GOTERM_CC_FAT	endoplasmic reticulum	180	7.60	1.3	2.40E-05
GOTERM_CC_FAT	proteasome complex	46	2.00	5.4	5.20E-26
GOTERM_CC_FAT	proteasome core complex	15	0.60	5.3	1.90E-08
GOTERM_BP_FAT	proteasomal ubiquitin-dependent protein catabolic process	53	2.20	3.6	1.40E-18
GOTERM_BP_FAT	proteasomal protein catabolic process	53	2.20	3.6	1.40E-18
GOTERM_BP_FAT	positive regulation of ubiquitin-protein ligase activity	44	1.90	4.4	9.70E-20
GOTERM_BP_FAT	positive regulation of ubiquitin-protein ligase activity during mitotic cell cycle	43	1.80	4.4	1.90E-19
GOTERM_BP_FAT	positive regulation of protein ubiquitination	45	1.90	3.7	1.60E-16
GOTERM_BP_FAT	proteasomal ubiquitin-dependent protein catabolic process	53	2.20	3.6	1.40E-18
GOTERM_BP_FAT	regulation of protein ubiquitination	48	2.00	3.4	4.20E-15
GOTERM_MF_FAT	unfolded protein binding	57	2.40	3.5	8.00E-19
GOTERM_BP_FAT	response to unfolded protein	27	1.10	2.7	2.40E-06
GOTERM_BP_FAT	protein folding	81	3.40	3.2	1.70E-23
GOTERM_CC_FAT	chaperonin-containing T-complex	7	0.30	7.1	4.70E-05
INTERPRO	Chaperone. tailless complex polypeptide 1	10	0.40	6.8	5.60E-07
INTERPRO	Chaperonin TCP-1. conserved site	9	0.40	6.8	3.40E-06
SP_PIR_KEYWORDS	molecular chaperone	10	0.40	6.3	2.80E-06
PIR_SUPERFAMILY	molecular chaperone t-complex-type	9	0.40	6.1	7.90E-06
INTERPRO	Heat shock chaperonin-binding	8	0.30	6	6.10E-05
INTERPRO	Chaperonin Cpn60/TCP-1	11	0.50	5.5	2.70E-06
SP_PIR_KEYWORDS	Chaperone	72	3.10	3.7	1.20E-24
INTERPRO	Molecular chaperone. heat shock protein. Hsp40. DnaJ	16	0.70	2.9	1.50E-04
GOTERM_CC_FAT	ER to Golgi transport vesicle	8	0.30	5.2	2.10E-04
GOTERM_CC_FAT	COPI vesicle coat	8	0.30	5.2	2.10E-04
GOTERM_BP_FAT	vesicle-mediated transport	145	6.10	1.8	2.70E-12
COG_ONTOLOGY	Intracellular trafficking and secretion	24	1.00	4.1	2.80E-10

: count F.E. :Fold enrichment

Then enriched GO-terms and pathways were identified using DAVID bioinformatics tool [153] for proteins whose total-peptide/phospho-peptide abundances were increased or decreased upon thapsigargin treatment compared to control samples. Pathway and GO-term enrichment analysis results for up/down protein sets were illustrated with the Venn diagrams shown in Figures 5.5, 5.6, and 5.7.

Enriched pathways and GO-terms for UP/DOWN gene sets obtained from whole-proteomics were presented in two Venn diagrams (see Figure 5.5 for KEGG-pathway and GO-BP, see Figure 5.6 for GO-CC and GO-MF), while those obtained from the phospho-proteomics were depicted in a single Venn diagram (Figure 5.7). As can be seen from Figure 5.5, the GO Biological Process terms of "IRE1-mediated unfolded protein response" and "Retrograde vesicle-mediate transport-Golgi to ER" were found to be enriched in the SIK2-WT-UP and SIK2-WT-DOWN lists, respectively (DAVID: $p < 0.05$, Benjamini < 0.1). Besides, GO-CC (Cellular component) terms of "ER chaperone complex", "Unfolded protein binding" and "ubiquitin protein ligase binding" were found to be enriched in the SIK-WT-UP protein set (Figure 5.6).

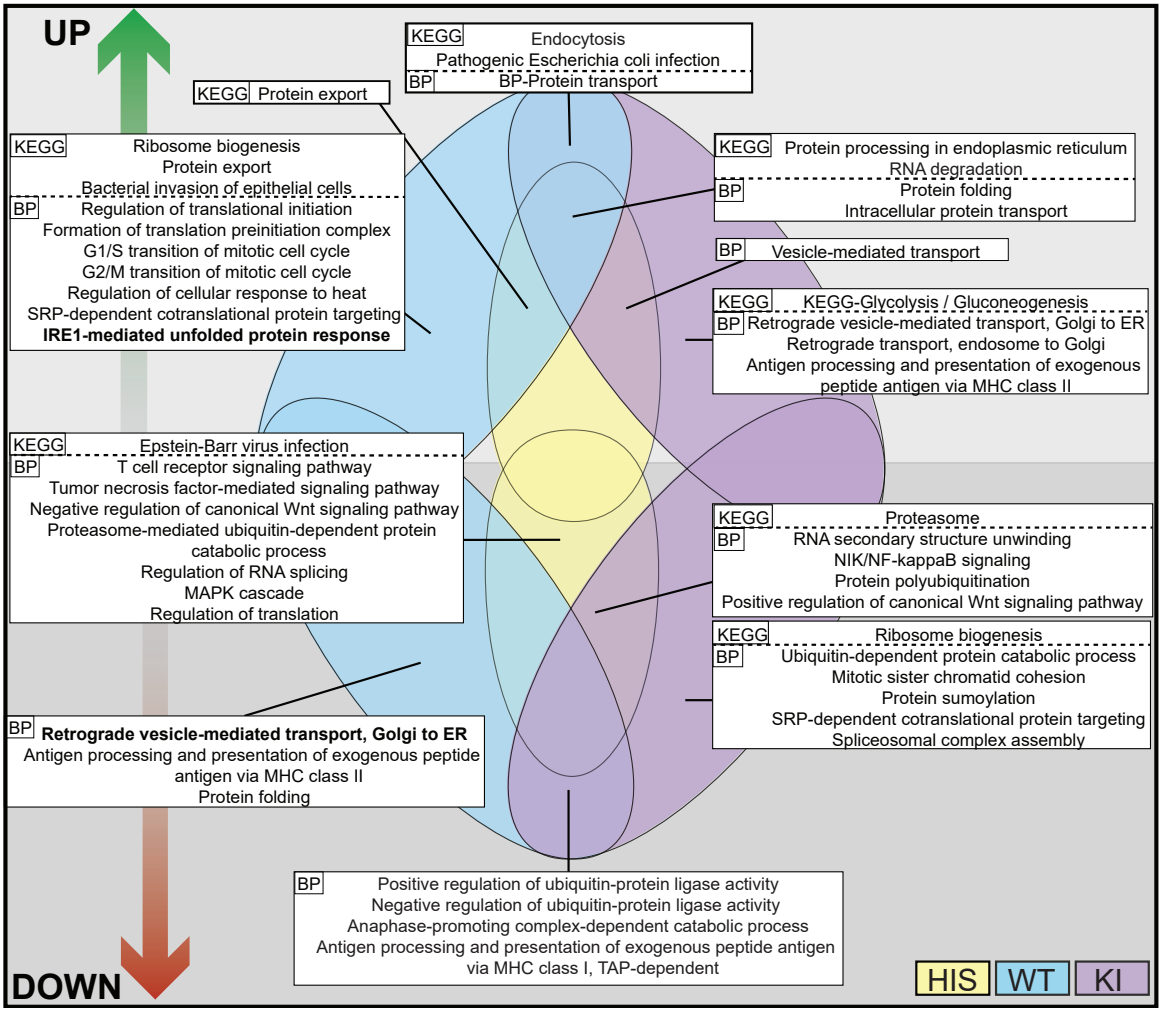

Figure 5.5. DAVID pathway enrichment analysis of protein sets (UP: proteins whose peptide abundances increased upon thapsigargin treatment, DOWN: proteins whose peptide abundances decreased upon thapsigargin treatment, BP:Biological function).

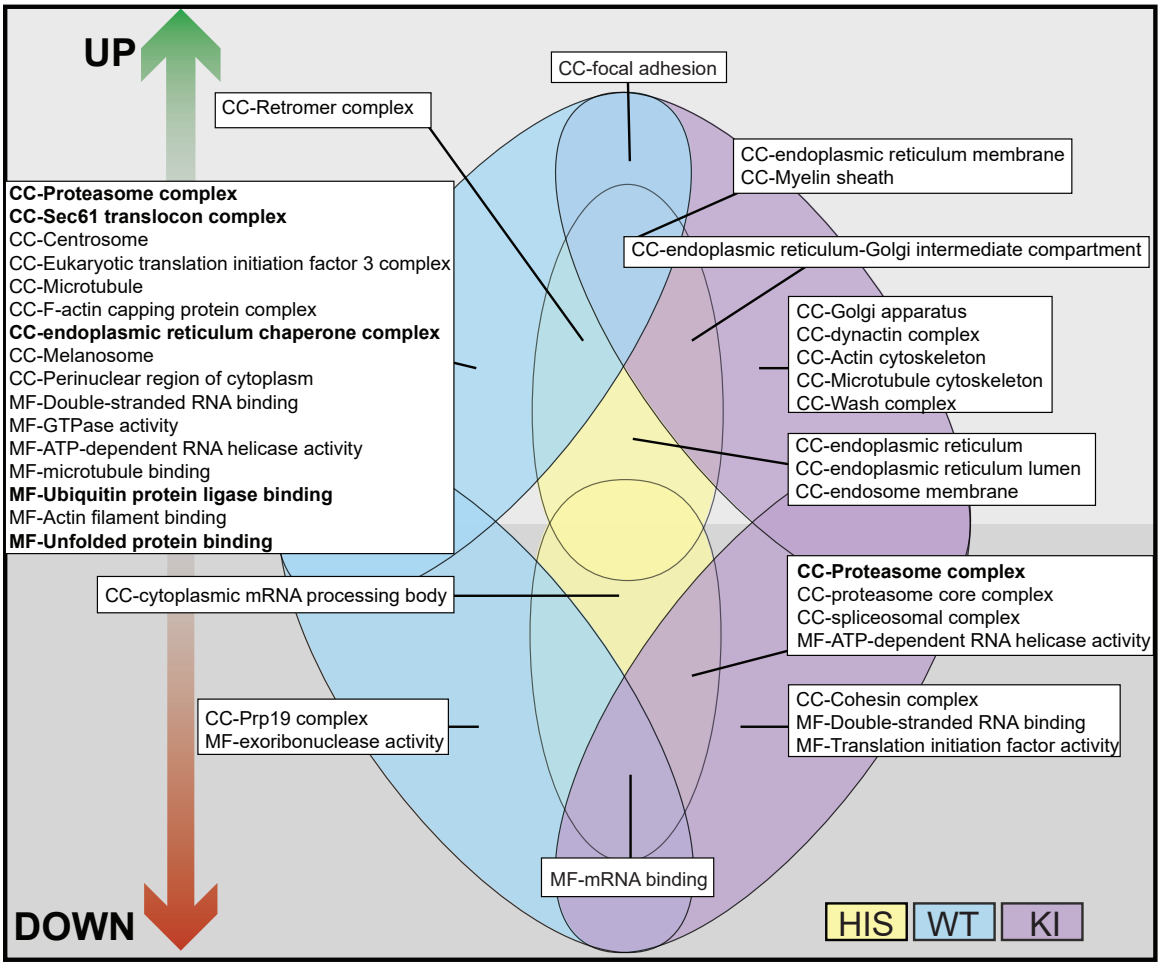

Figure 5.6. DAVID pathway enrichment analysis of protein sets (UP: proteins whose peptide abundances increased upon thapsigargin treatment, DOWN: proteins whose peptide abundances decreased upon thapsigargin treatment, CC:Cellular component, MF:Molecular function).

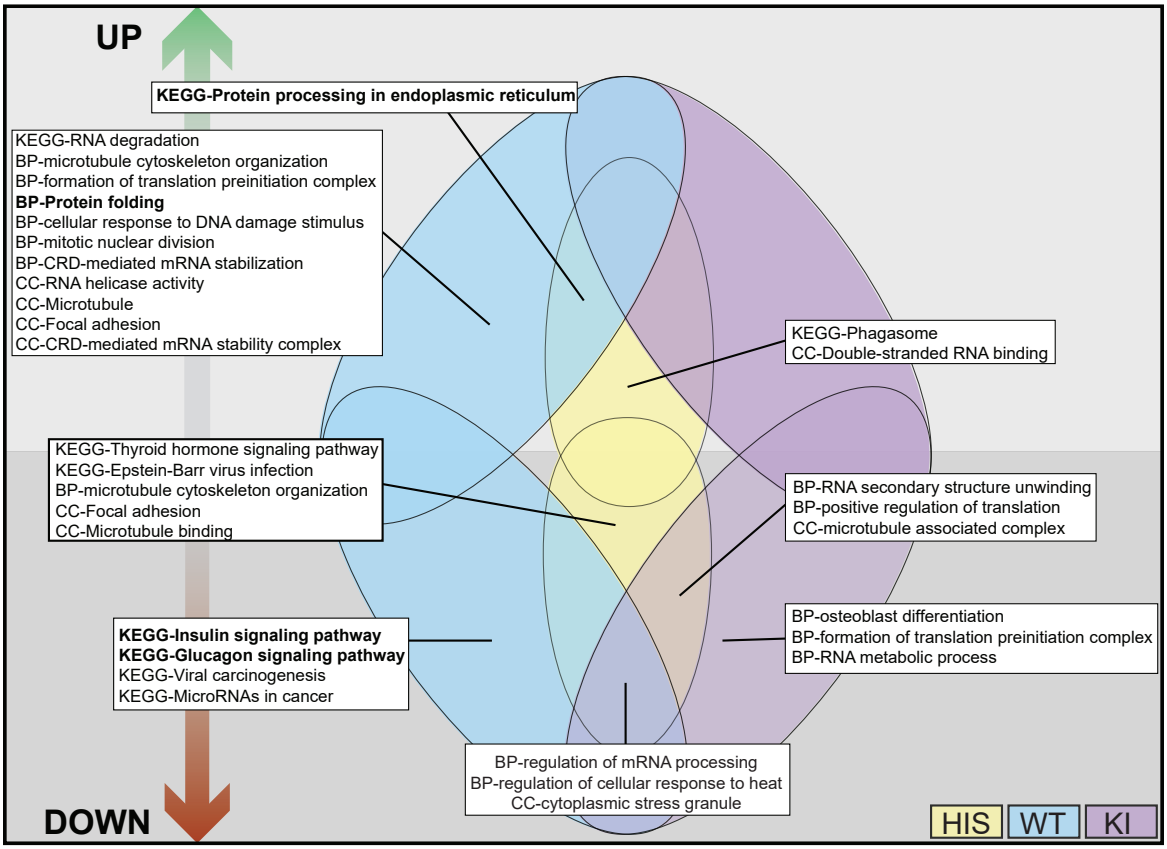

Figure 5.7. DAVID pathway and GO enrichment analysis of phospho-proteome. (UP: proteins whose phospho-peptide abundances increased upon thapsigargin treatment, DOWN: proteins whose phopsho-peptide abundances decreased upon thapsigargin treatment, BP:Biological function, CC:Cellular component MF:Molecular function).

5.2.1. Candidate protein selection

Based on the phospho-peptide abundances in each sample, candidate proteins (Table 5.4) were selected for further studies considering their involvement in ER-related molecular mechanisms (e.g. ERAD, vesicular transport and chaperone activity). Some representative proteins and their relative phospho-peptide abundances were shown in Figure 5.8.

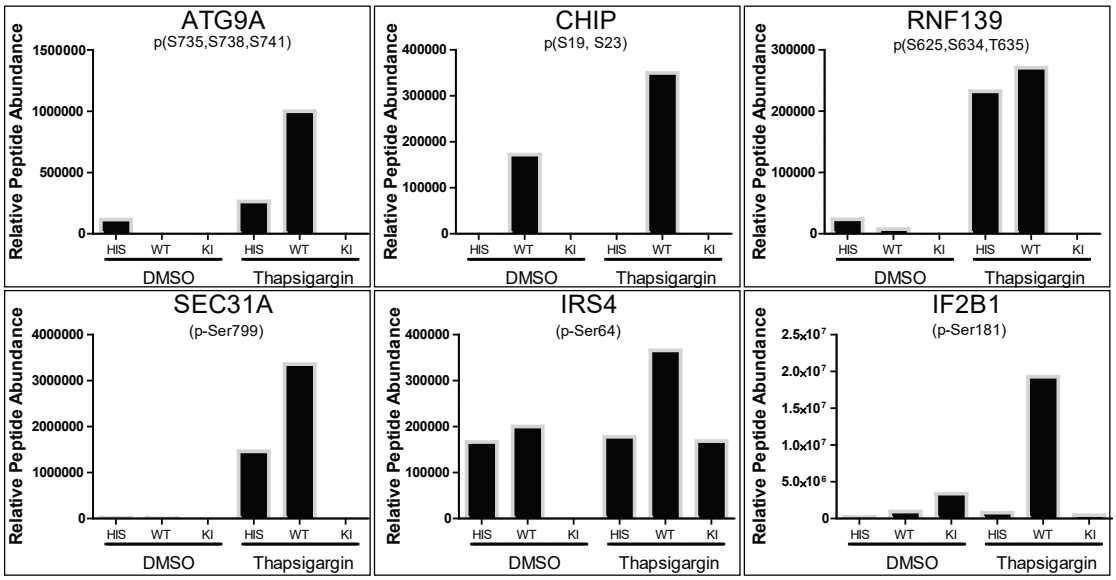

Figure 5.8. Relative phospho-peptide abundances of proteins in the candidate list. His: pcDNA4-HisC (empty backbone), WT:His-SIK2-WT, KI:His-SIK2-KI

Table 5.4. Candidate proteins chosen for validation and further studies.

Uniprot ID	**Description**	**Function**
ATG9A_HUMAN	Autophagy-related protein 9A	Autophagy
CHIP_HUMAN	E3 ubiquitin-protein ligase CHIP	E3-ubiquitin ligase
HUWE1_HUMAN	E3 ubiquitin ligase HUWE1	E3-ubiquitin ligase
RN139_HUMAN	E3 ubiquitin-protein ligase RNF139	E3-ubiquitin ligase
BRE1A_HUMAN	E3 ubiquitin-protein ligase BRE1A	E3-ubiquitin ligase
HS105_HUMAN	Heat shock protein 105 kDa	Chaperon
HSPB1_HUMAN	Heat shock protein beta-1	Chaperon
CMTR1_HUMAN	Cap-specific mRNA (nucleoside-2'-O-)-methyltransferase 1	RNA-modification
IF2B1_HUMAN	Insulin-like growth factor 2 mRNA-binding protein 1	RNA binding
RBM10_HUMAN	RNA-binding protein 10	RNA-binding

Table 5.4. Candidate proteins chosen for validation and further studies (cont.).

Uniprot ID	**Description**	**Function**
RBM26_HUMAN	RNA-binding protein 26	RNA-binding
RBM33_HUMAN	RNA-binding protein 33	RNA-binding
EXOS9_HUMAN	Exosome complex component RRP45	Exonuclease complex
SEC62_HUMAN	Translocation protein SEC62	Translocon
SC31A_HUMAN	Protein transport protein Sec31A	Protein export
IRS4_HUMAN	Insulin receptor substrate 4	Insulin-receptor substrate

The aminoacid sequences of proteins in the candidate list were scanned with the GPS3.0 bioinformatic tool [120] to identify putative SIK2 phosphorylation sites. The tool gave high SIK2 phosphorylation prediction score for some of the phospho-residues identified in the phospho-proteome analysis (Table 5.5).

Table 5.5. GPS3.0 Phosphorylation site prediction result (phospho-residues are marked with red. Underlined residues were the output of GPS3.0 as predicted SIK2 phosphorylation site).

Uniprot ID	**Residue (s)**	**GPS score**	**peptide(s)**
ATG9A_HUMAN	S735,S738,S741	7.5	HRRE<u>S</u>DE<u>S</u>GE<u>S</u>APDE
CHIP_HUMAN	S19,S23	7.833	GGG<u>S</u>PEK<u>S</u>PSAQELK
HUWE1_HUMAN	S1907	7	PRGSGTA<u>S</u>DDEFENL
RN139_HUMAN	S625,S634,T635	5.833	VREAAAE<u>S</u>DRELNED RELNEDD<u>ST</u>DCDDDV
BRE1A_HUMAN	S138	–	EPEPDSD<u>S</u>NQERKDD
HS105_HUMAN	S557	–	QTSQSPP<u>S</u>PELTSEE
HSPB1_HUMAN	S82	–	RALSRQL<u>S</u>SGVSEIR
CMTR1_HUMAN	S51,S53,S55	9.667	STTSL<u>S</u>G<u>S</u>D<u>S</u>ETEGK
RBM10_HUMAN	S61,S65	6.833	KHDYDD<u>S</u>SEEQ<u>S</u>AED
RBM26_HUMAN	S127	–	FSRRLNH<u>S</u>PPQSSSR
RBM33_HUMAN	S973	7	TVTHRTN<u>S</u>GGGDGPH

Table 5.5. GPS3.0 Phosphorylation site prediction result (cont.).

Uniprot ID	**Residue (s)**	**GPS score**	**peptide(s)**
IF2B1_HUMAN	S181,S314	–	RGQPRQGSPVAAGAP ETKITISSLQDLTLY
EXOS9_HUMAN	S392,S394	7.833	QDAPIILSDSEEEEM
SEC62_HUMAN	T375	–	KEELEQQTDGDCEED
SC31A_HUMAN	S799	9	EPVAGHESPKIPYEK
IRS4_HUMAN	S64	9.333	STATGSRSDSESEEE

Among these proteins, IRS4 and CHIP, having roles in biological processes related with metabolic pathways and ER functions, were selected for further functional studies.

5.3. SIK2 interacts with IRS4

Co-immunoprecipitation assay (co-IP) was performed using 293T cells transiently over-expressing FLAG-tagged IRS4 and HIS-tagged SIK2 to obtain direct evidence for the proposed interaction between SIK2 and IRS4. Western blot analysis showed that the FLAG antibody co-immunoprecipates IRS4 with SIK2 (Figure 5.9).

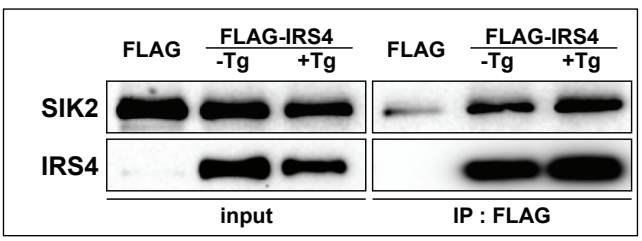

Figure 5.9. Co-immunoprecipitation of FLAG-IRS4 with HIS-SIK2 upon thapsigargin (Tg) treatment in 293T cells. 24 hours after transfection cells were either untreated or treated with 1μM Tg for 6 hours. IPs were carried out with anti-FLAG antibody and immunoprecipitates were analyzed by Western blotting using anti-SIK2, anti-IRS4 antibodies.

To further support the interaction between SIK2 and IRS4, co-localization assay was performed in 293T cells expressing mCherry-tagged SIK2 and sYFP-tagged IRS4.

As can be seen in Figure 5.10, SIK2 colocalized with IRS4 possibly in perinuclear region.

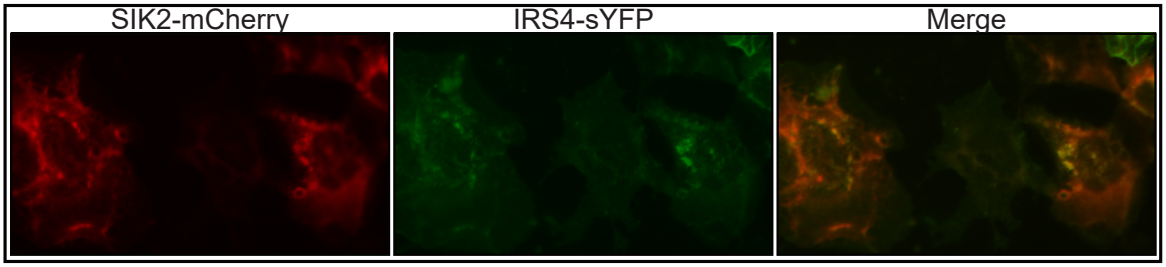

Figure 5.10. Co-localization analysis in 293T cells expressing IRS4-sYFP and SIK2-mCherry.

To identify region(s) of the SIK2-IRS4 physical interaction, various truncated IRS4 forms were generated and expressed in 293T cells (Figure 5.11). Co-IP assays demonstrated that the interaction between SIK2 and IRS4 was weakened in the absence of the PH and PTB domains.

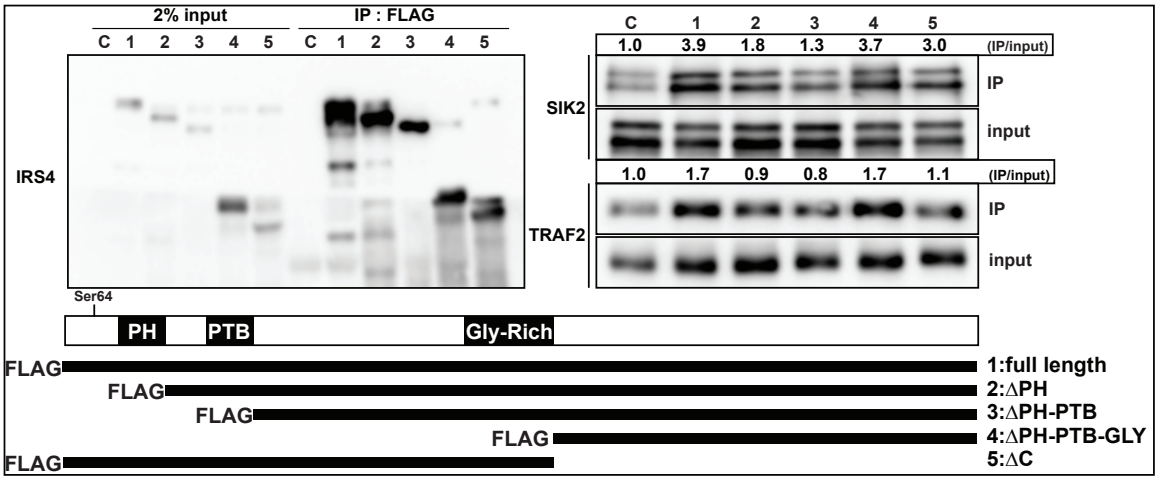

Figure 5.11. Mapping IRS4 regions innvolved in SIK2 interaction. Cells were transfected with wildtype and truncated IRS4 contructs and immunoprecipitations were performed 6 hours after thapsigargin treatment. Immunoprecipitates were analyzed by Western blotting using anti-IRS4, anti-SIK2 and anti-TRAF2 antibodies.

5.4. IRS4 interacts with IRE1

One of our initial proposed mechamisms about the possible roles of SIK2 in the UPR was that SIK2 might contribute to transmitting lumenal ER-stress signal to the cytosol through being a part of IRE1 signaling complex. For this purpose, IRE1-SIK2 interaction was tested with co-IP assays using different epitope-tagged constructs, but consistent results could not be obtained (data not shown). Nevertheless, TRAF2, which is a mediator of the IRE1/JNK pathway, was found to be immunoprecipitated with SIK2 (Figure 5.22). After capturing SIK2-TRAF2 and IRS4-TRAF2 (Figure 5.11) interactions, it was tested whether IRS4 interacts with IRE1. Both endogenous (Figure 5.12) and ectopically-expressed (Figure 5.13) IRE1 were immunoprecipitated with FLAG-IRS4.

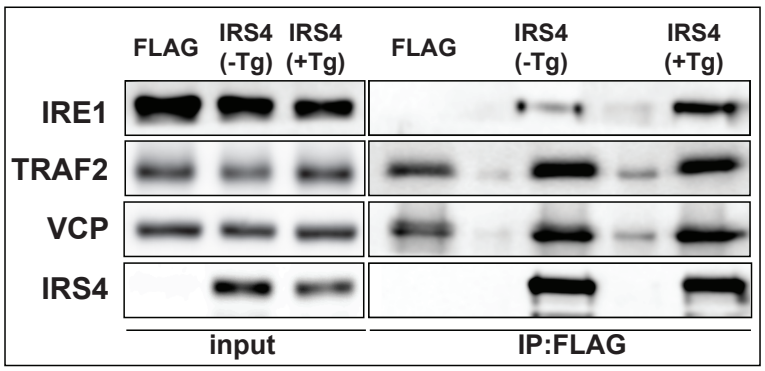

Figure 5.12. Co-immunoprecipitation of FLAG-IRS4 with endogenous IRE1 upon thapsigargin (Tg) treatment in 293T cells. 24 hours after transfection cells were either untreated or treated with Tg for 24 hours. IP's were carried out with anti-FLAG antibody and analyzed by Western blotting using anti-IRS4 and anti-IRE1 antibodies.

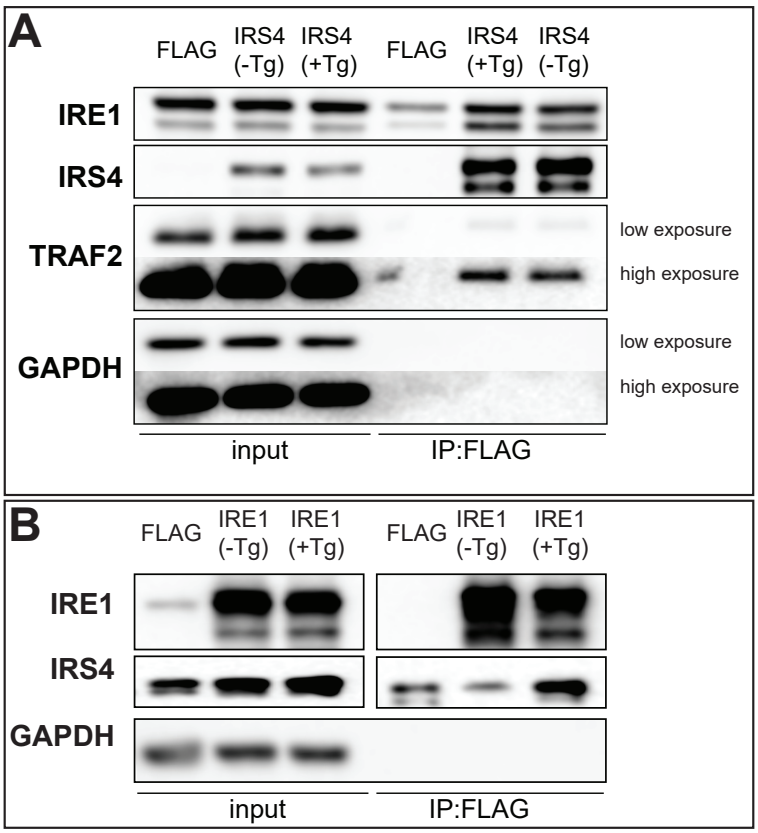

Figure 5.13. Co-immunoprecipitation of the ectopically expressed IRS4 and IRE1 proteins. 293T cells were transfected with Flag-IRS4/His-IRE1 (A) or mCherry-IRS4/FLAG-IRE1 (B) constructs. Cells were treated with Tg for 24 hours and lysates were immunoprecipitated with the anti-FLAG antibody.

A time-dependent study of the interaction following thapsigargin treatment was also conducted. As shown in Figure 5.14, the IRS4-IRE1 interaction reached a maximum at 6 hours of treatment and gradually decreased after that point.

To identify IRE1-interacting regions in the IRS4 protein, co-IP assays were performed using lysates of 293T cells expressing truncated-IRS4 forms. The interaction between IRE1 and IRS4 was found to be weakened when the PH or PTB domains were deleted from the N-terminus of IRS4, but not affected by C-terminal truncation (Figure 5.15).

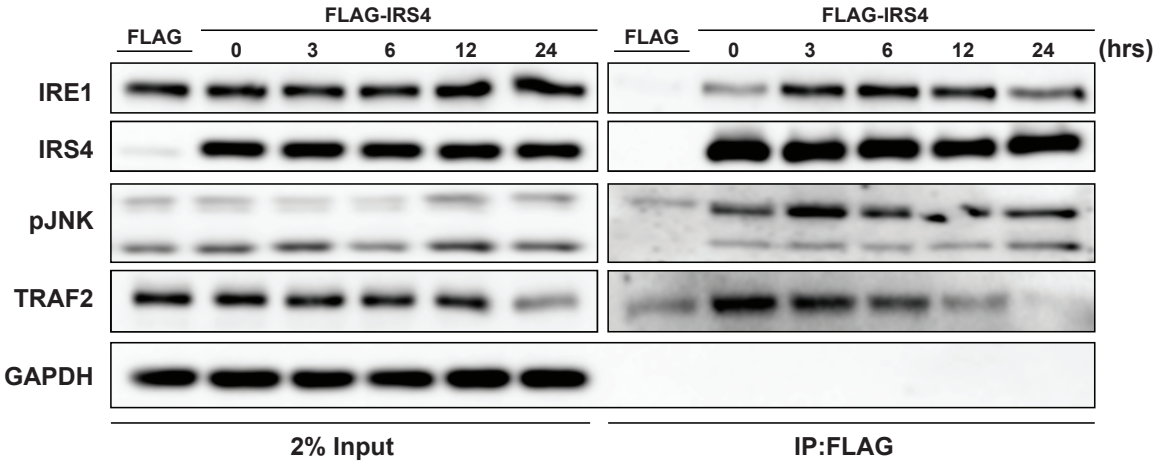

Figure 5.14. Co-immunoprecipitation of FLAG-IRS4 and endogenous IRE1 in different time points upon thapsigargin (1μM) treatment.

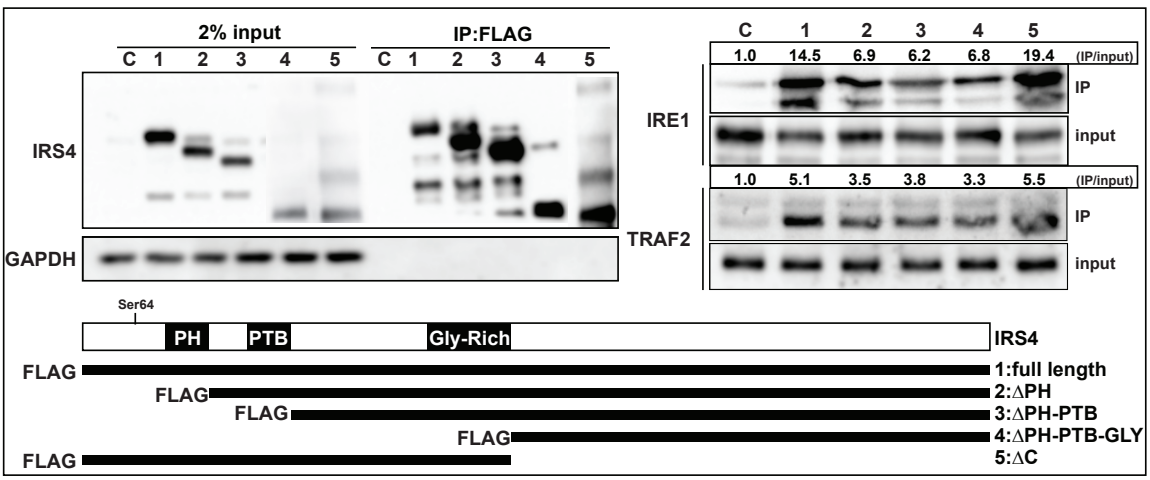

Figure 5.15. Mapping IRS4 regions involving in the IRS4-IRE1 interaction.

5.4.1. Effect of SIK2 on IRS4-IRE1 interaction

After detecting the IRS4-IRE1 interaction, we sought to determine whether there is any effect of SIK2 on this interaction. Co-IP assays, using the lysates of SIK2-overexpressing (wild-type and kinase inactive forms) and control 293T cells, indicated that SIK2 has a negative effect on the assembly of the IRE1-IRS4 complex in ER-stressed condition (Figure 5.16). On the other hand, it has been observed that SIK2 enhances the IRS4-TRAF2 interaction in both stressed and unstressed condition independent of its kinase activity.

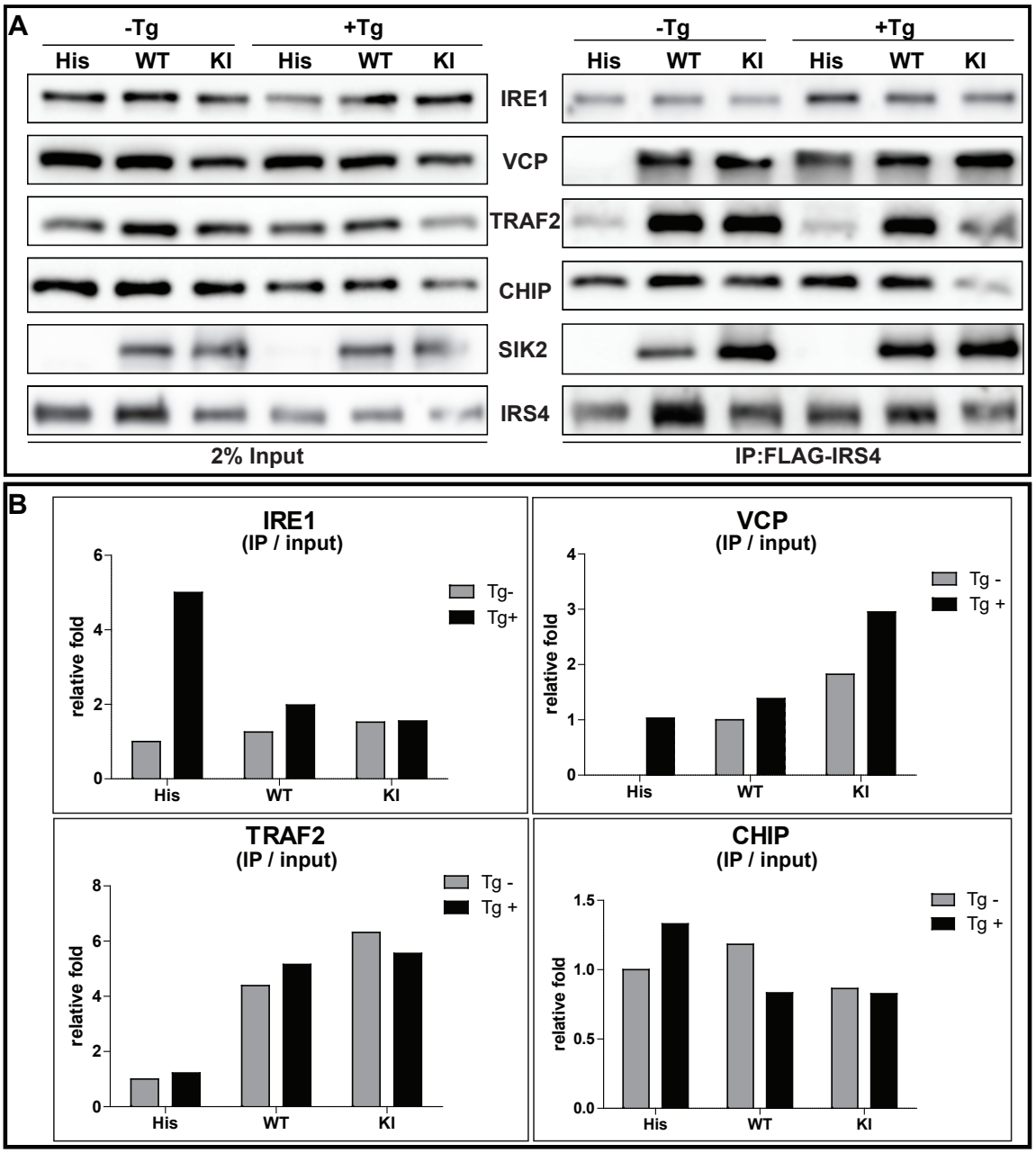

Figure 5.16. SIK2 negatively affects the formation of the IRS4-IRE1 complex and induces the interaction between IRS4 and TRAF2. Flag-tagged IRS4 over-expressing 293T cells were either transfected with empty plasmid (his) or SIK2 wt(wildtype)/ki(kinase-inactive) plasmids. 6 hours after thapsigargin treatment cellular lysates were immunoprecipitated using anti-flag antibody.

5.5. IRS4 and ER stress response

To unravel the possible physiological roles of IRS4 in the UPR, alteration in activities of ER stress related pathways were examined upon IRS4 overexpression. For this purpose, a series of experiments, including XBP-eYFP reporter assay and measuring CD3δ degradation, were conducted.

5.5.1. Analyses of XBP1 splicing activity and BiP protein levels in response to IRS4 overexpression

The effect of IRS4 on XBP1 mRNA splicing in response to thapsigargin treatment was evaluated. To monitor XBP1 splicing, a XBP1-eYFP reporter construct encoding DNA binding-deficient (ΔDBD) XBP1 was generated to follow the IRE1-mediated XBP1 splicing (Figure 5.17A). As presented in Figure 5.17B, more ΔDBD-XBP1 fusion proteins were accumulated in the IRS4 over-expressing 293T cells upon thapsigargin treatment. To support this, endogenous XBP1 mRNA splicing was also assessed by semiquantitative RT-PCR. XBP1 mRNA splicing is an early response and not continous during prolonged ER stress [155]. In control 293T cells, spliced XBP1 mRNA (s) was observed within 1 hour after thapsigargin treatment and at 12 hours unspliced form (u) became predominant again (Figure 5.17C). In IRS4-overexpressing cells, splicing gradually decreased after 6 hours, similar to control cells, but the time point, at which the unspliced form became the predominant transcript again, extended from 12th to 24th hours. BiP protein level was also checked to compare ER stress level between samples. Western blot analysis showed that IRS4 overexpression mildly alleviate thapsigargin-induced ER stress. Besides, IRS4 strongly reduced ER stress induced by tunicamycin, which is a chemical leading to unfolded protein accumulation through inhibiting glycosylation process (Figure 5.18).

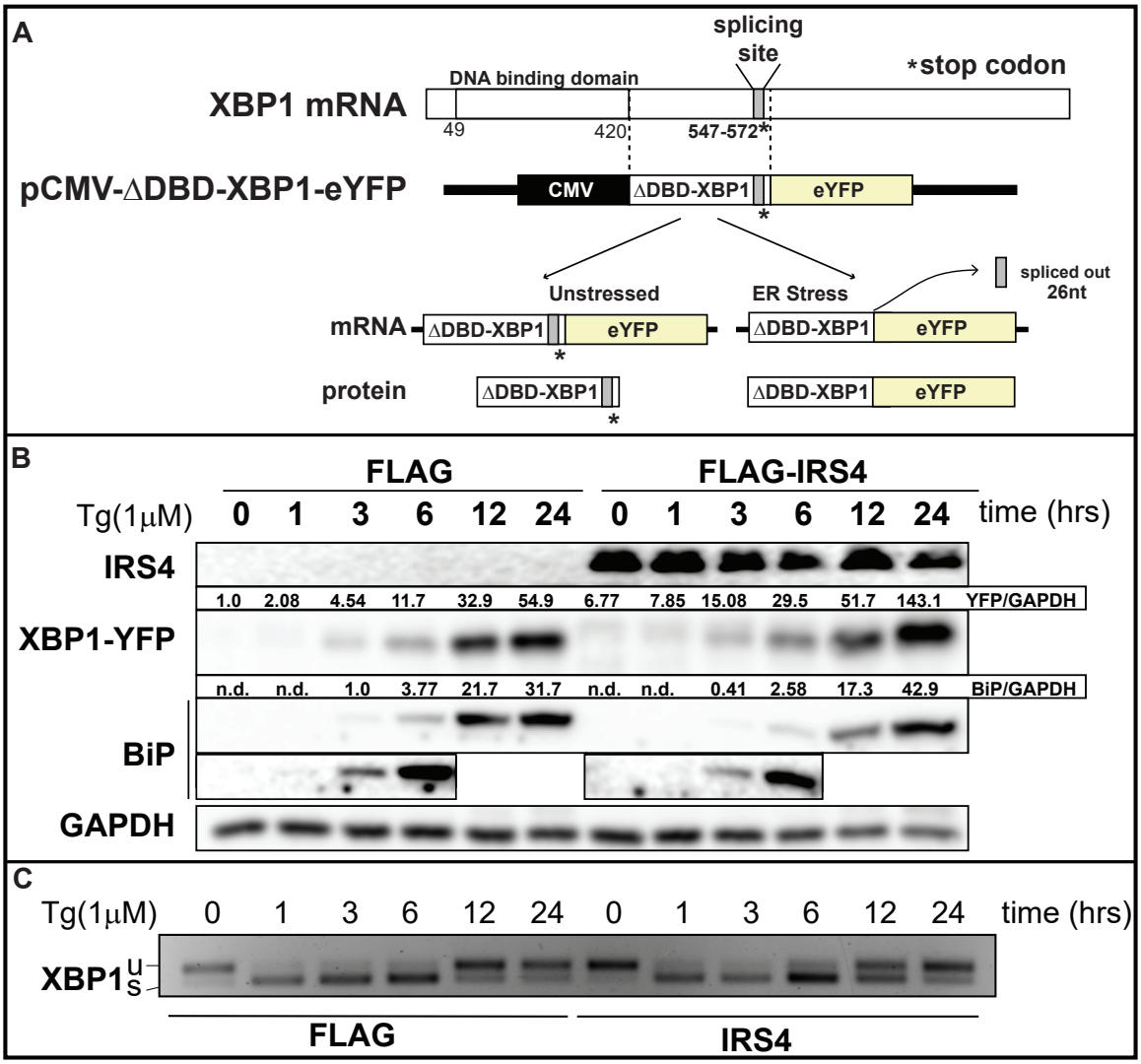

Figure 5.17. Effect of IRS4 over-expression on XBP1 splicing. XBP1 splicing assay was performed using the ΔDBD-XBP1-eYFP construct (A). Reporter fusion protein accumulation induced by ER stress and the BiP level were checked by Western blotting (B). Endogenous XBP1 mRNA level was detected by RT-PCR using primers amplifying both unspliced (u) and spliced (s) XBP1 transcripts (C).

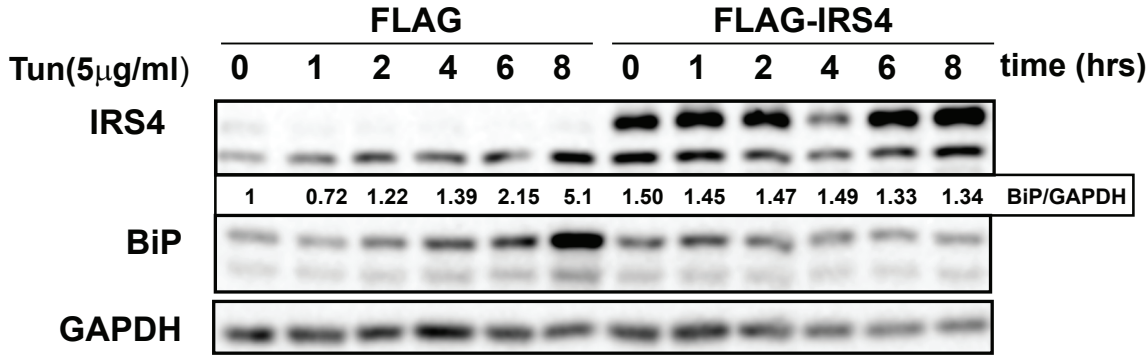

Figure 5.18. Effect of IRS4 over-expression on the BiP protein level in response to tunicamycin (5μg/ml) treatment at indicated time points.

5.5.2. Effect of IRS4 on ER-associated degradation (ERAD) and autophagic activity

To further investigate the functions of IRS4 in the UPR, ERAD activity was examined in response to IRS4 overexpression using recombinant CD3δ as ERAD substrate. CD3δ, which is a subunit of the T cell receptor, is degraded by ERAD when expressed individually in the absence of other subunits [156]. CD3δ-GFP fusion protein was expressed in 293T cells and its stability was followed upon overexpression of IRS4 individually or together with SIK2. SIK2 has previously been found to be critical for the proper degradation of ERAD substrates through participating in the ER retrotranslocon complex [123]. As expected, CD3δ protein level decreased in response to SIK2 overexpression. Interestingly, overexpression of IRS4 resulted in augmented CD3δ protein level compared to control sample, but could not prevent the reduction when it was co-expressed with SIK2 (Figure 5.19).

To support that alteration in the amount of CD3δ relies on its degradation, proteasome complex was inhibited using epoxomicin [157] and VR23 [158]. Consistently with the previous experiment presented in Figure 5.19, both SIK2 and IRS4 have similar effects on the stability of CD3δ in the absence of proteasome inhibitors (Figure 5.20, lanes 1 to 4). CD3δ-GFP levels increased in treated samples compared to their untreated counterparts. However, a similar pattern and ratios were observed that

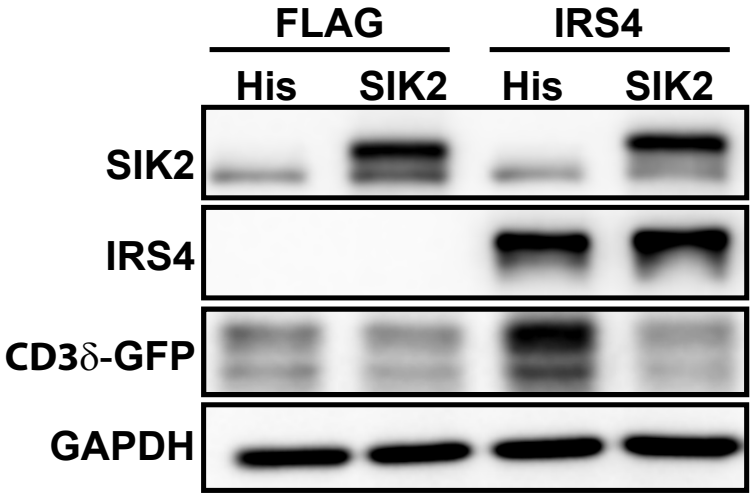

Figure 5.19. Effect of IRS4 overexpression either with or without SIK2 on the stability of the recombinant CD3δ-GFP protein.

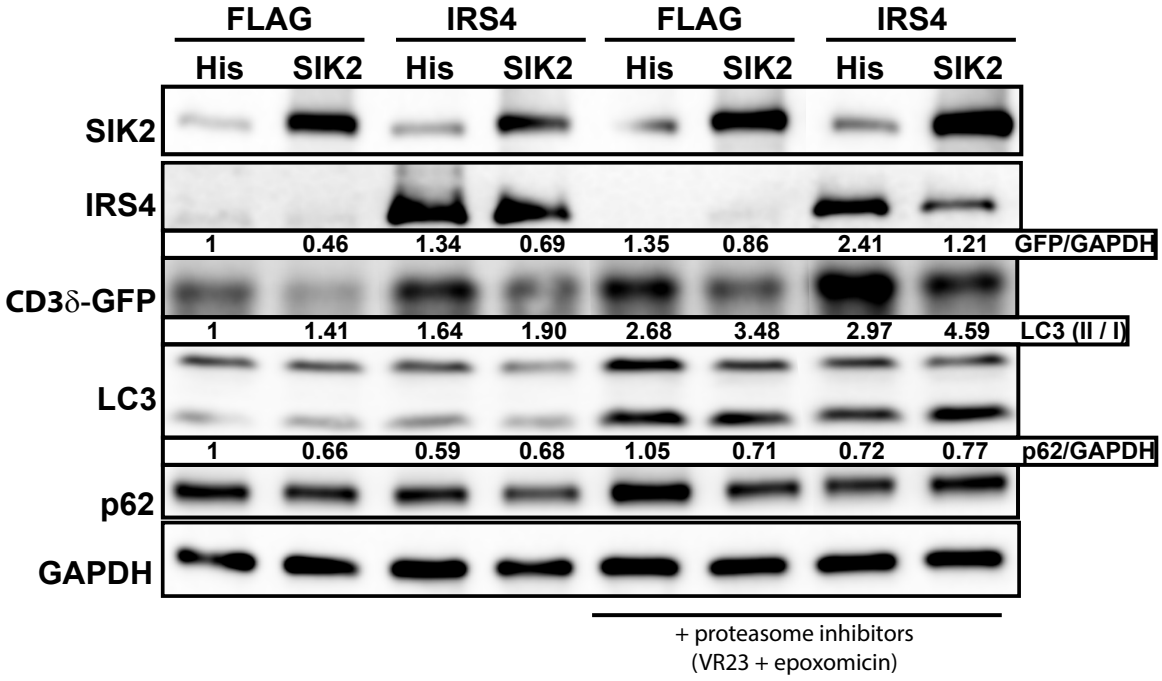

Figure 5.20. Effect of IRS4 overexpression on the stability of the recombinant CD3δ-GFP protein individually or together with SIK2 in the absence/presence of the proteasome inhibitors epoxomicin (250 nM) and VR23 (5 μM).

inhibitors did not equalize the CD3δ levels within samples. ERAD substrates are degraded by either the UPS or autophagy after their retranslocation into the cytosol. To probe the roles of IRS4 together with SIK2 in the autophagic clearance of ERAD substrates, the LC3-II/LC3-I ratio was examined. SIK2 over-expression (lane 1 and 2) consistently with the previously reported study [124] resulted in elevated LC3-II/LC3-I ratio which is an indication of increased autophagasome formation. Additionally, the ratio became higher in response to individual IRS4 overexpression (lane 1 and 3), but any synergistic effect of co-overexpression of SIK2 and IRS4 was not observed (lane 4). Inhibition of proteasome complex resulted in higher LC3-II/LC3-I ratio for each samples, but not changed the pattern within samples.

Stability of CD3δ-GFP was also checked by fluoroscence microscopy. As seen in Figure 5.21, the GFP fluoroscence increased in response to IRS4 overexpression and decreased when SIK2-WT was over-expressed either idividually or together with IRS4. The fluoroscence image seems to be consistent with the western blotting results (Figure 5.19).

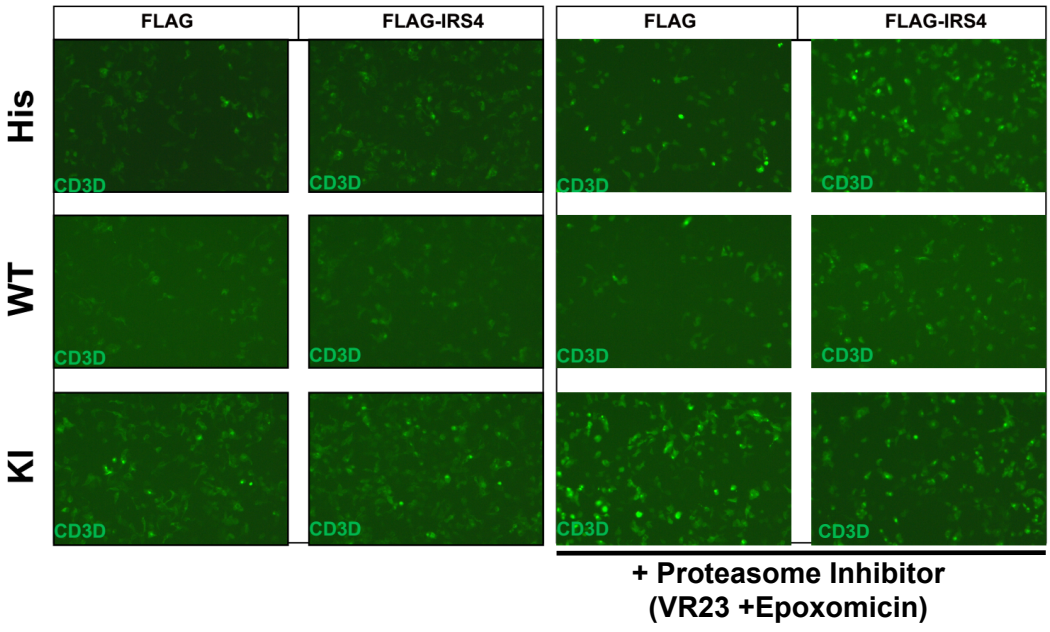

Figure 5.21. Effect of IRS4 and SIK2 on CD3δ-GFP fluoroscence in the absence/presence of proteasome inhibitors. WT:SIK2-wildtype, KI:SIK2-kinase inactive

5.6. SIK2-CHIP interaction

In phosphoproteomic data, a phospho-peptide (pSer19-pSer23) mapping to CHIP was detected specifically in the ER fraction of SIK2-WT over-expressing cells and its peptide abundance increased upon thapsigargin treatment (Figure 5.8). First, co-IP assay was performed to test possible interaction between SIK2 and CHIP. According to the first co-IP results, endogenous CHIP was immunoprecipitated with FLAG and HIS-tagged SIK2 (Figure 5.22).

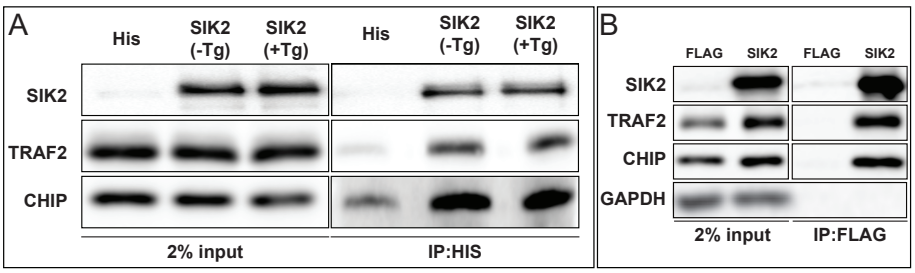

Figure 5.22. Co-immunopreciptation assays in 293T cells transiently overexpressing HIS-SIK2 (A) and FLAG-SIK2 (B).

Next, full-length and N-terminally deleted (Δ23) forms of CHIP were cloned into FLAG-tagged plasmids. Using these constructs, co-IP assays were carried out (Figure 5.23). Both endogenous(lane 2) and ectopically-expressed (HIS-tagged) SIK2 were immunoprecipitated with FLAG-tagged CHIP using the anti-FLAG antibody. N-terminal truncation of the first 23 amino acids of CHIP, where potential SIK2 phosphorylation sites reside, caused a weaker interaction for HIS-tagged SIK2 (lane 6) and the interaction almost disappeared for endogenous SIK2 (lane 3). Another finding from this experiment is that SIK2 protein levels decreased in response to over-expression of full-length CHIP and, to a lesser extent, N-terminal deleted form.

To test whether proteasomal degradation leads to this decline, cells were treated with proteasome inhibitors. As a result of Western blot analysis, we could not obtain any evidence to support that the decrease in SIK2 protein level is caused by CHIP-mediated proteasomal degradation (Figure 5.24). It was observed that over-expression of CHIP could reduce SIK2 level despite the inhibition of proteasome (lane 5 and 6).

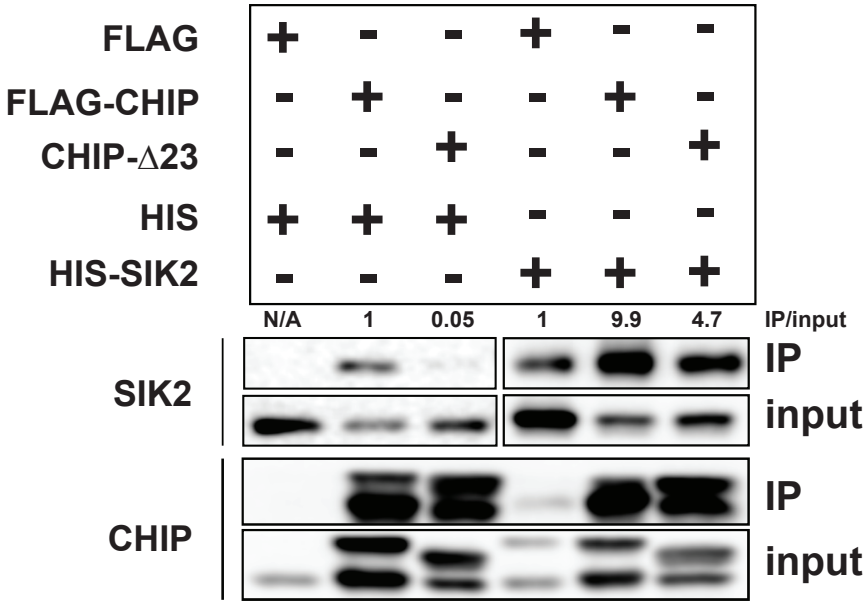

Figure 5.23. Co-immunopreciptation of endogenous and HIS-tagged SIK2 together with FLAG-tagged CHIP using the anti-FLAG antibody.

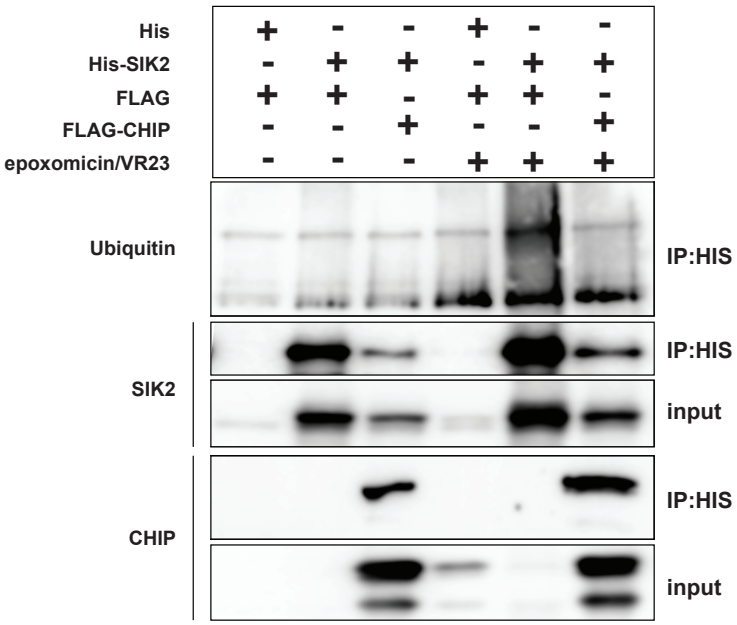

Figure 5.24. Western blot analysis of the immunoprecipitates from 293T cells transfected with indicated constructs. Cells were either untreated or treated with proteasome inhibitors.

6. DISCUSSION

As a consequence of the high-energy diet and sedentary lifestyle, obesity has reached epidemic levels worldwide. Obesity, with an increasing prevalence, has a high risk factor for the development of insulin resistance and type-2-diabetes. Several studies have shown that ER stress is involved in the pathalogic development of metabolic complications in obesity. Despite the accumulating evidence, it is not well known to what extent ER stress engages in, especially in different cell types. It is obvious that elucidating the relationship between ER-stress and metabolic diseases will facilitate the development of therapeutic interventions, as well as understanding the molecular aetiology of these diseases.

SIK2 is a serine/threonine kinase playing central roles in gluconeogenesis, lipogenesis and insulin signaling (See Section 1.3.1). Since SIK2 is involved in these metabolic pathways, it is an attractive pharmacological target for the development of therapautic drug against metabolic diseases such as insulin resistance, hepatic steatosis and type-2 diabetes. Recent studies have demonstrated that SIK2 has also critical roles in maintaining protein homeostasis by participating in ERAD, autophagy, and aggresome formation, which are also branches of the UPR. However, components of the protein regulatory networks in these biological processes, which are in cross-talk with SIK2, are not well known, yet.

Hitherto known protein interactions of SIK2 do not provide sufficient information to fully understand the role of SIK2 in aforementioned molecular mechanisms. Hence, we planned to use proteome-wide approaches as the first step to identify ER-localized proteins that are either directly phosphorylated or somehow regulated in response to increased SIK2 activity. For this purpose, ER fractions of stressed and unstressed 293T cells overexpressing the wildtype and kinase-inactive forms of SIK2 were isolated. ER-stress was induced by thapsigargin, which is more stable for a longer period in the cellular media compared to tunicamycin. Initial plan was using SIK2-overepxressing

stable HUH7 cells, hepatocyte derived cellular carcinoma cell line, for sub-proteomic studies. Although the metabolic and UPR pathways, in which SIK2 involved, are probably active, endoplasmic reticulum isolation was not efficient to provide enough amount of protein for the analysis part. Mass-spectrometry based label-free quantitative phospho-proteome analysis was performed with the protein samples isolated from ER-fractions to identify and quantify phospho-peptides. Based on peptide abundance scores we initially verified the Bip and SIK2 protein levels (Figure 5.4). In the phospho-proteome analysis, VCP, known SIK2 substrate, was found to be phosphorylated at its Ser770 residue in the cells expressing SIK2-WT upon thapsigargin treatment, consistently with the earlier report [123]. Furthermore, some phospho-residues of SIK2 were identified and their abundaces increased upon thapsigargin treatment. Two of them, Ser90 and Ser358 residues, were proposed in a study [159] as autophosphorylation sites and the latter was presented as a marker for SIK2 activity. The peptide containing pSer90 exihibited a sharp increase (around 60-fold) in its abundace upon thapsigargin treatment and identified only in SIK2-WT-overexpressing cells. Thapsigargin or overexpression dependent increase in phosphorylation of Ser358 was not observed. Because, we applied subproteome analysis, differential phospho-regulations of proteins within subcellular compartments might be possible. Then, GO-term and pathway enrichment analysis were made with UP (>2-fold increase) and DOWN (<0.5 decrease) protein sets. The most remarkable enriched term in the WT-UP proteins identified from full-protemic analysis was "IRE1-mediated unfolded protein response" (Figure 5.7). In phospho-proteomic analysis, "KEGG-Protein processing in endoplasmic reticulum" and "GO-BP-Protein folding" terms were found to be overrepresented in the SIK2-WT-UP protein set (Figure 5.7).

Around 20 of proteins in the candidate list, were selected as putative SIK2 substrates for further studies, taking into account their ER-related molecular functions. Initial co-IP assays were performed using primary antibodies against these proteins, but SIK2 was not detected in the majority of the immunoprecipitates (data not shown). Even if there were promising results for a few of them, considering time and cost we decided to use epitope-tagged recombinant proteins in co-IP studies. IRS4 was

one of the most intriguing proteins for us in the list, because of its involvement in insulin/leptin signaling and restricted expression in the arcuate nucleus of hypothalamus, where AgRP and POMC neurons are located. Intriguingly, the phopho-residue identified in mass-spec analyis, pSer64, is not present in other IRS isoforms (Figure 6.1) and the abundance of pSer64 containing phospho-peptide was found to be increased

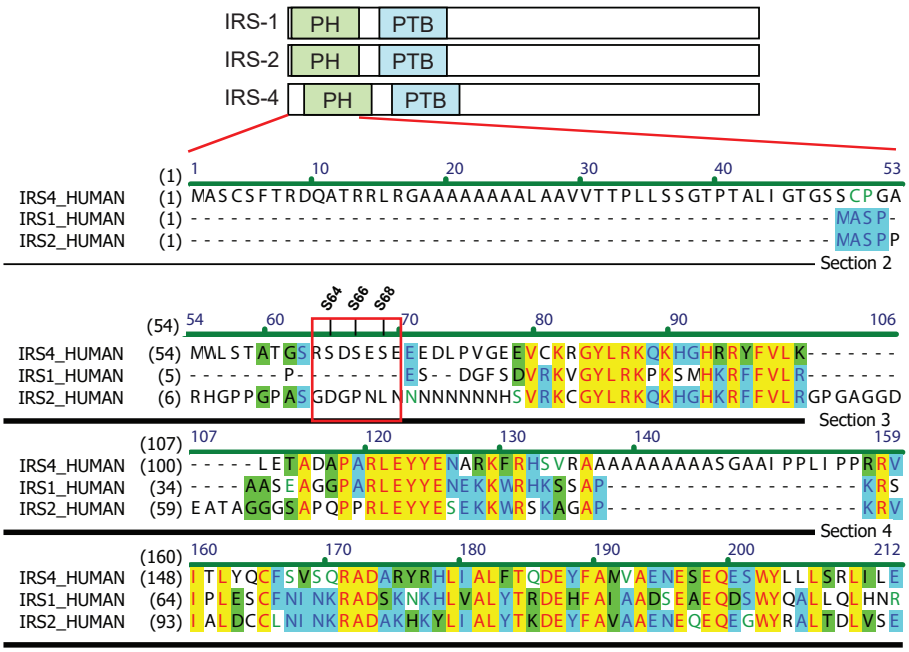

Figure 6.1. Multiple alignment of amino acid sequences of the human IRS proteins at indicated N-terminal regions.

in thapsigargin-treated cells overexpressing SIK2-WT (Figure 5.8). Therefore, experimental investigation of SIK2-IRS4 interaction was prioritized. The following co-IP experiments indicated an interaction between SIK2 and IRS4 (Figure 5.9) and deleting the PH and PTB domains weakened this interaction (Figure 5.11). This attenuation might be also due to the effect of truncated regions on the cellular localization or posttranslational modifications of IRS4. In a study, an inhibitory nuclear localization signal between the PH and PTB domains was suggested that deleting these domains caused accumulation of IRS4 in the nucleus [160]. It is plausible to suggest that phosphorylation of S64 by SIK2 may interfere with the nuclear localization of IRS4.

In the beginning of our project, we were speculating that SIK2, as a central mediator of the ERAD pathway, might be activated by the IRE1 signaling complex. A series of IP experiments were performed, but we were not able to capture IRE1-SIK2 interaction consistently. Detecting a kinase-kinase interaction is difficult, especially if one of the kinase is membrane localized. For this reason, instead of further studying the IRE1-SIK2 interaction, we focused on the other elements of the IRE1 signaling complex. We then found out that TRAF2 and CHIP, components of the IRE1/JNK pathway, interacts with SIK2 independently of ER-stress induction (Figure 5.22). Subsequently to this finding, we tested whether IRS4 interacts with IRE1. It was observed that IRS4 interacts with IRE1 in an ER-stress responsive manner (Figure 5.12 and 5.13) and the interaction was found to reach a maximum within 6 hours of thapsigargin treatment. The decline after a point might be informative about physiologic relevance of this interaction. It is known that at prolonged ER stress or later time points of thapsigargin treatment (after 4-6 hours), XBP1-splicing activity of IRE1 starts to decrease [161]. These co-IP results provided initial motivation to investigate possible effects of IRS4 on IRE1 signaling in the absence/presence of ER-stress. On the other hand, in ER-stressed condition SIK2 negatively affected the formation of the IRE1-IRS4 complex (Figure 5.16) independent of its kinase activity. However this does not exlude the idea that kinase inactive SIK2 may act as a dominat negative form to attenuate ERAD activity which may in turn increase the activity of endogenous SIK2 to dislodge IRS4 from IREsome complex.

To investigate the effects of IRS4 on IRE1/XBP1 signaling, XBP1 splicing activity was measured by XBP-YFP reporter assay and monitoring XBP1 transcript ratio (spliced/unspliced). As a result, some indications were obtained that IRS4 caused an increased XBP1 splicing activity (Figure 5.17B) and a delay in the timing of decline in the spliced-transcript ratio (Figure 5.17B). Later, IRS4 overexression was found to reduce the BiP protein amount to the basal level, which could be considered as an indication of recovery, under tunicamycin-induced ER stress (Figure 5.18). There are some major questions that need to be addressed concerning how IRS4 can execute such effects on the RNase activity of IRE1. Actually, this is directly related to the molecular

dynamics of the IRE1 signaling complex formation and activation states. IRE1 can trigger the activation of the XBP1 transcription factor and JNK pathway, having downstream effectors with distinct functions, which result in different physiological outputs in response to stress-condition. Order of IRE1 oligomerization and components of the IRE1 signaling complex are the main focus of the researches to decipher the molecular-switch mechanisms behind the regulation of IRE1 function [62, 162]. Hence, in the absence/presence of IRS4 examining the post-translational modifications of IRE1 and identifying other IREsome components could help to explore the physiological implications of this interaction.

Next, we investigated the possible involvement of IRS4 in the ERAD pathway. SIK2 has been previously found to phospho-regulate the ATPase activity of VCP, which mediates the retro-translocation of misfolded proteins from the ER lumen into the cytosol for their proteasomal degradation [123]. The degradation of CD3δ, which is a known ERAD substrate, was monitored to follow the changes in ERAD activity in response to IRS4 overexpression. IRS4 seems to prevent the reduction in the CD3δ level, but not when SIK2 is overexpressed (Figure 5.19). When using proteasome inhibitors, SIK2 enhanced the degradation of CD3δ to almost the same extent compared to untreated samples (Figure 5.20 and 5.21). Autophagy helps the mass-destruction of misfolded proteins. Autophagy and the UPS may not be mutually-exclusive to purge the misfolded proteins. By looking the LC3-II/LC3-I ratio, autophagic clearance of CD3δ in response to SIK2 and IRS4 overexpression was examined. Both IRS4 and SIK2 over-expressions increased the LC3-II/LC3-I ratio. The conversion of LC3-I to LC3-II is used as indication of autophagic activity, but inhibition of intermediate steps of autophagy, for instance inhibiting fusion of autophagasome with lysosome, can result in same output similar to increased autophagic activity. However, considering the role and requirement of SIK2 in the autophagosome-lysosome fusion reported in a study [124] and increased stability of CD3δ in response to IRS4 overexpression in our findings, we can speculate that IRS4 might negatively regulate autophagic activity. Another possibility is that IRS4 may participates in aggresome formation process preventing toxicity of misfolded proteins.

TRAF2 is also an adapter molecule in signal transduction of the TNF-α/NF-κB pathway, which is recruited to the plasma membrane upon stimulus. When we consider the cross-talk between ER stress and the inflammatory pathways (Section 1.2.7), whose molecular details are not well-known yet, probing the the possible roles of the IRS4-SIK2-TRAF2 molecular interactions in these pathways may be important in this aspect. Obesity is accepted as inflammatory condition that obese or overweight individuals have a low-grade systemic inflammation with elevated circulating blood inflammatory cytokine level [163]. Over-nutrion induced hypothalamic inflammation is an early event in the pathalogic development of metabolic diseases and disrupts the neuronal activities of the insulin/leptin sensitive cells in the arcuate nucleus of hypothalamus regulating energy balance and feeding behaviour [164]. The restricted expression of IRS4 in the ventral hypothalamus and arcuate nucleus [137] led us think of physiological relevance of these findings about the SIK2-IRS4 interaction in the insulin/leptin sensitive hypothalamic neurons (AgRP and POMC). Functional studies regarding ER stress, inflammatory pathways and insulin/leptin signaling, using a hypothalamic neuronal cell line, possess potential to yield intriguing results about this complex. We are currently pursuing the functional engagement of these IResome complex in the content of hyphothalamıc neurons.

Another issue not addressed in this study is the effect of IRS4 on RIDD activity. As an IRE1-interacting protein, IRS4 might regulate XBP1-independent RNase activity of IRE1, which causes decay of various ER-localized mRNAs. For this purpose, mRNA levels of known RIDD substrates (e.g. BLOSC and insulin) can be examined in response to ER-stress and genetic manipulation of IRS4.

As a result of the data obtained throughout this study, a molecular model can be drawn regarding the roles of the IRS4-SIK2 interaction in IRE1-XBP1 and ERAD pathways, as illustrated in Figure 6.2. Firstly, IRS4 and SIK2 may posses a molecular switch role between the IRE1/XBP1 signalling and protein degradation pathways by participating in the IRE1-signaling complex, autophagosome formation, or ERAD complex. In response to ER stress, SIK2, as a stress kinase, might be activated in

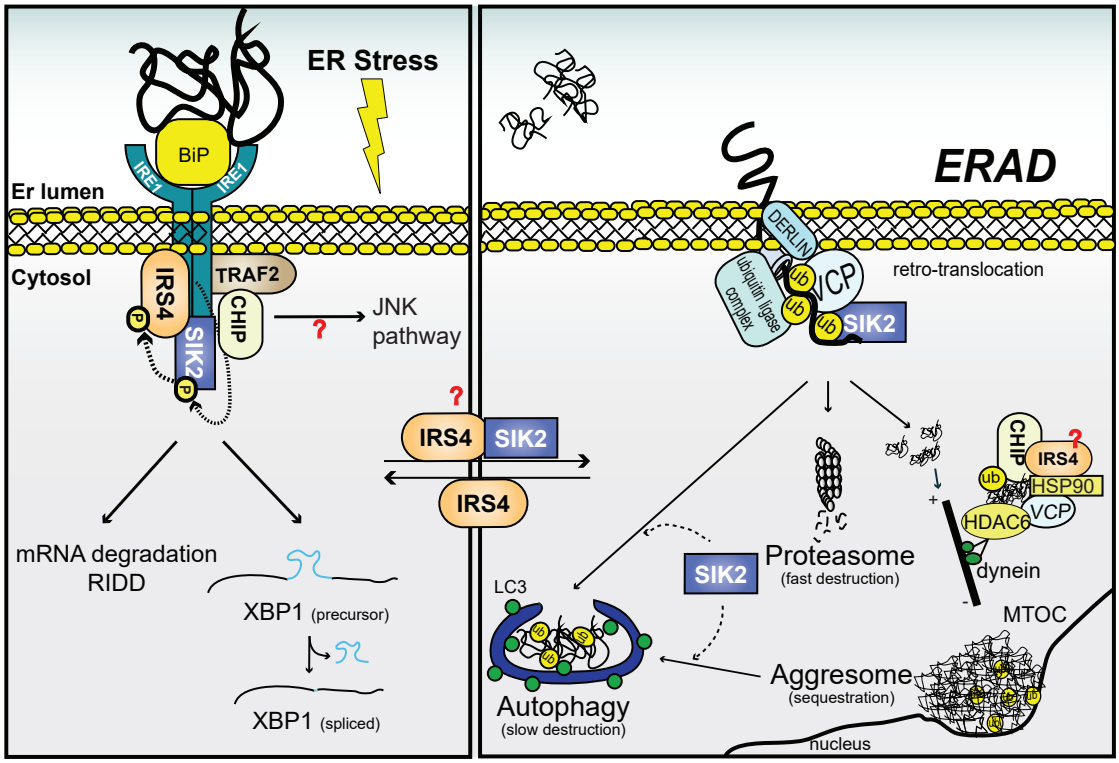

Figure 6.2. Proposed model suggesting molecular function of SIK2/IRS4/IRE1 signaling complex as a molecular switch between IRE1-mediated UPR and protein degradation pathways.

IRE1-dependent manner that LKB1 or elevated AMP/ATP ratio do not seem to take role as an upstream activator of SIK2 in its ERAD function [123]. In prolonged ER stress, SIK2 might disassociate IRS4 from IREsome complex resulting in decreased XBP1 splicing activity of IRE1.

CHIP was another candidate protein identified in the phospho-proteome study (Figure 5.8). The interaction between SIK2 and CHIP was detected by co-IP experiments (Figure 5.22). SIK2 protein level was also found to be decreased in response to over-expression of full-length CHIP and this decline seems to be unaffected upon proteasome inhibition (Figure 5.24). To test whether SIK2 is degraded during the autophagic process along with the client proteins, autophagic defective cells (e.g Atg5 knock-out cells) will be used for further studies. CHIP is an E3-ligase and other than tagging proteins for their proteasomal degradation, it has regulatory roles on proteins

with distinct functions, for example chaperones and kinases [165]. As mentioned earlier, CHIP regulates the IRE1/JNK pathway through direct ubiquitination of IRE1 [105] that ubiquitination of IRE1 can be examined in response to genetic manipulation of SIK2/CHIP and using phospho-mutants CHIP forms. CHIP regulates the NF-κB pathway through the degradation of TRAF2 [147], which was found to interact with SIK2 in this study. As suggested in the SIK2-IRS4 interaction, the possible effects of the CHIP-SIK2 interaction on this pathway will be evaluated. A recent raper has reported that CHIP negatively regulates insuling signaling through ubiquitination and subsequent degradation of insulin-receptor [166]. In addition to this study, considering CHIP-mediated degradation of PPARγ [146], SIK2-CHIP interaction may possess important function in metabolic pathways. SIK2 regulates insulin secretion in pancreatic β-cells through phosphorylation/degradation of CDK5R1, activator of CDK5 (cylic-dependen kinase 5) [119]. Interestingly, phosphorylation of CHIP by CDK5 has been documented, which disrupts the substrate binding of CHIP and causes neuronal cell death [167]. We identified the same residue in our phospho-proteomic analysis with increased peptide abundance in response to ER stress and SIK2-overexpression. In this context, it may be interesting to examine the effects of SIK2-CHIP interaction together with CDK5 activity on insulin secretion and neuronal cell death (Figure 6.3).

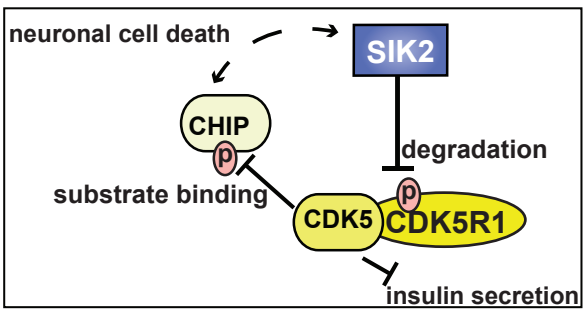

Figure 6.3. Molecular functions of CDK5 complex in neuronal cell death and insulin secretion, to which SIK2 and CHIP contribute as regulators.

Apart from CHIP and IRS4, studies on ATG9A and RNF139 from the candidate list shown in Figure 5.8 are ongoing. ATG9A, which is an autophagy related gene localized to ER-membrane, contributes to autophagasome formation upon nutritional

stress [168]. Any finding concerning ATG9A-SIK2 interaction will help to enlighten molecular details of the link between ER-stress and autophagy. RNF139 is an ER-resident E3-ligase, has been previously found to involve in ER-stress response through regulating the degradation of misfolded proteins in hepatocytes [169].

To sum up, results of this study strongly suggest novel interactions with a potential physiological relevance, especially in IRE1 signaling and proteostasis, whose dysregulations underlies the pathologic development of metabolic and neurological diseases. Therefore, we will expand our studies investigating eventual roles of these interactions in ER homeostasis, as the possible outputs from this work can create new opportıuties for the development of new therapeutic intervention.

REFERENCES

1. World Health Organization, "Obesity and overweight", 2016, `http://www.who.int/mediacentre/factsheets/fs311/en/`, accessed at January 2017.

2. Haslam, D. W. and W. P. T. James, "Obesity.", *Lancet*, Vol. 366, pp. 1197–1209, October 2005.

3. World Health Organization, "Global reports on diabetes", 2016, `http://www.who.int/diabetes/global-report/en/`, accessed at January 2017.

4. Barja-Fernandez, S., R. Leis, F. F. Casanueva and L. M. Seoane, "Drug development strategies for the treatment of obesity: how to ensure efficacy, safety, and sustainable weight loss.", *Drug Design, Development and Therapy*, Vol. 8, pp. 2391–2400, December 2014.

5. Anand, B. K. and J. R. Brobeck, "Localization of a 'feeding center' in the hypothalamus of the rat.", *Proceedings of the Society for Experimental Biology and Medicine*, Vol. 77, pp. 323–324, June 1951.

6. Leibowitz, S. F. and K. E. Wortley, "Hypothalamic control of energy balance: different peptides, different functions.", *Peptides*, Vol. 25, pp. 473–504, March 2004.

7. Hahn, T. M., J. F. Breininger, D. G. Baskin and M. W. Schwartz, "Coexpression of Agrp and NPY in fasting-activated hypothalamic neurons.", *Nature Neuroscience*, Vol. 1, pp. 271–272, August 1998.

8. Stanley, B. G., S. E. Kyrkouli, S. Lampert and S. F. Leibowitz, "Neuropeptide Y

chronically injected into the hypothalamus: a powerful neurochemical inducer of hyperphagia and obesity.", *Peptides*, Vol. 7, pp. 1189–1192, December 1986.

9. Halaas, J. L., K. S. Gajiwala, M. Maffei, S. L. Cohen *et al.*, "Weight-reducing effects of the plasma protein encoded by the obese gene", *Science*, Vol. 269, No. 5223, p. 543, July 1995.

10. Cowley, M. A., J. L. Smart, M. Rubinstein, M. G. Cerdan, S. Diano, T. L. Horvath, R. D. Cone and M. J. Low, "Leptin activates anorexigenic POMC neurons through a neural network in the arcuate nucleus.", *Nature*, Vol. 411, pp. 480–484, May 2001.

11. Farooqi, I. S., S. A. Jebb, G. Langmack, E. Lawrence, C. H. Cheetham, A. M. Prentice, I. A. Hughes, M. A. McCamish and S. O'Rahilly, "Effects of recombinant leptin therapy in a child with congenital leptin deficiency.", *The New England Journal of Medicine*, Vol. 341, pp. 879–884, September 1999.

12. Frederich, R. C., A. Hamann, S. Anderson, B. Löllmann, B. B. Lowell and J. S. Flier, "Leptin levels reflect body lipid content in mice: evidence for diet-induced resistance to leptin action", *Nature Medicine*, Vol. 1, No. 12, pp. 1311–1314, December 1995.

13. Maffei, M., J. Halaas, E. Ravussin, R. Pratley, G. Lee, Y. Zhang, H. Fei, S. Kim, R. Lallone, S. Ranganathan *et al.*, "Leptin levels in human and rodent: measurement of plasma leptin and ob RNA in obese and weight-reduced subjects", *Nature Medicine*, Vol. 1, No. 11, pp. 1155–1161, November 1995.

14. van den Top, M., K. Lee, A. D. Whyment, A. M. Blanks and D. Spanswick, "Orexigen-sensitive NPY/AgRP pacemaker neurons in the hypothalamic arcuate nucleus.", *Nature Neuroscience*, Vol. 7, pp. 493–494, May 2004.

15. Breen, T. L., I. M. Conwell and S. L. Wardlaw, "Effects of fasting, leptin, and

insulin on AGRP and POMC peptide release in the hypothalamus.", *Brain Research*, Vol. 1032, pp. 141–148, January 2005.

16. Griffin, M. E., M. J. Marcucci, G. W. Cline, K. Bell, N. Barucci, D. Lee, L. J. Goodyear, E. W. Kraegen, M. F. White and G. I. Shulman, "Free fatty acid-induced insulin resistance is associated with activation of protein kinase C theta and alterations in the insulin signaling cascade.", *Diabetes*, Vol. 48, pp. 1270–1274, June 1999.

17. Posey, K. A., D. J. Clegg, R. L. Printz, J. Byun, G. J. Morton, A. Vivekanandan-Giri, S. Pennathur, D. G. Baskin, J. W. Heinecke, S. C. Woods, M. W. Schwartz and K. D. Niswender, "Hypothalamic proinflammatory lipid accumulation, inflammation, and insulin resistance in rats fed a high-fat diet.", *American Journal of Physiology, Endocrinology and Metabolism*, Vol. 296, pp. E1003–E1012, May 2009.

18. Hotamisligil, G. S. and E. Erbay, "Nutrient sensing and inflammation in metabolic diseases.", *Nature Reviews. Immunology*, Vol. 8, pp. 923–934, December 2008.

19. Lumeng, C. N. and A. R. Saltiel, "Inflammatory links between obesity and metabolic disease.", *The Journal of Clinical Investigation*, Vol. 121, pp. 2111–2117, June 2011.

20. Ozcan, U., Q. Cao, E. Yilmaz, A.-H. Lee, N. N. Iwakoshi, E. Ozdelen, G. Tuncman, C. Grgn, L. H. Glimcher and G. S. Hotamisligil, "Endoplasmic reticulum stress links obesity, insulin action, and type 2 diabetes.", *Science*, Vol. 306, No. 5695, pp. 457–461, October 2004.

21. Hotamisligil, G. S., "Inflammation and endoplasmic reticulum stress in obesity and diabetes.", *International Journal of Obesity*, Vol. 32 Suppl 7, pp. S52–S54, December 2008.

22. Yang, L., P. Li, S. Fu, E. S. Calay and G. S. Hotamisligil, "Defective hepatic autophagy in obesity promotes ER stress and causes insulin resistance.", *Cell Metabolism*, Vol. 11, pp. 467–478, June 2010.

23. Nunez, C. E., V. S. Rodrigues, F. S. Gomes, R. F. d. Moura, S. C. Victorio, B. Bombassaro, E. A. Chaim, J. C. Pareja, B. Geloneze, L. A. Velloso and E. P. Araujo, "Defective regulation of adipose tissue autophagy in obesity.", *International Journal of Obesity*, Vol. 37, pp. 1473–1480, November 2013.

24. Meng, Q. and D. Cai, "Defective hypothalamic autophagy directs the central pathogenesis of obesity via the IkappaB kinase beta (IKKbeta)/NF-kappaB pathway.", *The Journal of Biological Chemistry*, Vol. 286, pp. 32324–32332, September 2011.

25. Fantuzzi, G., "Adipose tissue, adipokines, and inflammation.", *The Journal of Allergy and Clinical Immunology*, Vol. 115, pp. 911–9; quiz 920, May 2005.

26. Kawano, J. and R. Arora, "The role of adiponectin in obesity, diabetes, and cardiovascular disease.", *Journal of the Cardiometabolic Syndrome*, Vol. 4, pp. 44–49, January 2009.

27. Steppan, C. M., S. T. Bailey, S. Bhat, E. J. Brown, R. R. Banerjee, C. M. Wright, H. R. Patel, R. S. Ahima and M. A. Lazar, "The hormone resistin links obesity to diabetes.", *Nature*, Vol. 409, pp. 307–312, January 2001.

28. Antuna-Puente, B., B. Feve, S. Fellahi and J.-P. Bastard, "Adipokines: the missing link between insulin resistance and obesity.", *Diabetes & Metabolism*, Vol. 34, pp. 2–11, February 2008.

29. Kadowaki, T., T. Yamauchi, N. Kubota, K. Hara, K. Ueki and K. Tobe, "Adiponectin and adiponectin receptors in insulin resistance, diabetes, and the metabolic syndrome.", *The Journal of Clinical Investigation*, Vol. 116, pp. 1784–

1792, July 2006.

30. Zhang, X., G. Zhang, H. Zhang, M. Karin, H. Bai and D. Cai, "Hypothalamic IKKbeta/NF-kappaB and ER stress link overnutrition to energy imbalance and obesity.", *Cell*, Vol. 135, pp. 61–73, October 2008.

31. Uysal, K. T., S. M. Wiesbrock, M. W. Marino and G. S. Hotamisligil, "Protection from obesity-induced insulin resistance in mice lacking TNF-alpha function.", *Nature*, Vol. 389, pp. 610–614, October 1997.

32. Prada, P. O., H. G. Zecchin, A. L. Gasparetti, M. A. Torsoni, M. Ueno, A. E. Hirata, M. E. Corezola do Amaral, N. F. Her, A. C. Boschero and M. J. A. Saad, "Western diet modulates insulin signaling, c-Jun N-terminal kinase activity, and insulin receptor substrate-1ser307 phosphorylation in a tissue-specific fashion.", *Endocrinology*, Vol. 146, pp. 1576–1587, March 2005.

33. Hotamisligil, G. S., P. Peraldi, A. Budavari, R. Ellis, M. F. White and B. M. Spiegelman, "IRS-1-mediated inhibition of insulin receptor tyrosine kinase activity in TNF-alpha- and obesity-induced insulin resistance.", *Science*, Vol. 271, pp. 665–668, February 1996.

34. Purkayastha, S., G. Zhang and D. Cai, "Uncoupling the mechanisms of obesity and hypertension by targeting hypothalamic IKK-B and NF-KB.", *Nature Medicine*, Vol. 17, pp. 883–887, June 2011.

35. Niswender, K. D., G. J. Morton, W. H. Stearns, C. J. Rhodes, M. G. Myers and M. W. Schwartz, "Intracellular signalling. Key enzyme in leptin-induced anorexia.", *Nature*, Vol. 413, pp. 794–795, October 2001.

36. Harris, M., C. Aschkenasi, C. F. Elias, A. Chandrankunnel, E. A. Nillni, C. Bjorbaek, J. K. Elmquist, J. S. Flier and A. N. Hollenberg, "Transcriptional regulation of the thyrotropin-releasing hormone gene by leptin and melanocortin signaling.",

The Journal of Clinical Investigation, Vol. 107, pp. 111–120, January 2001.

37. Hakansson, M. L. and B. Meister, "Transcription factor STAT3 in leptin target neurons of the rat hypothalamus.", *Neuroendocrinology*, Vol. 68, pp. 420–427, December 1998.

38. Kitamura, T., Y. Feng, Y. I. Kitamura, S. C. Chua, A. W. Xu, G. S. Barsh, L. Rossetti and D. Accili, "Forkhead protein FoxO1 mediates Agrp-dependent effects of leptin on food intake.", *Nature Medicine*, Vol. 12, pp. 534–540, May 2006.

39. Ren, H., I. J. Orozco, Y. Su, S. Suyama, R. Gutierrez-Juarez, T. L. Horvath, S. L. Wardlaw, L. Plum, O. Arancio and D. Accili, "FoxO1 target Gpr17 activates AgRP neurons to regulate food intake.", *Cell*, Vol. 149, pp. 1314–1326, June 2012.

40. Plum, L., H. V. Lin, R. Dutia, J. Tanaka, K. S. Aizawa, M. Matsumoto, A. J. Kim, N. X. Cawley, J.-H. Paik, Y. P. Loh, R. A. DePinho, S. L. Wardlaw and D. Accili, "The obesity susceptibility gene Cpe links FoxO1 signaling in hypothalamic pro-opiomelanocortin neurons with regulation of food intake.", *Nature Medicine*, Vol. 15, pp. 1195–1201, October 2009.

41. Bjrbaek, C., J. K. Elmquist, J. D. Frantz, S. E. Shoelson and J. S. Flier, "Identification of SOCS-3 as a potential mediator of central leptin resistance.", *Molecular Cell*, Vol. 1, pp. 619–625, March 1998.

42. Mayer-Davis, E. J., S. Levin, R. N. Bergman, R. B. D'Agostino, A. J. Karter, M. F. Saad and I. R. A. S. (IRAS), "Insulin secretion, obesity, and potential behavioral influences: results from the Insulin Resistance Atherosclerosis Study (IRAS).", *Diabetes/Metabolism Research and Reviews*, Vol. 17, pp. 137–145, March 2001.

43. Cao, W., H.-Y. Liu, T. Hong and Z. Liu, "Excess exposure to insulin may be

the primary cause of insulin resistance.", *American Journal of Physiology, Endocrinology and Metabolism*, Vol. 298, p. E372, February 2010.

44. Boden, G. and G. I. Shulman, "Free fatty acids in obesity and type 2 diabetes: defining their role in the development of insulin resistance and beta-cell dysfunction.", *European Journal of Clinical Investigation*, Vol. 32 Suppl 3, pp. 14–23, June 2002.

45. Pankow, J. S., B. B. Duncan, M. I. Schmidt, C. M. Ballantyne, D. J. Couper, R. C. Hoogeveen, S. H. Golden and A. R. in Communities Study, "Fasting plasma free fatty acids and risk of type 2 diabetes: the atherosclerosis risk in communities study.", *Diabetes Care*, Vol. 27, pp. 77–82, January 2004.

46. Paolisso, G., P. A. Tataranni, J. E. Foley, C. Bogardus, B. V. Howard and E. Ravussin, "A high concentration of fasting plasma non-esterified fatty acids is a risk factor for the development of NIDDM.", *Diabetologia*, Vol. 38, pp. 1213–1217, October 1995.

47. Holzer, R. G., E.-J. Park, N. Li, H. Tran, M. Chen, C. Choi, G. Solinas and M. Karin, "Saturated fatty acids induce c-Src clustering within membrane subdomains, leading to JNK activation.", *Cell*, Vol. 147, pp. 173–184, September 2011.

48. Boden, G., "Obesity, insulin resistance and free fatty acids.", *Current Opinion in Endocrinology, Diabetes, and Obesity*, Vol. 18, pp. 139–143, April 2011.

49. Pal, D., S. Dasgupta, R. Kundu, S. Maitra, G. Das, S. Mukhopadhyay, S. Ray, S. S. Majumdar and S. Bhattacharya, "Fetuin-A acts as an endogenous ligand of TLR4 to promote lipid-induced insulin resistance.", *Nature Medicine*, Vol. 18, pp. 1279–1285, August 2012.

50. Cox, J. S. and P. Walter, "A novel mechanism for regulating activity of a tran-

scription factor that controls the unfolded protein response.", *Cell*, Vol. 87, pp. 391–404, November 1996.

51. Kaufman, R. J., "Stress signaling from the lumen of the endoplasmic reticulum: coordination of gene transcriptional and translational controls.", *Genes & Development*, Vol. 13, No. 10, pp. 1211–1233, May 1999.

52. Harding, H. P., Y. Zhang and D. Ron, "Protein translation and folding are coupled by an endoplasmic-reticulum-resident kinase.", *Nature*, Vol. 397, No. 6716, pp. 271–274, January 1999.

53. Travers, K. J., C. K. Patil, L. Wodicka, D. J. Lockhart, J. S. Weissman and P. Walter, "Functional and genomic analyses reveal an essential coordination between the unfolded protein response and ER-associated degradation.", *Cell*, Vol. 101, No. 3, pp. 249–258, April 2000.

54. McCracken, A. A. and J. L. Brodsky, "Assembly of ER-associated protein degradation in vitro: dependence on cytosol, calnexin, and ATP.", *The Journal of Cell Biology*, Vol. 132, No. 3, pp. 291–298, February 1996.

55. Kruse, K. B., J. L. Brodsky and A. A. McCracken, "Autophagy: an ER protein quality control process.", *Autophagy*, Vol. 2, pp. 135–137, April 2006.

56. Bernales, S., K. L. McDonald and P. Walter, "Autophagy counterbalances endoplasmic reticulum expansion during the unfolded protein response.", *PLoS Biology*, Vol. 4, p. e423, November 2006.

57. Rasheva, V. I. and P. M. Domingos, "Cellular responses to endoplasmic reticulum stress and apoptosis.", *Apoptosis*, Vol. 14, pp. 996–1007, August 2009.

58. Woo, C. W., D. Cui, J. Arellano, B. Dorweiler, H. Harding, K. A. Fitzgerald, D. Ron and I. Tabas, "Adaptive suppression of the ATF4-CHOP branch of the unfolded protein response by toll-like receptor signalling.", *Nature Cell Biology*,

Vol. 11, pp. 1473–1480, December 2009.

59. Bertolotti, A., Y. Zhang, L. M. Hendershot, H. P. Harding and D. Ron, "Dynamic interaction of BiP and ER stress transducers in the unfolded-protein response.", *Nature Cell Biology*, Vol. 2, No. 6, pp. 326–332, June 2000.

60. Kimata, Y., Y. Ishiwata-Kimata, T. Ito, A. Hirata, T. Suzuki, D. Oikawa, M. Takeuchi and K. Kohno, "Two regulatory steps of ER-stress sensor Ire1 involving its cluster formation and interaction with unfolded proteins", *Journal of Cell Biology*, Vol. 179, No. 1, pp. 75–86, October 2007.

61. Oikawa, D., Y. Kimata and K. Kohno, "Self-association and BiP dissociation are not sufficient for activation of the ER stress sensor Ire1.", *Journal of Cell Science*, Vol. 120, pp. 1681–1688, May 2007.

62. Zhou, J., C. Y. Liu, S. H. Back, R. L. Clark, D. Peisach, Z. Xu and R. J. Kaufman, "The crystal structure of human IRE1 luminal domain reveals a conserved dimerization interface required for activation of the unfolded protein response.", *Proceedings of the National Academy of Sciences of the United States of America*, Vol. 103, pp. 14343–14348, September 2006.

63. Sidrauski, C. and P. Walter, "The transmembrane kinase Ire1p is a site-specific endonuclease that initiates mRNA splicing in the unfolded protein response.", *Cell*, Vol. 90, No. 6, pp. 1031–1039, September 1997.

64. Calfon, M., H. Zeng, F. Urano, J. H. Till, S. R. Hubbard, H. P. Harding, S. G. Clark and D. Ron, "IRE1 couples endoplasmic reticulum load to secretory capacity by processing the XBP-1 mRNA.", *Nature*, Vol. 415, No. 6867, pp. 92–96, January 2002.

65. Yoshida, H., "Unconventional splicing of XBP-1 mRNA in the unfolded protein response.", *Antioxidants & redox signaling*, Vol. 9, No. 12, pp. 2323–2333, De-

cember 2007.

66. Wang, S. and R. J. Kaufman, "The impact of the unfolded protein response on human disease", *Journal of Cell Biology*, Vol. 197, No. 7, pp. 857–867, June 2012.

67. Hollien, J., J. H. Lin, H. Li, N. Stevens, P. Walter and J. S. Weissman, "Regulated Ire1-dependent decay of messenger RNAs in mammalian cells", *The Journal of Cell Biology*, Vol. 186, No. 3, pp. 323–331, August 2009.

68. Urano, F., X. Wang, A. Bertolotti, Y. Zhang, P. Chung, H. P. Harding and D. Ron, "Coupling of stress in the ER to activation of JNK protein kinases by transmembrane protein kinase IRE1.", *Science*, Vol. 287, No. 5453, pp. 664–666, January 2000.

69. Nishitoh, H., A. Matsuzawa, K. Tobiume, K. Saegusa, K. Takeda, K. Inoue, S. Hori, A. Kakizuka and H. Ichijo, "ASK1 is essential for endoplasmic reticulum stress-induced neuronal cell death triggered by expanded polyglutamine repeats", *Genes & Development*, Vol. 16, No. 11, pp. 1345–1355, June 2002.

70. Mauro, C., E. Crescenzi, R. De Mattia, F. Pacifico, S. Mellone, S. Salzano, C. de Luca, L. D'Adamio, G. Palumbo, S. Formisano, P. Vito and A. Leonardi, "Central role of the scaffold protein tumor necrosis factor receptor-associated factor 2 in regulating endoplasmic reticulum stress-induced apoptosis.", *The Journal of Biological Chemistry*, Vol. 281, pp. 2631–2638, February 2006.

71. Ogata, M., S.-i. Hino, A. Saito, K. Morikawa, S. Kondo, S. Kanemoto, T. Murakami, M. Taniguchi, I. Tanii, K. Yoshinaga, S. Shiosaka, J. A. Hammarback, F. Urano and K. Imaizumi, "Autophagy is activated for cell survival after endoplasmic reticulum stress.", *Molecular and Cellular Biology*, Vol. 26, pp. 9220–9231, December 2006.

72. Cheng, X., H. Liu, C.-C. Jiang, L. Fang, C. Chen, X.-D. Zhang and Z.-

W. Jiang, "Connecting endoplasmic reticulum stress to autophagy through IRE1/JNK/beclin-1 in breast cancer cells.", *International Journal of Molecular Medicine*, Vol. 34, pp. 772–781, September 2014.

73. Margariti, A., H. Li, T. Chen, D. Martin, G. Vizcay-Barrena, S. Alam, E. Karamariti, Q. Xiao, A. Zampetaki, Z. Zhang, W. Wang, Z. Jiang, C. Gao, B. Ma, Y.-G. Chen, G. Cockerill, Y. Hu, Q. Xu and L. Zeng, "XBP1 mRNA splicing triggers an autophagic response in endothelial cells through BECLIN-1 transcriptional activation.", *The Journal of Biological Chemistry*, Vol. 288, pp. 859–872, January 2013.

74. Harding, H. P., I. Novoa, Y. Zhang, H. Zeng, R. Wek, M. Schapira and D. Ron, "Regulated translation initiation controls stress-induced gene expression in mammalian cells.", *Molecular Cell*, Vol. 6, No. 5, pp. 1099–1108, November 2000.

75. Vattem, K. M. and R. C. Wek, "Reinitiation involving upstream ORFs regulates ATF4 mRNA translation in mammalian cells.", *Proceedings of the National Academy of Sciences of the United States of America*, Vol. 101, No. 31, pp. 11269–11274, August 2004.

76. Zinszner, H., M. Kuroda, X. Wang, N. Batchvarova, R. T. Lightfoot, H. Remotti, J. L. Stevens and D. Ron, "CHOP is implicated in programmed cell death in response to impaired function of the endoplasmic reticulum.", *Genes & Development*, Vol. 12, No. 7, pp. 982–995, April 1998.

77. McCullough, K. D., J. L. Martindale, L. O. Klotz, T. Y. Aw and N. J. Holbrook, "Gadd153 sensitizes cells to endoplasmic reticulum stress by down-regulating Bcl2 and perturbing the cellular redox state.", *Molecular and Cellular Biology*, Vol. 21, No. 4, pp. 1249–1259, February 2001.

78. Shen, J., X. Chen, L. Hendershot and R. Prywes, "ER stress regulation of ATF6 localization by dissociation of BiP/GRP78 binding and unmasking of Golgi local-

ization signals.", *Developmental Cell*, Vol. 3, pp. 99–111, July 2002.

79. Bommiasamy, H., S. H. Back, P. Fagone, K. Lee, S. Meshinchi, E. Vink, R. Sriburi, M. Frank, S. Jackowski, R. J. Kaufman and J. W. Brewer, "ATF6alpha induces XBP1-independent expansion of the endoplasmic reticulum.", *Journal of Cell Science*, Vol. 122, No. Pt 10, pp. 1626–1636, May 2009.

80. Johnston, J. A., C. L. Ward and R. R. Kopito, "Aggresomes: a cellular response to misfolded proteins.", *The Journal of Cell Biology*, Vol. 143, pp. 1883–1898, December 1998.

81. Garcia-Mata, R., Y.-S. Gao and E. Sztul, "Hassles with taking out the garbage: aggravating aggresomes.", *Traffic*, Vol. 3, pp. 388–396, June 2002.

82. Qin, L., Z. Wang, L. Tao and Y. Wang, "ER stress negatively regulates AKT/TSC/mTOR pathway to enhance autophagy.", *Autophagy*, Vol. 6, pp. 239–247, February 2010.

83. Lee, E. K., J. U. Jeong, J. W. Chang, W. S. Yang, S. B. Kim, S. K. Park, J. S. Park and S. K. Lee, "Activation of AMP-activated protein kinase inhibits albumin-induced endoplasmic reticulum stress and apoptosis through inhibition of reactive oxygen species.", *Nephron. Experimental Nephrology*, Vol. 121, pp. e38–e48, October 2012.

84. B'chir, W., A.-C. Maurin, V. Carraro, J. Averous, C. Jousse, Y. Muranishi, L. Parry, G. Stepien, P. Fafournoux and A. Bruhat, "The eIF2a/ATF4 pathway is essential for stress-induced autophagy gene expression.", *Nucleic Acids Research*, Vol. 41, pp. 7683–7699, September 2013.

85. Yorimitsu, T., U. Nair, Z. Yang and D. J. Klionsky, "Endoplasmic reticulum stress triggers autophagy.", *The Journal of Biological Chemistry*, Vol. 281, pp. 30299–30304, October 2006.

86. Lee, H., J.-Y. Noh, Y. Oh, Y. Kim, J.-W. Chang, C.-W. Chung, S.-T. Lee, M. Kim, H. Ryu and Y.-K. Jung, "IRE1 plays an essential role in ER stress-mediated aggregation of mutant huntingtin via the inhibition of autophagy flux.", *Human Molecular Genetics*, Vol. 21, pp. 101–114, January 2012.

87. Zhou, Y., J. Lee, C. M. Reno, C. Sun, S. W. Park, J. Chung, J. Lee, S. J. Fisher, M. F. White, S. B. Biddinger and U. Ozcan, "Regulation of glucose homeostasis through a XBP-1-FoxO1 interaction.", *Nature Medicine*, Vol. 17, pp. 356–365, March 2011.

88. Guo, Q., Q. Shi, H. Li, J. Liu, S. Wu, H. Sun and B. Zhou, "Glycolipid Metabolism Disorder in the Liver of Obese Mice Is Improved by TUDCA via the Restoration of Defective Hepatic Autophagy.", *International Journal of Endocrinology*, Vol. 2015, p. 687938, November 2015.

89. Kim, O.-K., D.-E. Nam, W. Jun and J. Lee, "Cudrania tricuspidata water extract improved obesity-induced hepatic insulin resistance in db/db mice by suppressing ER stress and inflammation.", *Food & Nutrition Research*, Vol. 59, p. 29165, October 2015.

90. Kars, M., L. Yang, M. F. Gregor, B. S. Mohammed, T. A. Pietka, B. N. Finck, B. W. Patterson, J. D. Horton, B. Mittendorfer, G. S. Hotamisligil and S. Klein, "Tauroursodeoxycholic Acid may improve liver and muscle but not adipose tissue insulin sensitivity in obese men and women.", *Diabetes*, Vol. 59, pp. 1899–1905, August 2010.

91. Mao, T., M. Shao, Y. Qiu, J. Huang, Y. Zhang, B. Song, Q. Wang, L. Jiang, Y. Liu, J.-D. J. Han, P. Cao, J. Li, X. Gao, L. Rui, L. Qi, W. Li and Y. Liu, "PKA phosphorylation couples hepatic inositol-requiring enzyme 1alpha to glucagon signaling in glucose metabolism.", *Proceedings of the National Academy of Sciences of the United States of America*, Vol. 108, pp. 15852–15857, September 2011.

92. Rutkowski, D. T., J. Wu, S.-H. Back, M. U. Callaghan, S. P. Ferris, J. Iqbal, R. Clark, H. Miao, J. R. Hassler, J. Fornek, M. G. Katze, M. M. Hussain, B. Song, J. Swathirajan, J. Wang, G. D.-Y. Yau and R. J. Kaufman, "UPR pathways combine to prevent hepatic steatosis caused by ER stress-mediated suppression of transcriptional master regulators.", *Developmental Cell*, Vol. 15, No. 6, pp. 829–840, December 2008.

93. Ozcan, U., E. Yilmaz, L. Ozcan, M. Furuhashi, E. Vaillancourt, R. O. Smith, C. Z. Grgn and G. S. Hotamisligil, "Chemical chaperones reduce ER stress and restore glucose homeostasis in a mouse model of type 2 diabetes.", *Science*, Vol. 313, No. 5790, pp. 1137–1140, August 2006.

94. Xiao, C., A. Giacca and G. F. Lewis, "Sodium phenylbutyrate, a drug with known capacity to reduce endoplasmic reticulum stress, partially alleviates lipid-induced insulin resistance and beta-cell dysfunction in humans.", *Diabetes*, Vol. 60, pp. 918–924, March 2011.

95. Hosoi, T., M. Sasaki, T. Miyahara, C. Hashimoto, S. Matsuo, M. Yoshii and K. Ozawa, "Endoplasmic reticulum stress induces leptin resistance.", *Molecular Pharmacology*, Vol. 74, pp. 1610–1619, December 2008.

96. Ozcan, L., A. S. Ergin, A. Lu, J. Chung, S. Sarkar, D. Nie, M. G. Myers and U. Ozcan, "Endoplasmic reticulum stress plays a central role in development of leptin resistance.", *Cell Metabolism*, Vol. 9, pp. 35–51, January 2009.

97. Won, J. C., P.-G. Jang, C. Namkoong, E. H. Koh, S. K. Kim, J.-Y. Park, K.-U. Lee and M.-S. Kim, "Central administration of an endoplasmic reticulum stress inducer inhibits the anorexigenic effects of leptin and insulin.", *Obesity*, Vol. 17, pp. 1861–1865, October 2009.

98. Deng, J., P. D. Lu, Y. Zhang, D. Scheuner, R. J. Kaufman, N. Sonenberg, H. P. Harding and D. Ron, "Translational repression mediates activation of nuclear

factor kappa B by phosphorylated translation initiation factor 2.", *Molecular and Cellular Biology*, Vol. 24, pp. 10161–10168, December 2004.

99. Tuncman, G., J. Hirosumi, G. Solinas, L. Chang, M. Karin and G. S. Hotamisligil, "Functional in vivo interactions between JNK1 and JNK2 isoforms in obesity and insulin resistance.", *Proceedings of the National Academy of Sciences of the United States of America*, Vol. 103, pp. 10741–10746, July 2006.

100. Tam, A. B., E. L. Mercado, A. Hoffmann and M. Niwa, "ER stress activates NF-KB by integrating functions of basal IKK activity, IRE1 and PERK.", *PLoS One*, Vol. 7, p. e45078, October 2012.

101. Gargalovic, P. S., N. M. Gharavi, M. J. Clark, J. Pagnon, W.-P. Yang, A. He, A. Truong, T. Baruch-Oren, J. A. Berliner, T. G. Kirchgessner and A. J. Lusis, "The unfolded protein response is an important regulator of inflammatory genes in endothelial cells.", *Arteriosclerosis, Thrombosis, and Vascular Biology*, Vol. 26, pp. 2490–2496, November 2006.

102. Gao, M., C. Zhang, Y. Ma, L. Bu, L. Yan and D. Liu, "Hydrodynamic delivery of mIL10 gene protects mice from high-fat diet-induced obesity and glucose intolerance.", *Molecular Therapy*, Vol. 21, pp. 1852–1861, October 2013.

103. Gao, M., Y. Ma and D. Liu, "Rutin suppresses palmitic acids-triggered inflammation in macrophages and blocks high fat diet-induced obesity and fatty liver in mice.", *Pharmaceutical Research*, Vol. 30, pp. 2940–2950, November 2013.

104. Yamazaki, H., N. Hiramatsu, K. Hayakawa, Y. Tagawa, M. Okamura, R. Ogata, T. Huang, S. Nakajima, J. Yao, A. W. Paton, J. C. Paton and M. Kitamura, "Activation of the Akt-NF-kappaB pathway by subtilase cytotoxin through the ATF6 branch of the unfolded protein response.", *Journal of Immunology*, Vol. 183, pp. 1480–1487, July 2009.

105. Liu, J. and L. Du, "PERK pathway is involved in oxygen-glucose-serum deprivation-induced NF-kB activation via ROS generation in spinal cord astrocytes.", *Biochemical and Biophysical Research Communications*, Vol. 467, pp. 197–203, November 2015.

106. Xue, X., J.-H. Piao, A. Nakajima, S. Sakon-Komazawa, Y. Kojima, K. Mori, H. Yagita, K. Okumura, H. Harding and H. Nakano, "Tumor necrosis factor alpha (TNFalpha) induces the unfolded protein response (UPR) in a reactive oxygen species (ROS)-dependent fashion, and the UPR counteracts ROS accumulation by TNFalpha.", *The Journal of Biological Chemistry*, Vol. 280, pp. 33917–33925, October 2005.

107. Yoon, Y.-S., W.-Y. Seo, M.-W. Lee, S.-T. Kim and S.-H. Koo, "Salt-inducible kinase regulates hepatic lipogenesis by controlling SREBP-1c phosphorylation.", *The Journal of Biological Chemistry*, Vol. 284, No. 16, pp. 10446–10452, April 2009.

108. Du, J., Q. Chen, H. Takemori and H. Xu, "SIK2 can be activated by deprivation of nutrition and it inhibits expression of lipogenic genes in adipocytes.", *Obesity*, Vol. 16, No. 3, pp. 531–538, March 2008.

109. Henriksson, E., J. Sall, A. Gormand, S. Wasserstrom, N. A. Morrice, A. M. Fritzen, M. Foretz, D. G. Campbell, K. Sakamoto, M. Ekelund, E. Degerman, K. G. Stenkula and O. Gransson, "SIK2 regulates CRTCs, HDAC4 and glucose uptake in adipocytes.", *Journal of Cell Science*, Vol. 128, pp. 472–486, February 2015.

110. Park, J., Y.-S. Yoon, H.-S. Han, Y.-H. Kim, Y. Ogawa, K.-G. Park, C.-H. Lee, S.-T. Kim and S.-H. Koo, "SIK2 is critical in the regulation of lipid homeostasis and adipogenesis in vivo.", *Diabetes*, Vol. 63, pp. 3659–3673, November 2014.

111. Ruiz, J. C., F. L. Conlon and E. J. Robertson, "Identification of novel protein

kinases expressed in the myocardium of the developing mouse heart.", *Mechanisms of Development*, Vol. 48, No. 3, pp. 153–164, December 1994.

112. Wang, Z., H. Takemori, S. K. Halder, Y. Nonaka and M. Okamoto, "Cloning of a novel kinase (SIK) of the SNF1/AMPK family from high salt diet-treated rat adrenal.", *FEBS Letters*, Vol. 453, No. 1-2, pp. 135–139, June 1999.

113. Okamoto, M., H. Takemori and Y. Katoh, "Salt-inducible kinase in steroidogenesis and adipogenesis.", *Trends in Endocrinology and Metabolism*, Vol. 15, No. 1, pp. 21–26, January 2004.

114. Horike, N., H. Takemori, Y. Katoh, J. Doi, L. Min, T. Asano, X. J. Sun, H. Yamamoto, S. Kasayama, M. Muraoka, Y. Nonaka and M. Okamoto, "Adipose-specific expression, phosphorylation of Ser794 in insulin receptor substrate-1, and activation in diabetic animals of salt-inducible kinase-2.", *The Journal of Biological Chemistry*, Vol. 278, No. 20, pp. 18440–18447, May 2003.

115. Qiao, L.-Y., R. Zhande, T. L. Jetton, G. Zhou and X. J. Sun, "In vivo phosphorylation of insulin receptor substrate 1 at serine 789 by a novel serine kinase in insulin-resistant rodents.", *The Journal of Biological Chemistry*, Vol. 277, pp. 26530–26539, July 2002.

116. Bricambert, J., J. Miranda, F. Benhamed, J. Girard, C. Postic and R. Dentin, "Salt-inducible kinase 2 links transcriptional coactivator p300 phosphorylation to the prevention of ChREBP-dependent hepatic steatosis in mice.", *The Journal of Clinical Investigation*, Vol. 120, No. 12, pp. 4316–4331, December 2010.

117. Screaton, R. A., M. D. Conkright, Y. Katoh, J. L. Best, G. Canettieri, S. Jeffries, E. Guzman, S. Niessen, J. R. Yates, H. Takemori, M. Okamoto and M. Montminy, "The CREB coactivator TORC2 functions as a calcium- and cAMP-sensitive coincidence detector.", *Cell*, Vol. 119, No. 1, pp. 61–74, October 2004.

118. Dentin, R., Y. Liu, S.-H. Koo, S. Hedrick, T. Vargas, J. Heredia, J. Yates and M. Montminy, "Insulin modulates gluconeogenesis by inhibition of the coactivator TORC2.", *Nature*, Vol. 449, No. 7160, pp. 366–369, September 2007.

119. Sakamaki, J.-I., A. Fu, C. Reeks, S. Baird, C. Depatie, M. A. Azzabi, N. Bardeesy, A.-C. Gingras, S.-P. Yee and R. A. Screaton, "Role of the SIK2-p35-PJA2 complex in pancreatic B-cell functional compensation.", *Nature Cell Biology*, Vol. 16, No. 3, pp. 234–244, March 2014.

120. Xue, Y., J. Ren, X. Gao, C. Jin, L. Wen and X. Yao, "GPS 2.0, a tool to predict kinase-specific phosphorylation sites in hierarchy.", *Molecular & Cellular Proteomics : MCP*, Vol. 7, No. 9, pp. 1598–1608, September 2008.

121. Ye, Y., H. H. Meyer and T. A. Rapoport, "Function of the p97-Ufd1-Npl4 complex in retrotranslocation from the ER to the cytosol: dual recognition of nonubiquitinated polypeptide segments and polyubiquitin chains.", *The Journal of Cell Biology*, Vol. 162, No. 1, pp. 71–84, July 2003.

122. Topcu, M., *The role of SIK2 in endoplasmic reticulum associated degradation*, Master's Thesis, Gebze Institute of Technology, 2013.

123. Yang, F.-C., Y.-H. Lin, W.-H. Chen, J.-Y. Huang, H.-Y. Chang, S.-H. Su, H.-T. Wang, C.-Y. Chiang, P.-H. Hsu, M.-D. Tsai, B. C.-M. Tan and S.-C. Lee, "Interaction between salt-inducible kinase 2 (SIK2) and p97/valosin-containing protein (VCP) regulates endoplasmic reticulum (ER)-associated protein degradation in mammalian cells.", *The Journal of Biological Chemistry*, Vol. 288, No. 47, pp. 33861–33872, November 2013.

124. Yang, F.-C., B. C.-M. Tan, W.-H. Chen, Y.-H. Lin, J.-Y. Huang, H.-Y. Chang, H.-Y. Sun, P.-H. Hsu, G.-G. Liou, J. Shen, C.-J. Chang, C.-C. Han, M.-D. Tsai and S.-C. Lee, "Reversible acetylation regulates salt-inducible kinase (SIK2) and its function in autophagy.", *The Journal of Biological Chemistry*, Vol. 288, pp.

6227–6237, March 2013.

125. Kahn, C. R., M. F. White, S. E. Shoelson, J. M. Backer, E. Araki, B. Cheatham, P. Csermely, F. Folli, B. J. Goldstein and P. Huertas, "The insulin receptor and its substrate: molecular determinants of early events in insulin action.", *Recent Progress in Hormone Research*, Vol. 48, pp. 291–339, 1993.

126. Johnston, J. A., L. M. Wang, E. P. Hanson, X. J. Sun, M. F. White, S. A. Oakes, J. H. Pierce and J. J. O'Shea, "Interleukins 2, 4, 7, and 15 stimulate tyrosine phosphorylation of insulin receptor substrates 1 and 2 in T cells. Potential role of JAK kinases.", *The Journal of Biological Chemistry*, Vol. 270, pp. 28527–28530, December 1995.

127. Kellerer, M., M. Koch, E. Metzinger, J. Mushack, E. Capp and H. U. Haring, "Leptin activates PI-3 kinase in C2C12 myotubes via janus kinase-2 (JAK-2) and insulin receptor substrate-2 (IRS-2) dependent pathways.", *Diabetologia*, Vol. 40, pp. 1358–1362, November 1997.

128. Backer, J. M., M. G. Myers, S. E. Shoelson, D. J. Chin, X. J. Sun, M. Miralpeix, P. Hu, B. Margolis, E. Y. Skolnik and J. Schlessinger, "Phosphatidylinositol 3'-kinase is activated by association with IRS-1 during insulin stimulation.", *The EMBO Journal*, Vol. 11, pp. 3469–3479, September 1992.

129. Shepherd, P. R., D. J. Withers and K. Siddle, "Phosphoinositide 3-kinase: the key switch mechanism in insulin signalling.", *The Biochemical Journal*, Vol. 333 (Pt 3), pp. 471–490, August 1998.

130. Weissmann, L., P. G. F. Quaresma, A. C. Santos, A. H. B. de Matos, V. D. B. Pascoal, T. M. Zanotto, G. Castro, D. Guadagnini, J. M. da Silva, L. A. Velloso, J. C. Bittencourt, I. Lopes-Cendes, M. J. A. Saad and P. O. Prada, "IKKb is key to induction of insulin resistance in the hypothalamus, and its inhibition reverses obesity.", *Diabetes*, Vol. 63, pp. 3334–3345, October 2014.

131. Dong, X. C., K. D. Copps, S. Guo, Y. Li, R. Kollipara, R. A. DePinho and M. F. White, "Inactivation of hepatic Foxo1 by insulin signaling is required for adaptive nutrient homeostasis and endocrine growth regulation.", *Cell Metabolism*, Vol. 8, pp. 65–76, July 2008.

132. Lin, X., A. Taguchi, S. Park, J. A. Kushner, F. Li, Y. Li and M. F. White, "Dysregulation of insulin receptor substrate 2 in beta cells and brain causes obesity and diabetes.", *The Journal of Clinical Investigation*, Vol. 114, pp. 908–916, October 2004.

133. Fantin, V. R., Q. Wang, G. E. Lienhard and S. R. Keller, "Mice lacking insulin receptor substrate 4 exhibit mild defects in growth, reproduction, and glucose homeostasis.", *American Journal of Physiology, Endocrinology and Metabolism*, Vol. 278, pp. E127–E133, January 2000.

134. Liu, S. C., Q. Wang, G. E. Lienhard and S. R. Keller, "Insulin receptor substrate 3 is not essential for growth or glucose homeostasis.", *The Journal of Biological Chemistry*, Vol. 274, pp. 18093–18099, June 1999.

135. Tsuruzoe, K., R. Emkey, K. M. Kriauciunas, K. Ueki and C. R. Kahn, "Insulin receptor substrate 3 (IRS-3) and IRS-4 impair IRS-1- and IRS-2-mediated signaling.", *Molecular and Cellular Biology*, Vol. 21, pp. 26–38, January 2001.

136. Tseng, Y.-H., K. M. Kriauciunas, E. Kokkotou and C. R. Kahn, "Differential roles of insulin receptor substrates in brown adipocyte differentiation.", *Molecular and Cellular Biology*, Vol. 24, pp. 1918–1929, March 2004.

137. Numan, S. and D. S. Russell, "Discrete expression of insulin receptor substrate-4 mRNA in adult rat brain.", *Brain Research. Molecular Brain Research*, Vol. 72, pp. 97–102, September 1999.

138. Wauman, J., A.-S. De Smet, D. Catteeuw, D. Belsham and J. Tavernier, "Insulin

receptor substrate 4 couples the leptin receptor to multiple signaling pathways.", *Molecular Endocrinology*, Vol. 22, pp. 965–977, April 2008.

139. Ballinger, C. A., P. Connell, Y. Wu, Z. Hu, L. J. Thompson, L. Y. Yin and C. Patterson, "Identification of CHIP, a novel tetratricopeptide repeat-containing protein that interacts with heat shock proteins and negatively regulates chaperone functions.", *Molecular and Cellular Biology*, Vol. 19, pp. 4535–4545, June 1999.

140. Connell, P., C. A. Ballinger, J. Jiang, Y. Wu, L. J. Thompson, J. Hhfeld and C. Patterson, "The co-chaperone CHIP regulates protein triage decisions mediated by heat-shock proteins.", *Nature Cell Biology*, Vol. 3, pp. 93–96, January 2001.

141. Murata, S., Y. Minami, M. Minami, T. Chiba and K. Tanaka, "CHIP is a chaperone-dependent E3 ligase that ubiquitylates unfolded protein.", *EMBO Reports*, Vol. 2, pp. 1133–1138, December 2001.

142. Jana, N. R., P. Dikshit, A. Goswami, S. Kotliarova, S. Murata, K. Tanaka and N. Nukina, "Co-chaperone CHIP associates with expanded polyglutamine protein and promotes their degradation by proteasomes.", *The Journal of Biological Chemistry*, Vol. 280, pp. 11635–11640, March 2005.

143. Meacham, G. C., C. Patterson, W. Zhang, J. M. Younger and D. M. Cyr, "The Hsc70 co-chaperone CHIP targets immature CFTR for proteasomal degradation.", *Nature Cell Biology*, Vol. 3, pp. 100–105, January 2001.

144. Zhu, X., J. Zhang, H. Sun, C. Jiang, Y. Dong, Q. Shan, S. Su, Y. Xie, N. Xu, X. Lou and S. Liu, "Ubiquitination of inositol-requiring enzyme 1 (IRE1) by the E3 ligase CHIP mediates the IRE1/TRAF2/JNK pathway.", *The Journal of Biological Chemistry*, Vol. 289, pp. 30567–30577, October 2014.

145. Kim, J.-H., S. Shin, J. Seo, E.-W. Lee, M. Jeong, M.-S. Lee, H.-J. Han and J. Song,

"C-terminus of HSC70-Interacting Protein (CHIP) Inhibits Adipocyte Differentiation via Ubiquitin- and Proteasome-Mediated Degradation of PPARg.", *Scientific Reports*, Vol. 7, p. 40023, January 2017.

146. Lv, Y., S. Song, K. Zhang, H. Gao and R. Ma, "CHIP regulates AKT/FoxO/Bim signaling in MCF7 and MCF10A cells.", *PLoS One*, Vol. 8, p. e83312, 2013.

147. Jang, K. W., K. H. Lee, S. H. Kim, T. Jin, E. Y. Choi, H. J. Jeon, E. Kim, Y. S. Han and J. H. Chung, "Ubiquitin ligase CHIP induces TRAF2 proteasomal degradation and NF-KB inactivation to regulate breast cancer cell invasion.", *Journal of Cellular Biochemistry*, Vol. 112, pp. 3612–3620, December 2011.

148. Wang, Y., F. Ren, Y. Wang, Y. Feng, D. Wang, B. Jia, Y. Qiu, S. Wang, J. Yu, J. J. Sung, J. Xu, N. Zeps and Z. Chang, "CHIP/Stub1 functions as a tumor suppressor and represses NF-KB-mediated signaling in colorectal cancer.", *Carcinogenesis*, Vol. 35, pp. 983–991, May 2014.

149. Gao, Y., C. Han, H. Huang, Y. Xin, Y. Xu, L. Luo and Z. Yin, "Heat shock protein 70 together with its co-chaperone CHIP inhibits TNF-alpha induced apoptosis by promoting proteasomal degradation of apoptosis signal-regulating kinase1.", *Apoptosis*, Vol. 15, pp. 822–833, July 2010.

150. Guo, D., Z. Ying, H. Wang, D. Chen, F. Gao, H. Ren and G. Wang, "Regulation of autophagic flux by CHIP.", *Neuroscience Bulletin*, Vol. 31, pp. 469–479, August 2015.

151. Sha, Y., L. Pandit, S. Zeng and N. T. Eissa, "A critical role for CHIP in the aggresome pathway.", *Molecular and Cellular Biology*, Vol. 29, pp. 116–128, January 2009.

152. Küser, G., *SIK2: a key player in FGF2-induced proliferation and insulin-induced survivale/hyperglycemia-dependent apoptosis in müller cells*, Ph.D. The-

sis, Boğaziçi University, 2011.

153. Huang, D. W., B. T. Sherman and R. A. Lempicki, "Systematic and integrative analysis of large gene lists using DAVID bioinformatics resources.", *Nature Protocols*, Vol. 4, pp. 44–57, 2009.

154. Schönthal, A., J. Sugarman, J. H. Brown, M. R. Hanley and J. R. Feramisco, "Regulation of c-fos and c-jun protooncogene expression by the Ca(2+)-ATPase inhibitor thapsigargin.", *Proceedings of the National academy of Sciences of the United States of America*, Vol. 88, No. 16, pp. 7096–7100, August 1991.

155. van Schadewijk, A., E. F. A. van't Wout, J. Stolk and P. S. Hiemstra, "A quantitative method for detection of spliced X-box binding protein-1 (XBP1) mRNA as a measure of endoplasmic reticulum (ER) stress.", *Cell stress & Chaperones*, Vol. 17, pp. 275–279, March 2012.

156. Yang, M., S. Omura, J. S. Bonifacino and A. M. Weissman, "Novel aspects of degradation of T cell receptor subunits from the endoplasmic reticulum (ER) in T cells: importance of oligosaccharide processing, ubiquitination, and proteasome-dependent removal from ER membranes.", *The Journal of Experimental Medicine*, Vol. 187, pp. 835–846, March 1998.

157. Meng, L., R. Mohan, B. H. Kwok, M. Elofsson, N. Sin and C. M. Crews, "Epoxomicin, a potent and selective proteasome inhibitor, exhibits in vivo antiinflammatory activity.", *Proceedings of the National Academy of Sciences of the United States of America*, Vol. 96, pp. 10403–10408, August 1999.

158. Pundir, S., H.-Y. Vu, V. R. Solomon, R. McClure and H. Lee, "VR23: A Quinoline-Sulfonyl Hybrid Proteasome Inhibitor That Selectively Kills Cancer via Cyclin E-Mediated Centrosome Amplification.", *Cancer Research*, Vol. 75, pp. 4164–4175, October 2015.

159. Miranda, F., D. Mannion, S. Liu, Y. Zheng, L. S. Mangala, C. Redondo, S. Herrero-Gonzalez, R. Xu, C. Taylor, D. F. Chedom, M. Karaminejadranjbar, A. Albukhari, D. Jiang, S. Pradeep, C. Rodriguez-Aguayo, G. Lopez-Berestein, E. Salah, K. R. Abdul Azeez, J. M. Elkins, L. Campo, K. A. Myers, D. Klotz, S. Bivona, S. Dhar, R. C. Bast, H. Saya, H. G. Choi, N. S. Gray, R. Fischer, B. M. Kessler, C. Yau, A. K. Sood, T. Motohara, S. Knapp and A. A. Ahmed, "Salt-Inducible Kinase 2 Couples Ovarian Cancer Cell Metabolism with Survival at the Adipocyte-Rich Metastatic Niche.", *Cancer Cell*, Vol. 30, pp. 273–289, August 2016.

160. Hoxhaj, G., K. Dissanayake and C. MacKintosh, "Effect of IRS4 levels on PI 3-kinase signalling.", *PLoS One*, Vol. 8, p. e73327, September 2013.

161. Lin, J. H., H. Li, D. Yasumura, H. R. Cohen, C. Zhang, B. Panning, K. M. Shokat, M. M. Lavail and P. Walter, "IRE1 signaling affects cell fate during the unfolded protein response.", *Science*, Vol. 318, pp. 944–949, November 2007.

162. Li, H., A. V. Korennykh, S. L. Behrman and P. Walter, "Mammalian endoplasmic reticulum stress sensor IRE1 signals by dynamic clustering.", *Proceedings of the National Academy of Sciences of the United States of America*, Vol. 107, pp. 16113–16118, September 2010.

163. Das, U. N., "Is obesity an inflammatory condition?", *Nutrition*, Vol. 17, pp. 953–966, 2001.

164. Cai, D. and T. Liu, "Hypothalamic inflammation: a double-edged sword to nutritional diseases.", *Annals of the New York Academy of Sciences*, Vol. 1243, pp. E1–39, December 2011.

165. Joshi, V., A. Amanullah, A. Upadhyay, R. Mishra, A. Kumar and A. Mishra, "A Decade of Boon or Burden: What Has the CHIP Ever Done for Cellular Protein Quality Control Mechanism Implicated in Neurodegeneration and Aging?",

Frontiers in Molecular Neuroscience, Vol. 9, p. 93, 2016.

166. Tawo, R., W. Pokrzywa, v. Kevei, M. E. Akyuz, V. Balaji, S. Adrian, J. Hhfeld and T. Hoppe, "The Ubiquitin Ligase CHIP Integrates Proteostasis and Aging by Regulation of Insulin Receptor Turnover.", *Cell*, Vol. 169, pp. 470–482.e13, April 2017.

167. Kim, C., N. Yun, J. Lee, M. B. H. Youdim, C. Ju, W.-K. Kim, P.-L. Han and Y. J. Oh, "Phosphorylation of CHIP at Ser20 by Cdk5 promotes tAIF-mediated neuronal death.", *Cell Death and Differentiation*, Vol. 23, pp. 333–346, February 2016.

168. Papinski, D., M. Schuschnig, W. Reiter, L. Wilhelm, C. A. Barnes, A. Maiolica, I. Hansmann, T. Pfaffenwimmer, M. Kijanska, I. Stoffel, S. S. Lee, A. Brezovich, J. H. Lou, B. E. Turk, R. Aebersold, G. Ammerer, M. Peter and C. Kraft, "Early steps in autophagy depend on direct phosphorylation of Atg9 by the Atg1 kinase.", *Molecular Cell*, Vol. 53, pp. 471–483, February 2014.

169. Chang, P.-C., H.-W. Tsai, M.-T. Chiang, P.-L. Huang, S.-K. Shyue and L.-Y. Chau, "TRC8 downregulation contributes to the development of non-alcoholic steatohepatitis by exacerbating hepatic endoplasmic reticulum stress.", *Biochimica et Biophysica Acta*, Vol. 1852, pp. 2339–2351, November 2015.

APPENDIX A: PLASMID MAPS

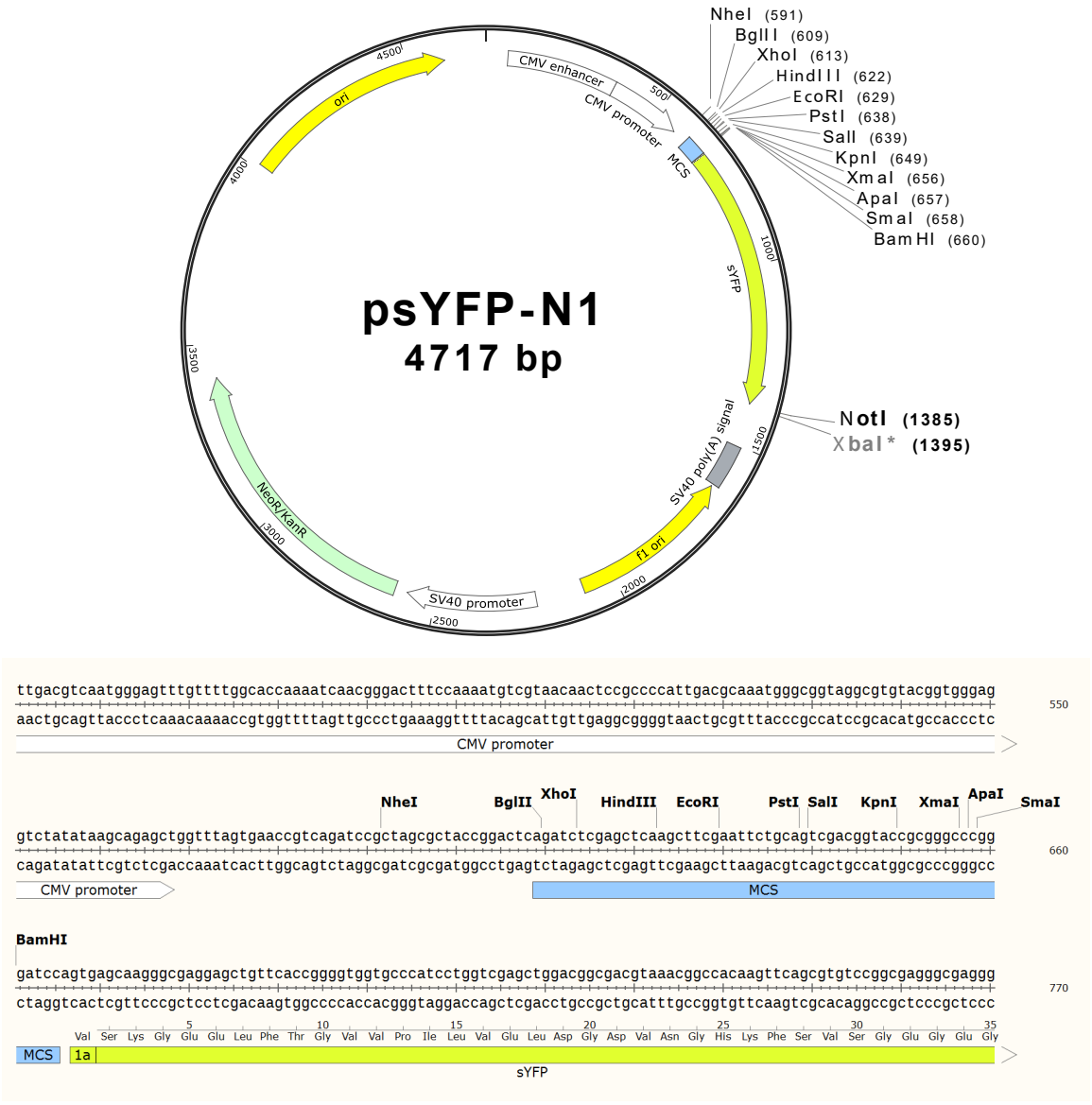

Figure A.1. Restriction map and multiple cloning site of the psYFP-N1 plasmid.

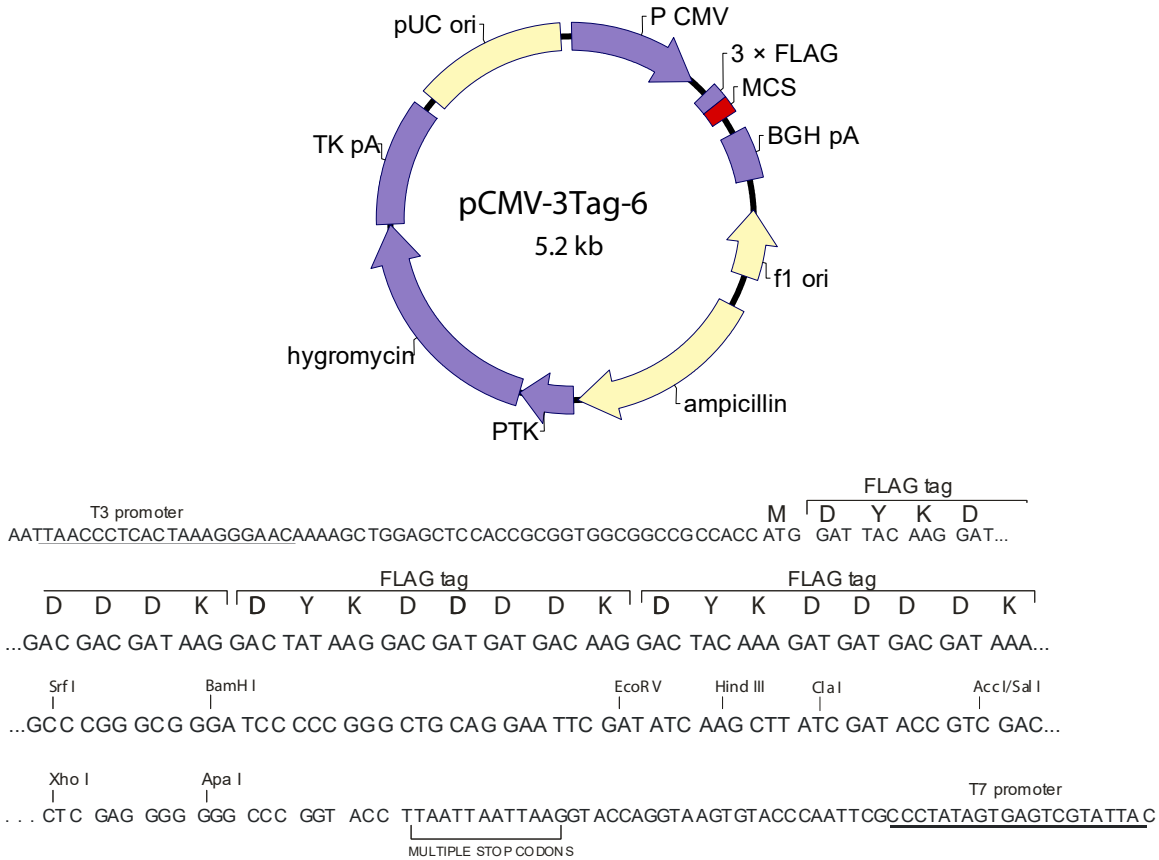

Figure A.2. Restriction map of the pCMV-3Tag-6 plasmid.